OUKA
Osaka University Knowledge Archive

Title	Study on Culture-Driven Epigenetic Memory during Expansion of Human Induced Pluripotent Stem Cells
Author(s)	Thanuthanakhun, Naruchit
Citation	大阪大学, 2022, 博士論文
Version Type	VoR
URL	https://doi.org/10.18910/88011
rights	
Note	

Osaka University Knowledge Archive : OUKA

https://ir.library.osaka-u.ac.jp/

Osaka University

Doctoral Dissertation

Study on Culture-Driven Epigenetic Memory during Expansion of Human Induced Pluripotent Stem Cells

Naruchit Thanuthanakhun

January 2022

Graduate School of Engineering

Osaka University

Contents

	Pages
Abstract	**1**
General introduction	**3**
1. Human induced pluripotent stem cells as a cell source for regenerative medicine	3
2. Epigenetic and transcriptional regulation of state and potential in pluripotent stem cells	6
3. Chapter outline	12
Chapter 1 Investigation of epigenetic memory formation and initialization during cultures of human iPS cells	**15**
1.1 Introduction	15
1.2 Materials and methods	17
1.3 Results	24
1.3.1 Morphological and growth phenotypes of hiPSCs in 2D and 3D cultures	24
1.3.2 Regulation of cell behaviors in different culture conditions	26
1.3.3 Culture-induced rearrangement of actomyosin cytoskeleton	27
1.3.4 Epigenetic memory formation and initialization in 2D and 3D cultures	32
1.3.5 Pluripotent state and differentiation potential of hiPSCs in 2D and 3D cultures	35
1.4 Discussion	39
1.5 Chapter summary	43
Chapter 2 Investigation of epigenetic memory consolidation in prolonged cultures of human iPS cells	**44**
2.1 Introduction	44
2.2 Materials and methods	46

Contents (continued)

	Pages
2.3 Results	51
2.3.1 Cell behavioral and nucleoskeletal charataceristics of hiPSCs with different initial seeding densities	51
2.3.2 Epigenetic memory formation during growth phase transition in correlation with the activation of core pluripotent gene expression	56
2.3.3 Epigenetic memory initialization and consolidation after subculture from different growth phases	59
2.3.4 Association between epigenetic memory formation in past culture and lineage differentiation potential	64
2.4 Discussion	68
2.5 Chapter summary	72
Concluding remarks	**73**
3.1 General conclusion	73
3.2 Future perspectives	76
Nomenclature	**79**
Abbreviations	**80**
References	**82**
Lists of publications	**98**
Acknowledgements	**99**

Abstract

Human induced pluripotent stem cells (hiPSCs) are a promising source of stem cells for regenerative medicine. To control the quality and stability of hiPSC expansion for practical applications, understanding how the cell properties are affected by culture environmental factors during expansion process is critical. The main objective of this thesis is to elucidate the culture-driven epigenetic memory and its role in modulating the quality of cultured hiPSCs.

In chapter 1, formation of epigenetic memory was firstly investigated in hiPSCs under general expansion conditions including two-dimensional (2D) monolayer and three-dimensional (3D) aggregate cultures. Quantitative analysis of global histone methylation by western blotting revealed that cells in 2D culture upregulated active H3K4me3 mark and downregulated repressive H3K27me3 mark, whereas the cells in 3D culture significantly earlier upregulated the H3K4me3 but constantly maintained the H3K27me3. After subculture into new culture vessels, the cells collected from both 2D and 3D cultures exhibited their ability to reset and initialize the epigenetic memory to baseline levels detected in the initial culture period before subculture. Moreover, compared to cells in 2D culture, the cells in 3D culture demonstrated distinct transcriptional activation of naïve pluripotency signatures. Overall, this chapter described the effect of different culture conditions on epigenetic memory formation and its initialization after subculture.

In chapter 2, the epigenetic memory of hiPSCs was further examined during prolonged expansion culture at different cell growth phases. Cells collected from exponential and stationary growth phases maintained the capability of epigenetic memory initialization after subculture; however, the cells collected from long-term stationary growth phase that formed and lasted the epigenetic memory for several days in past culture distinctly showed consolidation of epigenetic memory after subculture. In addition, the epigenetic memory

formed at different growth phases in past culture was found associated with the lineage differentiation preference. Concisely, prolonged expansion of hiPSCs under long-term stationary phase resulted in the epigenetic memory consolidation after subculture.

Taken together, this thesis demonstrated epigenetic memory formation during expansion of hiPSCs and the impact of past culture experience on epigenetic memory initialization and consolidation after subculture. This study paves the way for controlling the cell quality by considering epigenetic memory mechanism, and the improved understanding of cellular responses to the culture environments may help enable the process design and optimization for manufacturing of hiPSCs.

General introduction

1. Human induced pluripotent stem cells as a cell source for regenerative medicine

Pluripotent stem cells (PSCs), including embryonic stem cells (ESCs) and induced pluripotent stem cells (iPSCs), are cells that have the ability to undergo unlimited self-renewal and to differentiate into all somatic cell types (Shi et al., 2016). iPSCs can be generated by reprogramming somatic cells to a pluripotent state through ectopic expression of a defined set of transcription factors, which were firstly established by Yamanaka and Takahashi in 2006. Advances in stem cell research have demonstrated that human iPSCs (hiPSCs) can be directed *in vitro* towards many different types of specialized cells, such as hepatocytes, cardiomyocytes, neurons (Gunhanlar et al., 2018; Kaneko et al., 2016; Yoshida et al., 2018). Moreover, a wide range of hiPSC generation methods has been to date introduced to create safe, clinical-grade cells in an individual-/allele-specific manner (Ji et al., 2016). The given advantages of hiPSC technology highlight the feasibility of using these accessible stem cells for cell-based therapies and regenerative medicine, which seek to regenerate or repair tissues that have been damaged by diseases, injuries, or aging.

In the translation of hiPSCs into therapeutic applications, efficient cell production is essential to provide the cells in clinically relevant numbers with stable quality for further processing and differentiation (Galvanauskas et al., 2017; Polak & Mantalaris, 2008). Recent researches and developments in hiPSC production provide various culture platforms for expanding the cell quantity (Horiguchi & Kino-oka, 2021; Le & Hasegawa, 2019; Valamehr et al., 2012). Two-dimensional (2D) monolayer culture represents a traditional method, which has been exploited to culture cells since the early 1900s and modified for growing PSCs by applying cell-based feeder layers or proteins of the extracellular matrix (ECM) or their fragments to support the adhesion of PSCs on the culture surfaces and to enable maintenance

of their self-renewal and proliferation (Chan et al., 2020; Jensen & Teng, 2020). Cultures in 2D monolayers support uniform distributions of nutrients, oxygen, and growth factors to the cells, which thought to facilitate homogeneous cell expansion and promote batch-to-batch reproducibility; whereas the scalability of 2D culture is considered as its limitations (Duval et al., 2017). At present, a scale out of 2D approach has been suggested for large-scale production of PSCs by exploiting multi-layered flasks in cell factories or cell stacks under automated operation (Kropp et al., 2017). In addition, three-dimensional (3D) aggregate culture serves as an alternative format in the PSC production, which relied on the ability of cells to adhere to each other and form spheroid structure in suspension without sticking to a culture surface (Kato et al., 2018). This approach provides advantages for scaling up under controlled conditions and mimicking native stem cell niche; however, the chemical diffusion gradients possibly develop within the 3D structure, and the sequential cell passaging is still operationally critical to achieve high-fold cell expansion (Lei & Schaffer, 2013; Mirbagheri et al., 2019). The emergence of various culture platforms offers options for cell production; however, there is the need for much optimization of culture conditions, and the comprehensive quality management is required in parallel to validate and trace the cellular properties upon the expansion (Adil & Schaffer, 2017).

With an aspect of the quality of produced cells, quality attributes must be defined according to regulatory guidelines for biologics and be thoroughly monitored to assure the manufacturing process (Rehakova et al., 2020). Quality criteria for hiPSCs typically include pluripotency, differentiation capacity, cellular viability, genomic instability, tumorigenicity as well as microbiological sterility (Huang et al., 2019; Seki & Fukuda, 2016). The properties of undifferentiated hiPSCs are defined as cell state, while the abilities of hiPSCs to differentiate into other cell types are defined as cell potential (Kim & Kino-oka, 2020). Maintenance of the cell state and potential in hiPSCs could be characterized using well-established assays, such as measurement of the transcriptional or protein expression of pluripotent markers in

undifferentiated cells or the expression of lineage-specific markers in hiPSC derivatives following spontaneous or lineage-specific differentiation induction (Baghbaderani et al., 2016). Assessment of the functional properties in the cultured hiPSCs is routinely performed to verify the selection of cell lines for intended applications and to evaluate and trace the cell quality during and after manufacturing (Liu & Zheng, 2019). **Fig. 1** demonstrated that hiPSC quality can be influenced by variable factors during expansion process including raw material adaptability, operator's skill and sense, and culture conditions (Kim & Kino-oka, 2020). In order to control the culture-induced fluctuation contributing to hiPSC quality, it is thus foremost to comprehend how each variable culture factor has an impact on the cellular properties as well as its underlying mechanism.

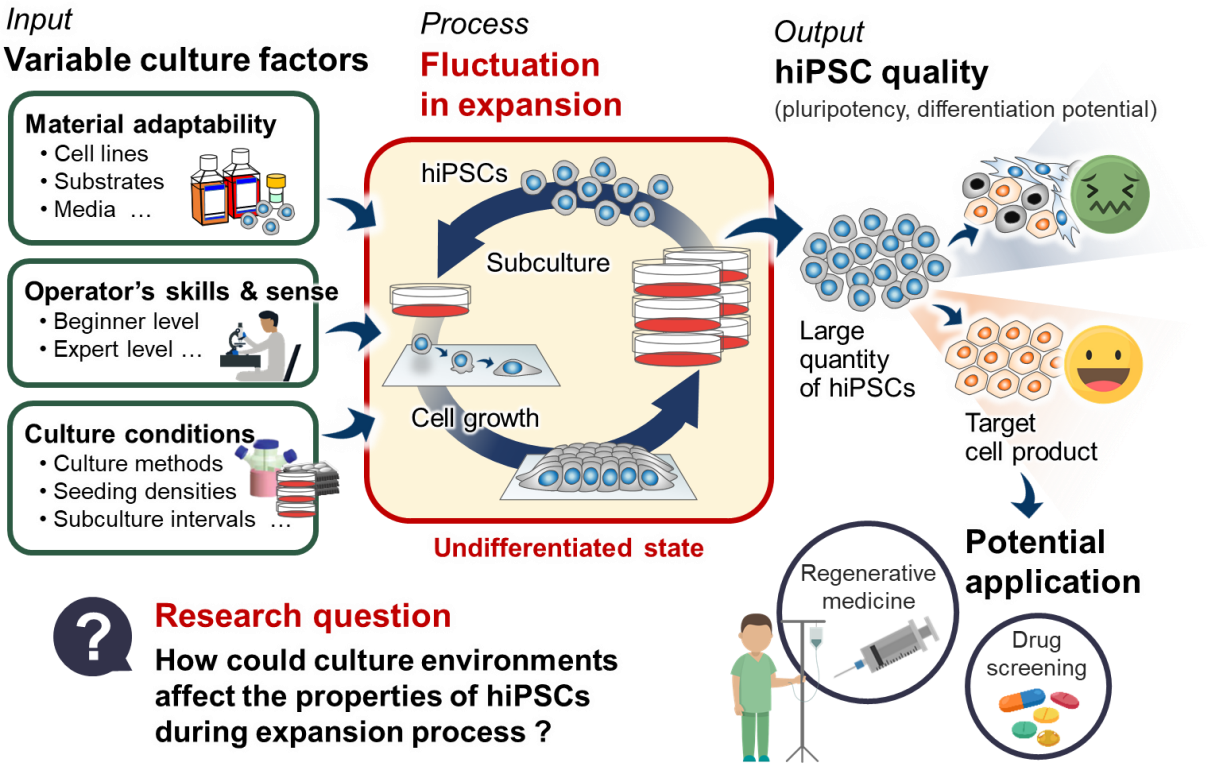

Figure 1 Culture-induced fluctuation of cell quality during expansion of undifferentiated hiPSCs contributing to their downstream application.

2. Epigenetic and transcriptional regulation of state and potential in pluripotent stem cells

In PSCs, the pluripotency and differentiation specification are orchestrated by the coordinated regulatory networks of many transcription factors and epigenetic regulators. In the 1950s, Conrad Waddington proposed the concept of an epigenetic landscape to explain the multistep and multifactorial developmental pathways from pluripotent stem cells to terminally differentiated cells (Creighton & Waddington, 1958; Wu et al., 2017). In the landscape framework as shown in **Fig. 2A**, the developing cell is depicted as a ball rolling down a hillside marked by uneven ridges and valleys until reaching the bottom. The topography of the landscape represents developmental path choices during cell differentiation that are hypothetically shaped by the intrinsic gene regulatory networks (Banerji et al., 2013). The dynamics of a gene regulatory circuit beneath the landscape can be attributed to the change of height and slope of the ridges expressed on the landscape, constructing branching points and navigating cells to different states via binary decisions in sequence (Gilbert, 2000). Valleys on the landscape in which the ball is retained also describe the states during development where the potency of cells could be preserved (Chen et al., 2015). Moreover, this theoretical landscape was used to quantify the possibility of reverse differentiation process under certain circumstance, explaining the generation of iPSCs by which a specialized cell at the bottom of landscape can be de-differentiated into a pluripotent state at the summit of landscape (Takahashi, 2012). A growing number of studies based on mechanistic exploration as well as mathematical modelling have been conducted to provide experimental evidence recapitulating the metaphor of Waddington's epigenetic landscape (Banerji et al., 2013; Li & Wang, 2013). The molecular insight into the regulation of each cell state on this landscape has been extensively investigated as it is a key for stem cell research and further applications.

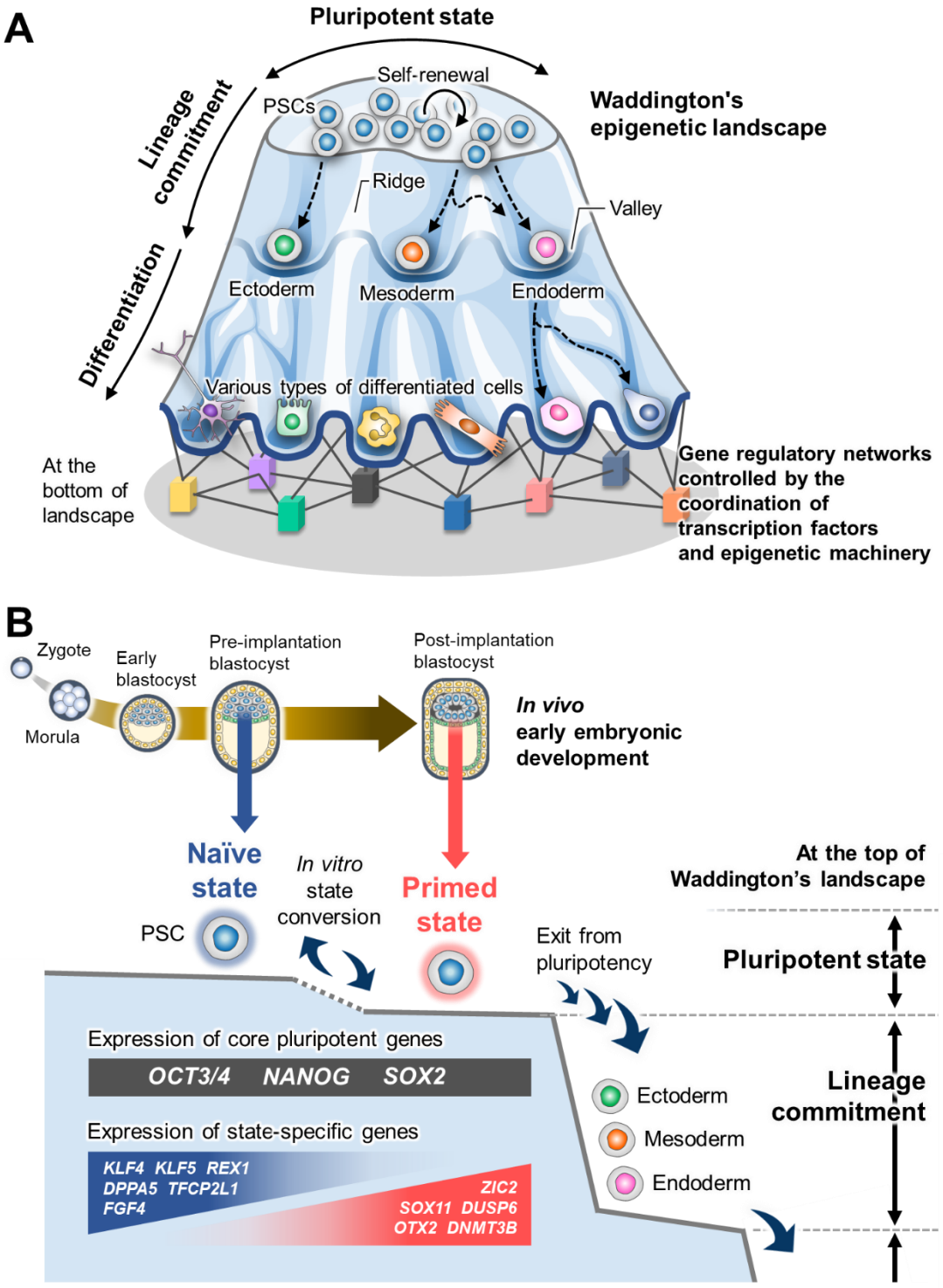

Figure 2 Regulation of the cell state and fate decision in pluripotent stem cells. (A) Concept of Waddington's epigenetic landscape. (B) Existence of two distinct pluripotent states, including naïve and primed states, during *in vivo* early embryonic development, and in *in vitro* cultures.

In the maintenance of pluripotent state of PSCs (**Fig. 2B**), core pluripotency circuitry of OCT3/4, NANOG and SOX2 has been shown to co-occupy a considerable portion of their target genes including their own regulatory regions, simultaneously activating and keeping the expression of pluripotency-associated genes required for self-renewal while repressing the expression of differentiation-associated genes required for pluripotency exit and differentiation commitment (Boyer et al., 2005; Yeo & Ng, 2013). The pluripotent state of PSCs have been characterized and classified into two different states corresponding to the existence of two distinct PSC populations during the early *in vivo* embryonic development (Nichols & Smith, 2009; Takahashi et al., 2018). PSCs derived from the inner cell mass of a pre-implantation blastocyst have been considered to be in the naïve state, whereas PSCs derived from the epiblast of a post-implantation blastocyst have been considered to be in the primed state (Dundes & Loh, 2020). Conversion from naïve to primed state represents a major step in mammalian embryogenesis as it sets the state for the self-organization into cells of the three germ layers, ectoderm, mesoderm and endoderm, that would further develop into distinct organs and tissues (Dundes & Loh, 2020).

In traditional *in vitro* cultures, hESCs and hiPSCs were grown and maintained in a primed state as the molecular characterization indicates a close similarity of their properties to those in the primed epiblast (Nichols & Smith, 2012). Recently, several studies show that these two pluripotent states could be interconverted *in vitro* by supplementing the stem cell culture medium with specific sets of small molecules and growth factors (Duggal et al., 2015; Gafni et al., 2013). In addition, 3D culture systems have been found to support the transition and maintenance of naïve pluripotency through modulating intracellular mechanosensitive pathways (Chang et al., 2021; Lipsitz et al., 2018; McKee et al., 2019). Differences in gene expression, epigenetic states and metabolic activity present between the different cell states (Weinberger et al., 2016). As shown in **Fig. 2B**, transcriptional expression of state-specific

genes has been used to distinguish the two pluripotent states of PSCs, including naïve pluripotency-associated genes: *KLF4, KLF5, DPPA5, FGF4, REX1, TFCP2L1*; primed-pluripotency associated genes: *ZIC2, SOX11, OTX2, DUSP6, DNMT3B* (Lipsitz et al., 2018; McKee et al., 2019; Messmer et al., 2019; Theunissen et al., 2016). Although broad differentiation potential is shared among the naïve and primed PSCs, previous studies elucidated that induction of naïve pluripotency in PSCs might help increase the clonogenicity of cell expansion and overcome the limited differentiation and maturation capacity of primed PSCs (Warrier et al., 2017). However, advantages of the different pluripotent states of PSCs in future applications remain controversial, and the molecular mechanism regulating the state transition still needs further clarifications (Ortmann et al., 2020; Rohani et al., 2020). Current knowledge importantly indicated the pluripotency plasticity in PSC population under *in vivo* and *in vitro* environments.

In concert with the pluripotent transcription factors, epigenetic modifications have been implicated in regulating the state and potential of PSCs by organizing the chromatin structure and accessibility, in turn programing global gene transcription and cellular functions (Friman et al., 2019; Roberts et al., 2021). Epigenetic histone modifications and DNA methylation form a complex regulatory network that attunes genome function (Barrand & Collas, 2010; Bhanu et al., 2016). Comparative epigenetic profiling studies in PSCs and their differentiated progeny have elucidated that simultaneous presence of two epigenetic histone modifications including histone H3 trimethylation at lysine 4 (H3K4me3) and at lysine 27 (H3K27me3), defined as bivalent histone mark, represents a key and prevalent epigenetic signature of PSCs that contributes to the preservation of cell identity while keeping their genome in a flexible state to allow for broad differentiation (**Fig. 3**; Azuara et al., 2006; Bernstein et al., 2006; Mikkelsen et al., 2007).

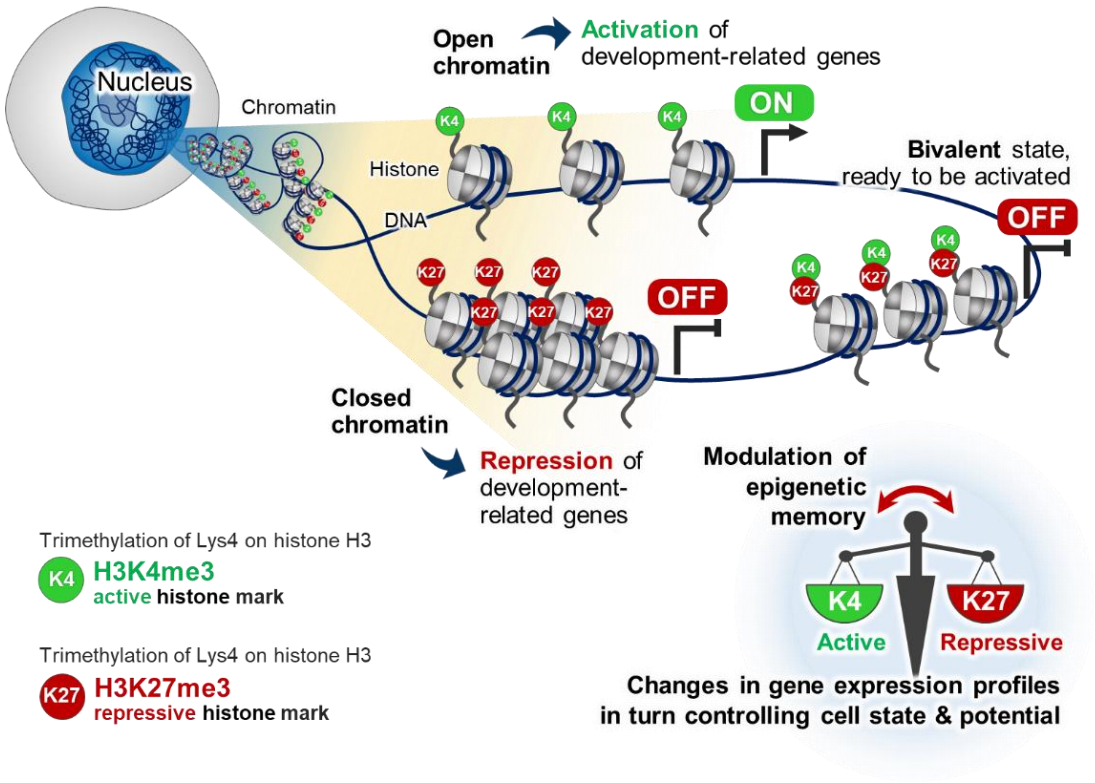

Figure 3 Role of epigenetic histone modifications in controlling the chromatin remodeling and gene transcriptional regulation.

Generally, H3K4me3 mark is associated with active or open chromatin, while H3K27me3 mark is associated with repressive or closed chromatin (Amabile & Meissner, 2009; Rada-Iglesias & Wysocka, 2011). Deposition of these active and repressive epigenetic histone marks, defined as epigenetic memory formation, regulates transcriptional activation or repression of diverse pluripotency and development-related genes (Azuara et al., 2006; Mikkelsen et al., 2007). In particular, it has been identified that the active H3K4me3 mark is positively correlated with the expression of constitutive housekeeping genes fundamentally required for cell growth and survival of PSCs, and also found to be relevant to the maintenance of pluripotent gene activation (Bogliotti et al., 2018). Differences in global abundance of the repressive H3K27me3 mark that acts on regulation of lineage priming features were linked with the distinction between naïve and primed pluripotent states of PSCs (van Mierlo et al.,

2019). Furthermore, enrichment with bivalent modifications of H3K4me3 and H3K27me3 at promoters of differentiation-related genes across the genome takes part in sustaining the PSCs in an undifferentiated state by retaining the genes in a poised state transcriptionally silent but ready to be switched on in response to differentiation stimuli (Bertero et al., 2015; Grandy et al., 2016; Wang et al., 2017). Upon the differentiation progression, the number of promoters with bivalent histone marks temporally reduced in a correlation with the decreased cell potency (Aranda et al., 2009). Regulation of epigenetic memory in PSCs is thus key to determine their gene transcriptional profile and supervise cell fate specification process by which cells would make a decision to maintain their pluripotent state or undergo differentiation and lineage commitment (Cheedipudi et al., 2014; Roberts et al., 2021).

The epigenetic memory can be formed, modified and transferred from one cell generation to another without alterations of DNA sequence (Dean, 2017; Kim et al., 2010). During generation of hiPSCs, global patterns of mature somatic epigenetic modifications must be reset to the ESC-like state; however, recent studies unveiled a retention of residual epigenetic information from their donor cells, namely cell origin-derived epigenetic memory (Kim et al., 2010). The existence of cell origin-derived epigenetic memory resulted in a preference for differentiation into their original cell lineage (Bar-Nur et al., 2011). Moreover, in stem cell cultures, epigenetic memory can also be established through adaptive cellular mechanism in response to culture environmental cues (McEwen et al., 2013; Scesa et al., 2021; Weissbein et al., 2017). Epigenetic modifications can be enzymatically reversed after cessation of exposure to a specific environment, but some modifications of epigenetic memory seem to persist, indicating irreversible changes in cellular adaptability (Killaars et al., 2019). Therefore, the culture-derived epigenetic memory may also reflect the cell culture experiences and govern cellular properties and their application potential. To understand how the culture environmental factors rearrange the gene and epigenetic regulatory networks of hiPSCs as well as how the

disturbance of this regulatory system reflects the cell quality, the culture-induced cellular changes, and fundamental epigenetic mechanisms during expansion of hiPSCs still need to be clarified.

3. Chapter outline

The quality of PSCs and their further differentiation could be affected by culture-induced fluctuation (Kanie et al., 2019; Kim et al., 2018; Shibata et al., 2018). Hence, understanding mechanism how the changes in culture environmental factors can instruct cell properties would be critical for the quality-controlled production of PSCs.

To date, it becomes clear that cells are responsive to the mechanical stimuli from their surrounding environments via a process collectively known as mechanotransduction (**Fig. 4A**). As an adaptive cellular response to the culture environments, cells modulate their phenotypic and functional cell behaviors, such as cell conformation, cell-cell and cell-substrate interactions, and cell migration (Kim & Kino-oka, 2020). Changes of the cell behaviors over time, defined as cell behavioral dynamic, can trigger biochemical signaling and cytoskeletal reorganization, in turn altering the intranuclear modification of epigenetic memory and gene transcriptional expression, and consequently altering the cell properties (Alisafaei et al., 2019; Le et al., 2016). However, the epigenetic memory regulation in cultured hiPSCs and its role in dictating the cell properties has been still less studied. The thesis was thus aimed to elucidate the culture-driven epigenetic memory regulation during expansion process and its role in modulating the state and potential of hiPSCs. This study has been divided into two following chapters (**Fig. 4B**).

Chapter 1 firstly investigates the formation of epigenetic memory during expansion of hiPSCs in general culture conditions. hiPSCs were grown under 2D monolayer culture and 3D aggregate culture in stem cell maintenance medium for 120 h and observed for cell behavioral

changes and cytoskeletal organization. During culture, epigenetic memory formation and pluripotency regulation were evaluated by quantitative analyses of global histone methylation and pluripotency-associated gene expression, respectively. Moreover, the ability of cells to reset and initialize the epigenetic memory that formed in past culture was evaluated by measuring the histone methylation after subculture into new culture vessels and comparing with those before subculture. This chapter would describe the epigenetic memory formation of hiPSCs in 2D and 3D culture conditions and their epigenetic memory initialization after subculture.

Chapter 2 further clarifies the epigenetic memory initialization and consolidation after subculturing the hiPSCs from different growth phases and different initial seeding density cultures. In this chapter, the cells were grown under 2D culture with low and high initial seeding densities in stem cell maintenance medium and the culture time was prolonged until 216 h. The cells at different culture time points were subcultured into new culture vessels and evaluated for the histone methylation to observe the epigenetic memory initialization and consolidation after subculture. In addition, the cells at different culture time points were also investigated for the three-lineage differentiation potential to explicate a relationship between the epigenetic memory in past culture and their subsequent lineage differentiation preference. To summarize, this chapter would examine the epigenetic memory consolidation after subculture from prolonged expansion of hiPSCs.

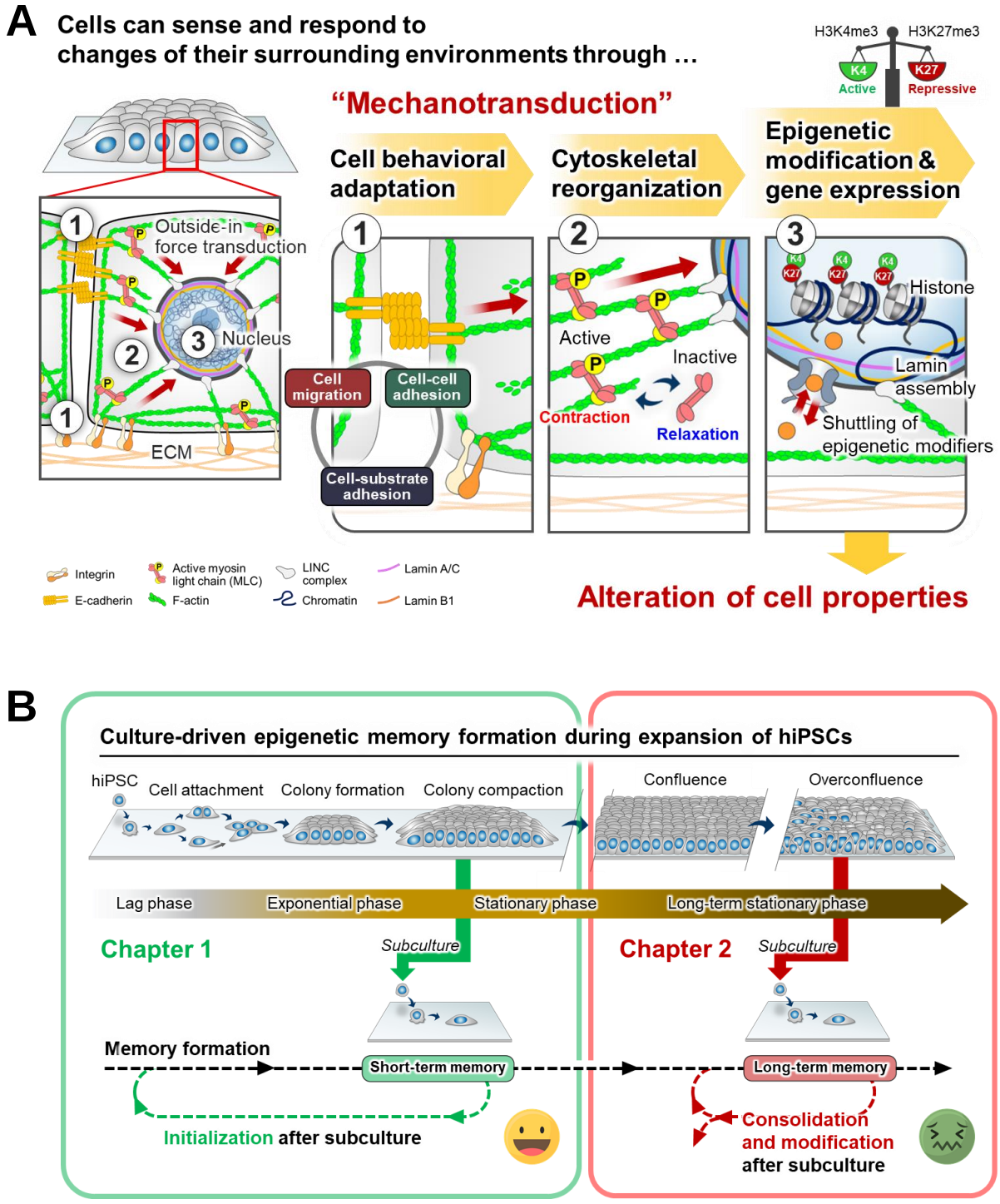

Figure 4 Schematic diagram showing the outline of this study. (A) Plausible influence of culture environments on the intracellular mechanotransduction and epigenetic modification which may contribute to the alteration of hiPSC properties. (B) Chapter outline.

Chapter 1

Investigation of epigenetic memory formation and initialization during cultures of human iPS cells

1.1 Introduction

Cells are basically capable of sensing and responding to the properties of local environment in order to keep their homeostasis (Kshitiz et al., 2016; Shih et al., 2011; Sreenivasappa et al., 2014). Changes in mechanical cues arising in the cellular microenvironment, such as intercellular tension, ECM stiffness, geometric constraint, can be transmitted through mechanosensors at the cell-cell and cell-substrate interfaces, and transduced into biochemical signals and behavioral responses via a mechanotransduction process (Kshitiz et al., 2016; Vining & Mooney, 2017). Inside the cells, one of the key intermediates in mechanotransduction is remodeling of the actomyosin cytoskeletal structure and contractility by regulating actin polymerization and myosin motor activity (Gupta et al., 2015). Since the actomyosin cytoskeleton physically links the cell surface to the nucleus via the linker of nucleoskeleton and cytoskeleton (LINC) complex, alteration of the actomyosin contraction directly exert forces on the nucleus, affecting dynamics of nuclear morphology and intranuclear compartments (Alam et al., 2016; Alisafaei et al., 2019; Chanet et al., 2017). In addition, tensional forces generated by the actomyosin contraction also direct nuclear import and export of diverse epigenetic factors, consequently triggering epigenetic modifications, such as histone methylation, as well as reorganizing the chromatin architecture (Alisafaei et al., 2019; Keeling et al., 2017). Mechanotransduction-induced epigenetic modifications control flexibility of chromatin states to regulate gene transcriptional activation and repression,

permitting the cells to adapt to differential mechanical environments (Ankam et al., 2018; Damodaran et al., 2018).

Prior studies indicated that specific patterns of epigenetic modifications in the cell's DNA and histones can be passed on to next generation cells due to existence of epigenetic memory (Levenson & Sweatt, 2005; Saxton & Rine, 2019). In response to the mechanical cues of cellular environments, the epigenetic modifications can temporarily or permanently alter stem cell features, such as proliferation and fate determination (Crowder et al., 2016; Hazeltine et al., 2013; Killaars et al., 2019, 2020). Despite previous studies showing the effect of culture environments on several properties of cultured cells, less studies explore how they could influence the epigenetic memory regulation of hPSCs as well as their undifferentiated state and differentiation potential during the expansion process, which are considered to be essential for refining critical culture environmental factors and optimizing proper expansion conditions to control the quality of hiPSCs.

The purpose of this chapter is to investigate the effect of different culture conditions including conventional 2D monolayer culture and 3D aggregate culture on the epigenetic memory of hiPSCs during culture and after subculture.

1.2 Materials and methods

1.2.1 Cell line and maintenance culture

The hiPSC line 1383D2 was provided by the Center for iPS Cell Research and Application at Kyoto University (Kato et al., 2019). Cells were routinely maintained on laminin-511 E8 fragment (iMatrix-511; Nippi Inc., Japan)-coated polystyrene culture dishes (0.25 μg/cm^2) in stem cell maintenance medium (StemFit AK02N medium; Ajinomoto, Japan) with a seeding density of 7.5 × 10^3 cells/cm^2. Cells were incubated at 37°C in a humidified atmosphere of 5% CO_2; the medium was changed daily. When hiPSCs reached a confluency level of approximately 80% on day 4 (2.0 to 3.0 × 10^5 cells/cm^2), they were subcultured by treating with 5 mM ethylenediaminetetraacetic acid (EDTA)/phosphate-buffered saline (PBS) with 10 μM of a Rho-associated protein kinase (ROCK) inhibitor (Y-27632; Wako Pure Chemical Industries, Japan) for 10 min at room temperature (RT), and later, a dissociation reagent (TrypLE Select^{TM}; Invitrogen, USA) with 10 μM Y-27632 was added for 7 min at 37°C. Finally, they were resuspended as single cells, re-seeded and cultured in StemFit AK02N medium containing 10 μM Y-27632 for the first 24 h. The culture medium was replaced every day with fresh medium in the absence of Y-27632.

1.2.2 Experimental cultures

hiPSCs were cultured in two different stem cell expansion conditions: 2D monolayer and 3D aggregate cultures. Outlines of experimental cultures and evaluation procedures were shown in **Fig. 1.1**. In 2D monolayer culture, single dissociated cells were seeded at a density of 2.5 × 10^3 cells/cm^2 onto dishes coated with iMatrix-511 (0.25 μg/cm^2). In 3D aggregate culture, single dissociated cells were seeded at a density of 6.0 × 10^5 cells/well (200 cells/aggregate) into micro-space culture plates (Elplasia; Kuraray Co., Ltd., Japan). In both conditions, cells were cultured in StemFit AK02N medium supplemented with 10 μM Y-27632

for the first 24 h after seeding. The culture medium was changed every day with fresh medium without Y-27632. The cultures were further grown for 120 h.

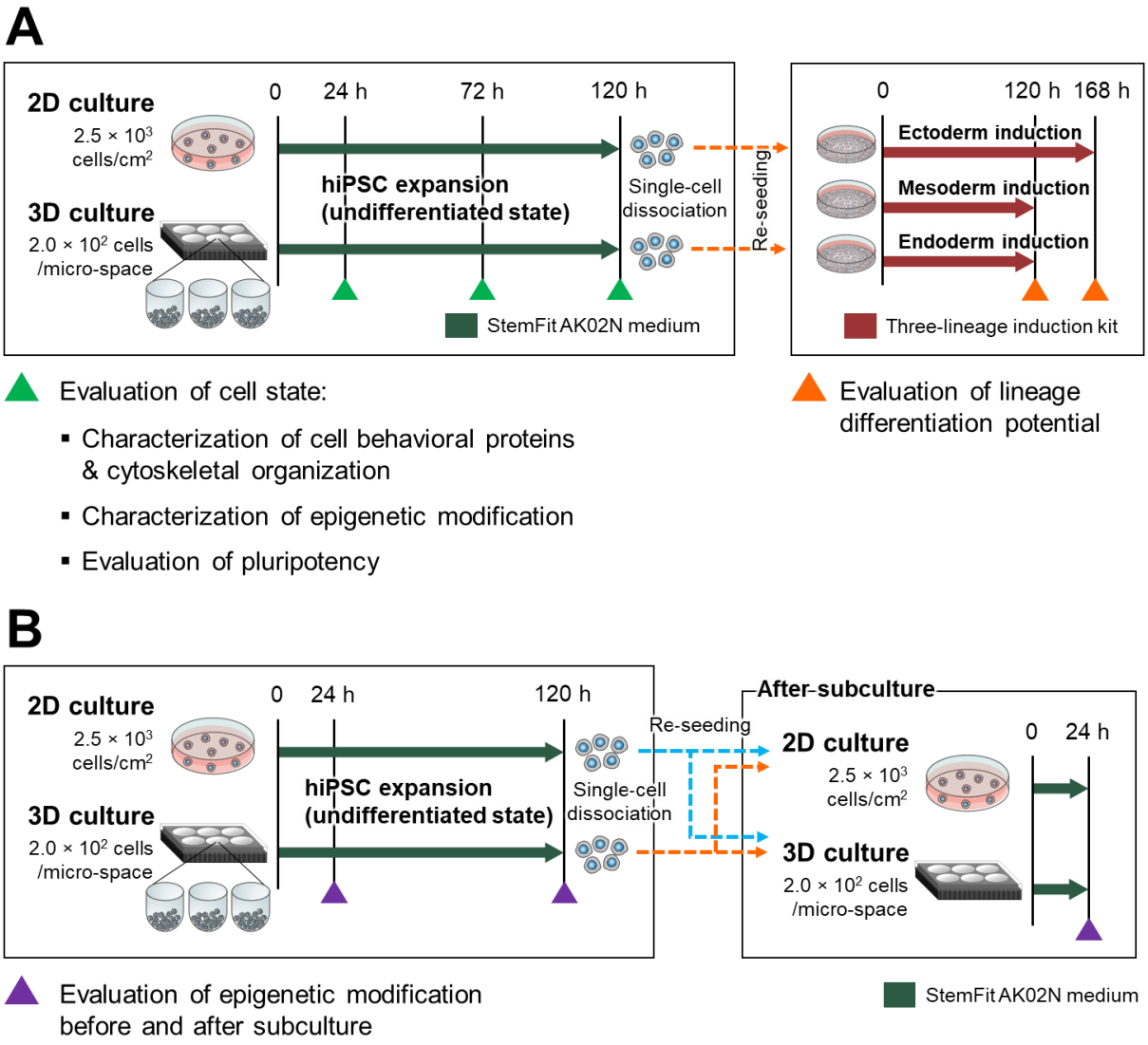

Figure 1.1 Schematic diagram showing the experimental outline in chapter 1. (A) Evaluation of cell behaviors, epigenetic memory, pluripotency, and differentiation potential in 2D and 3D cultures of hiPSCs. (B) Evaluation of epigenetic memory after subculture.

1.2.3 Evaluation of cell proliferative ability

Evaluation of the cell proliferation under 2D and 3D cultures based on two parameters including attachment efficiency (α) and apparent specific growth rate (μ_{app}) was conducted similar to that described previously (Koaykul et al., 2019; Nath et al., 2017). At 24 and 120 h after seeding, cells in 2D and 3D cultures were dissociated into single cells using TrypLE™ Select, and the number of viable cells was counted by trypan blue exclusion assay. The α was calculated as a ratio of the number of viable cells at 24 h (X_{24}) to the number of seeded cells at 0 h. The μ_{app} was calculated using the following equation: $\mu = \ln (X_{120}/X_{24})/\Delta t$, where X_{120} is the number of viable cells at 120 h, and Δt is the differential time of 96 h.

1.2.4 Assay for trilineage differentiation potential

To assess the differentiation potential of hiPSCs, the cells were induced to differentiate into three germ lineages using Stemdiff™ trilineage differentiation kit (StemCell Technologies, Canada). Single dissociated cells obtained at the end of 2D and 3D cultures (120 h) were re-seeded onto plates coated with iMatrix-511 (0.25 μg/cm^2) at a density of 2.0 ×10^5 cells/cm^2 for ectoderm and endoderm differentiation, and 5.0 × 10^4 cells/cm^2 for mesoderm differentiation. According to the manufacturer's instructions, for ectoderm differentiation, cells were plated in Stemdiff™ trilineage ectoderm medium with 10 μM Y-27632. For endoderm and mesoderm differentiation, cells were plated in a maintenance culture medium with 10 μM Y-27632. At the first 24 h after seeding, the media were replaced with each lineage-specific differentiation medium in the absence of Y-27632. The media were changed every day.

1.2.5 Immunofluorescence staining

Immunofluorescence staining was carried out as described previously (Kato et al., 2019). Cells were washed with PBS and fixed with 4% paraformaldehyde (Wako Pure Chemical Industries, Japan). For 2D monolayers, cells were fixed and maintained on the culture plates throughout the staining procedures. For 3D cell aggregates, the fixed aggregates were embedded in optical cutting temperature solution (Tissue-Tek, Sakura Finetek Japan Co., Ltd., Japan) prior to rapid freezing in a liquid nitrogen bath and storage at -80°C. The fixed specimens were sectioned at 10 μm using a cryostat microtome and placed onto glass slides (Leica CM1850, Germany). For sectioned aggregate samples, all following staining procedures were performed in a humidified chamber. The prepared samples from 2D and 3D cultures were then permeabilized with 0.5% Triton X-100 in PBS for 10 min. After blocking with Block Ace solution (Dainippon Sumitomo Pharma Co. Ltd., Japan) for 90 min at RT, the cells were incubated overnight at 4°C with the following primary antibodies: anti-NANOG, anti-phospho-myosin light chain 2, anti-SOX17 (Cell Signaling Technology Inc., USA); anti-brachyury, anti-OCT3/4 (Santa Cruz Biotechnology, USA); and anti-PAX6 (Sigma-Aldrich, USA). The stained cells were rinsed with Tris-buffered saline (TBS) and then incubated with fluorescent-dye conjugated secondary antibodies (Thermo Fisher, USA) for 1 h at RT. After TBS rinses, the cells were stained with 4′,6-diamidino-2-phenylindole (DAPI, Life Technologies, USA) and rhodamine phalloidin (Thermo Fisher, USA) for 30 min at RT to stain the nuclei and F-actin, respectively. Stained samples were visualized by a confocal laser-scanning microscope (FV-1000; Olympus, Japan) with a 60× objective lens.

1.2.6 Protein extraction and western blot analysis

Protein extraction and western blot analysis were performed as described previously (Koaykul et al., 2019). Total proteins from cultured cells (3.0 to 5.0 × 10^6 cells) were extracted by solubilization in radioimmunoprecipitation assay (RIPA) lysis buffer (Sigma, USA) containing protease and phosphatase inhibitor cocktail (Thermo Scientific, USA), whereas nuclear and cytoplasmic proteins were extracted by the Nuclear Extraction Kit (Abcam, USA). Equal amounts of protein (25 to 40 µg protein from the extracted samples) were separated by sodium dodecyl sulphate–polyacrylamide gel electrophoresis (SDS-PAGE) and blotted onto polyvinylidene difluoride (PVDF) membranes (BioRad, USA). The membranes were blocked with 5% ECL blocking agent (GE Healthcare, USA) in TBS for 60 min at RT and incubated overnight at 4°C with the following primary antibodies: anti-β-actin, anti-histone H3, anti-integrin β1, anti-myosin light chain 2, anti-phosphorylated myosin light chain 2 (Ser19), anti-tri-methyl-histone H3 (Lys4), anti-tri-methyl-histone H3 (Lys27) (Cell Signaling Technology Inc., USA); anti-E-cadherin, anti-Rac1, anti-RhoA (Santa Cruz Biotechnology, USA). After rinses with TBS containing 0.1% Tween-20 (TBST), incubation with fluorescent-dye conjugated secondary antibodies (BioRad, USA) was conducted for 1 h at RT, followed by rinses with TBST. The signals were detected using infrared fluorescence with ChemiDoc MP imaging system (BioRad, USA). β-actin, total myosin light chain (MLC), and histone H3 were used as an internal control for sample loading. The signal intensity of target protein bands was normalized to the intensity of the internal loading control for that sample, and then the normalized intensity from each lane was divided by the normalized intensity of the sample in lane 1 in order to compare the relative expression across conditions.

1.2.7 Quantitative reverse transcription-polymerase chain reaction

RNA extraction and quantitative reverse transcription-polymerase chain reaction (qRT-PCR) were conducted as described previously (Koaykul et al., 2019). Total RNA was extracted from the cells (1.0×10^6 cells) using RNeasy mini kit (Qiagen, Germany) and reverse transcribed to cDNA by PrimeScript RT reagent kit (Takara Bio, Inc., Japan) following the manufacturer's protocols. qRT-PCR analysis was performed using SYBR Premix Ex Taq (Takara Bio, Inc., Japan) on a 7300 real-time PCR system (Applied Biosystems, USA). Amplification specificity for each real-time RT-PCR analysis was confirmed by melting curve analysis. Expression of target genes was normalized to the expression of β-actin (*ACTB*) as an internal reference gene, and relative expression was then determined by the $2^{-\Delta\Delta Ct}$ method. The primers used in this study are indicated in **Table 1.1**.

Table 1.1 List of primers used for qRT-PCR in chapter 1

Genes	Forward sequence (5' → 3')	Reverse sequence (5' → 3')
OCT3/4	CAAAACCCGGAGGAGGAGTC	CACATCGGCCTGTGTATATC
NANOG	TGATTTGTGGGCCTGAAGAAAA	GAGGCATCTCAGCAGAAGACA
SOX2	TGGCGAACCATCTCTGTGGT	CCAACGGTGTCAACCTGCAT
FGF4	CGTGGTGAGCATCTTCGGC	GTAGGACTCGTAGGCGTTGT
DPPA5	ATATCCCGCCGTGGGTGAAAGTTC	ACTCAGCCATGGACTGGAGCATCC
KLF5	GCTCACCTGAGGACTCACAC	CTTCATATGCAGGGCCAGGT
DUSP6	TCCCTGAGGCCATTTCTTTCATAGATG	GCAGCTGACCCATGAAGTTGAAGT
SOX11	CCAGGACAGAACCACCTGAT	CCCCACAAACCACTCAGACT

Table 1.1 (continued) List of primers used for qRT-PCR in chapter 1

Genes	Forward sequence (5' → 3')	Reverse sequence (5' → 3')
ZIC2	CATGCACGGTCCACACCTC	CTCATGGACCTTCATGTGCTT
PAX6	TCTTTGCTTGGGAAATCCG	CTGCCCGTTCAACATCCTTAG
OTX2	CAAAGTGAGACCTGCCAAAAAGA	TGGACAAGGGATCTGACAGTG
SOX1	ATGCACCGCTACGACATGG	CTCATGTAGCCCTGCGAGTTG
MAP2	CGAAGCGCCAATGGATTCC	TGAACTATCCTTGCAGACACCT
T	GCAAAAGCTTTCCTTGATGC	ATGAGGATTTGCAGGTGGAC
CDX2	TTCACTACAGTCGCTACATCACCAT	TTGTTGATTTTCCTCTCCTTTGCT
MYH6	CTCAAGCTCATGGCCACTCT	GCCTCCTTTGCTTTTACCACT
NKX2.5	ACCCTGAGTCCCCTGGATTT	TCACTCATTGCACGCTGCAT
SOX17	GAGCCAAGGGCGAGTCCCGTA	CCTTCCACGACTTGCCCAGCAT
FOXA2	GTCCGACTGGAGCAGCTACTA	GTACGTGTTCATGCCGTTCATC
GATA4	ACACCCCAATCTCGATATGTTTG	GTTGCACAGATAGTGACCCGT
GATA6	GCGGGCTCTACAGCAAGATG	ACAGTTGGCACAGGACAATCC
ACTB	AGGCACCAGGGCGTGAT	GCCCACATAGGAATCCTTCTGAC

1.2.8 Statistical analysis

All experimental data are expressed as the mean ± standard deviation (SD). *P*-values were calculated using Student's *t* test to compare means between two groups. Statistically significant differences were considered at a *P*-value of less than 0.05 or 0.01.

1.3 Results

1.3.1 Morphological and growth phenotypes of hiPSCs in 2D and 3D cultures

To examine the behavioral adaptation and growth process of hiPSCs under 2D and 3D expansion cultures, single dissociated cells were cultivated as 2D monolayers on iMatrix-511 coated dishes or as 3D aggregates in micro-space cell-culture plates, and later observed by time-course and time-lapse phase contrast microscopy. After seeding, hiPSCs in 2D culture adhered and spread on the substrate (**Fig. 1.2A**). Single cells migrated randomly and came into contact with other surrounding cells. After forming intercellular connection, the cells collectively migrate as an epithelial colony. Cell colonies grew and spontaneously fused with nearby clusters until near confluence at 120 h. In contrast, cells in 3D culture initially settled into each micro-space by gravity and gathered on the bottom of micro-spaces. In the first 24 h, cells self-assembled to form 3D aggregates, and the aggregates showed their smooth surface and regular spherical structure (**Fig. 1.2B**). The aggregates gradually expanded in size and became highly compact with rougher surface until 120 h. Attachment efficiency (α) and apparent specific growth rate (μ_{app}) were used to measure cell proliferation ability in 2D and 3D cultures. Compared with those in 2D culture, the values of α (**Fig. 1.2B**) and μ_{app} (**Fig. 1.2C**) of cells in 3D culture were significantly 1.8- and 2.0-fold lower, respectively, revealing the influence of culture platforms on growth properties of hiPSCs.

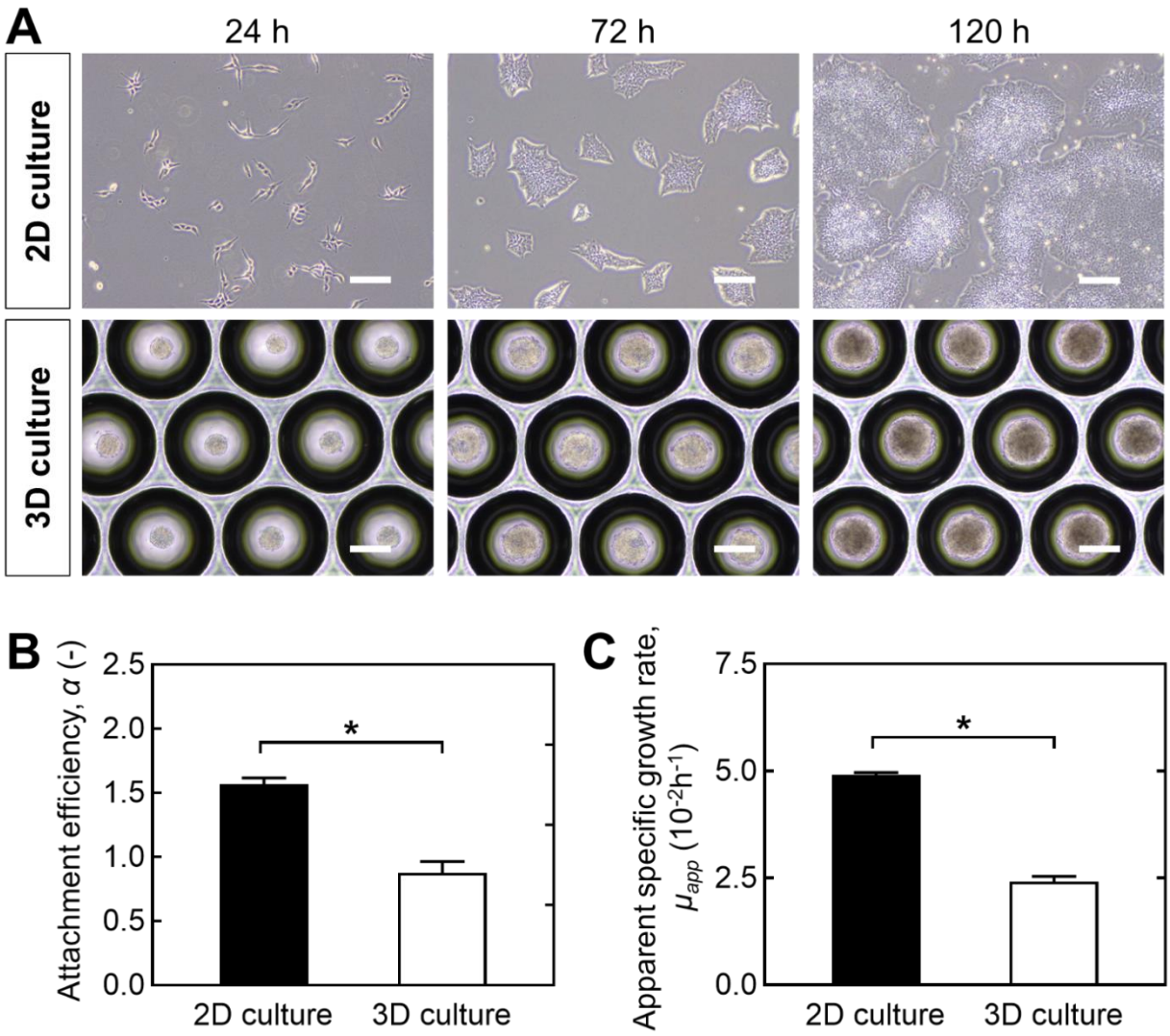

Figure 1.2 Differences in cell morphology and proliferation of hiPSCs under 2D monolayer culture and 3D aggregate culture conditions. (A) Observation of cell morphology by phase-contrast microscopy during 2D and 3D cultures. Scale bars, 200 μm. (B) Attachment efficiency and (C) apparent specific growth rate. The data are shown as mean ± SD (n = 3). * P-value < 0.01, compared between 2D and 3D cultures.

1.3.2 Regulation of cell behaviors in different culture conditions

To further clarify the behavioral characteristics of hiPSCs in the different culture conditions, protein expression of two cell adhesion-mediated molecules (E-cadherin and integrin β1) and two members of the Rho family GTPases (Rac1 and RhoA) was evaluated by western blot analysis. Cell adhesion molecules E-cadherin and integrin β1 were expressed within the first 24 h after seeding; however, changes of the two adhesion protein levels over culture time were found not statistically significant in each culture condition (**Fig. 1.3A**). Compared to that in 3D culture, the expression of integrin β1 was significantly 3.0-fold higher in 2D culture at 120 h, while there was no difference of E-cadherin levels between 2D and 3D cultures.

In addition, the quantitative analysis of Rac1 and RhoA exhibited distinct time-dependent changes in the expression among the two culture conditions (**Fig. 1.3B**). In 2D culture, from 24 to 72 h, the expression of Rac1 was slightly increased, while the expression of RhoA was maintained. At 120 h, the expression of both Rac1 and RhoA was found significantly upregulated. In 3D culture, the expression of Rac1 was maintained at relatively low levels throughout the culture period, while the expression of RhoA was found highly upregulated at 72 and 120 h. Comparison of the protein expression between conditions indicated that cells in 3D culture kept the Rac1 expression at relatively low level, while the cells in 2D culture dramatically increased the level of Rac1 from 24 to 120 h, resulting in its significantly 2.4-fold higher level than that in 3D culture at 120 h. On the contrary, the cells in 3D culture exhibited an earlier upregulation of RhoA, showing its significantly 2.2-fold higher level than that in 2D culture at 72 h; however, the expression of RhoA in two culture conditions finally reached a similar level at the end of culture period (120 h). These results demonstrate the dynamics of cell behavioral regulation during cell expansion in 2D and 3D cultures.

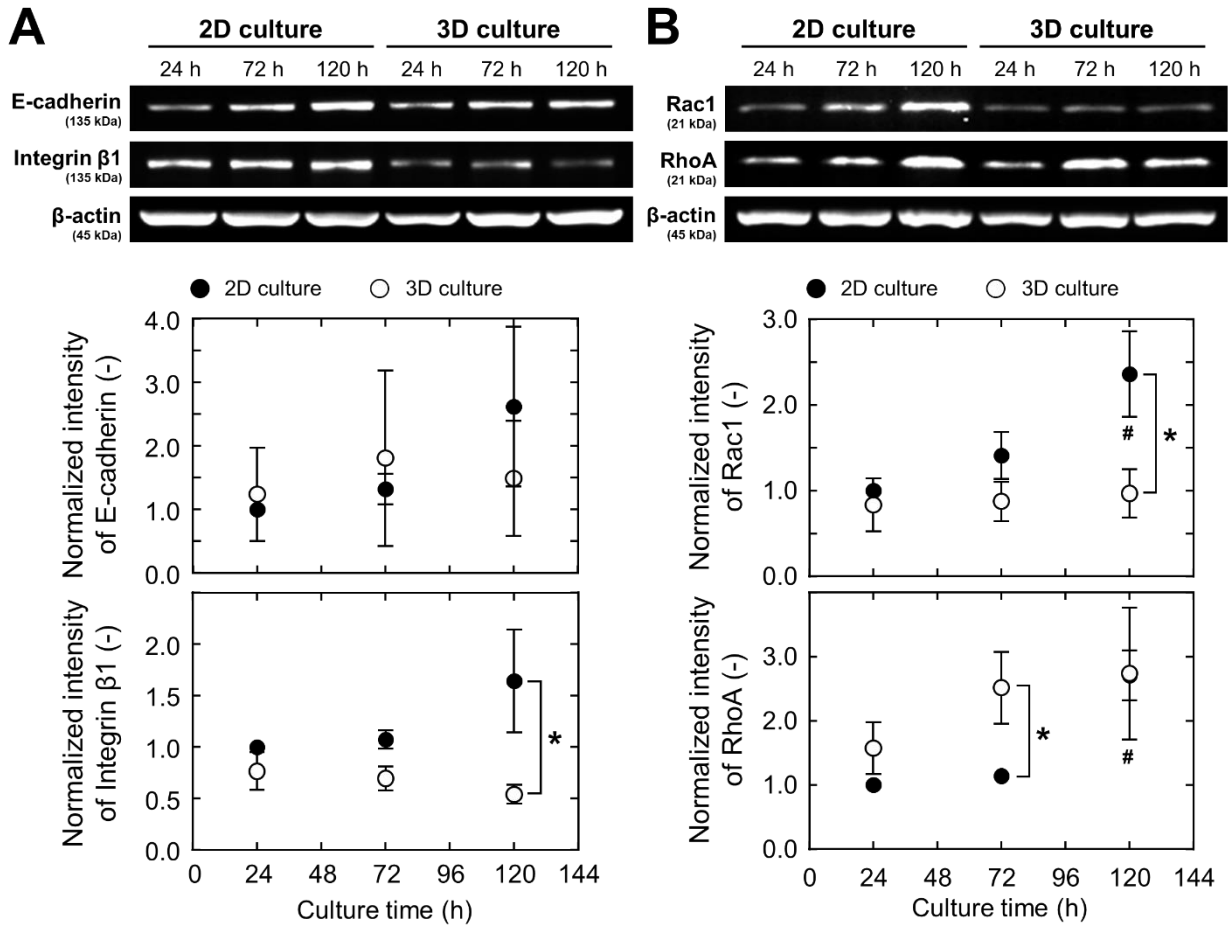

Figure 1.3 Dynamic regulation of protein expression associated with cell behaviors during 2D and 3D cultures of hiPSCs. Western blot images and quantitative analysis of (A) E-cadherin and integrin β1, and (B) Rac1 and RhoA. The intensity of each target protein was normalized to that of β-actin. The data are shown as mean ± SD (n = 3). $^{\#,*}$ P-value < 0.05, compared with that measured at 24 h ($^{\#}$), compared between 2D and 3D cultures at the same time points (*).

1.3.3 Culture-induced rearrangement of actomyosin cytoskeleton

As the arrangement of actomyosin cytoskeleton is critical for cell mechanics and force distribution, and has been shown to be strongly cooperated with cell morphological and behavioral changes (Alisafaei et al., 2019; Keeling et al., 2017), the organization of actomyosin cytoskeleton in hiPSCs during expansion under 2D and 3D cultures were investigated. Firstly,

localization of the actomyosin cytoskeleton was observed by immunofluorescence staining of its two key components including filamentous actin (F-actin) and phosphorylated myosin light chain (pMLC), an activated part of myosin motor protein (**Fig. 1.4**).

At the early time point after seeding, hiPSCs in 2D culture displayed long-branched projections of F-actin elongated from the cell body with large spread areas of the cells (**Fig. 1.4A**) and flattened cell nuclei detected in *XZ* cross-sections (**Fig. 1.4A2**). pMLC was found highly colocalized with the F-actin especially at the cell periphery (**Fig. 1.4A1**). From 72 h to the end of culture period, cell colonies exhibited a polarized organization of the actomyosin cytoskeleton along the apical-basal axis as shown in *XZ* cross-sections (**Fig. 1.4B-C**). Thick bundles of actin filaments were aligned as a continuous belt underlying apical intercellular junctions and colocalized with the circumferential myosin enrichment (**Fig. 1.4B1-C1**). Compared with that at 72 h, structural alignment of F-actin at 120 h was found more complex, and the cortical myosin showed its poorly organized distribution across the apical domain of actomyosin networks (**Fig. 1.4B2-C2**). Cell nuclei were in close proximity to each other, and their shape turned to be prolate ellipsoid within densely packed areas of the 2D monolayers.

In 3D culture, initial cell aggregation at 24 h showed formation of cell-cell contacts with thick branched actin networks partially colocalized with pMLC at the cell cortex (**Fig. 1.4D**), while the cells maintained a spheroid shape of cell nuclei within the loosely aggregated structure. At 72 h, cell expansion and cytoskeletal rearrangement appeared to lead to a more compact structure of 3D aggregates (**Fig. 1.4E**). Cells at the periphery of aggregates showed a spontaneous assembly of actin bundle rings with an abundance of the pMLC (**Fig. 1.4E-F**). Inside the aggregates, complex, highly branched networks of actomyosin cytoskeleton in the absence of polarization continued to grow at the cell-cell boundaries (**Fig. 1.4 E1-F1**). Cells became elongated and stretched. The nuclei were also found to deform in the same fashion as that of the cells until 120 h (**Fig. 1.4E2-F2**).

In addition, western blotting of pMLC and total MLC was performed to quantitatively compare the myosin motor activity in cells under 2D and 3D cultures (**Fig. 1.5**). The analysis demonstrated that the ratio of pMLC per total MLC levels was reduced over time in 3D culture, and the phosphorylation ratios at 72 and 120 h in 3D culture was significantly 2.0- and 2.7-fold lower than those in 2D culture, respectively.

Overall, the results indicated that hiPSCs are responsive to the different culture conditions and subsequent behavioral changes along culture time by distinctly reorganizing the structural orientation of actomyosin cytoskeleton as well as regulating the activation of myosin motor activity.

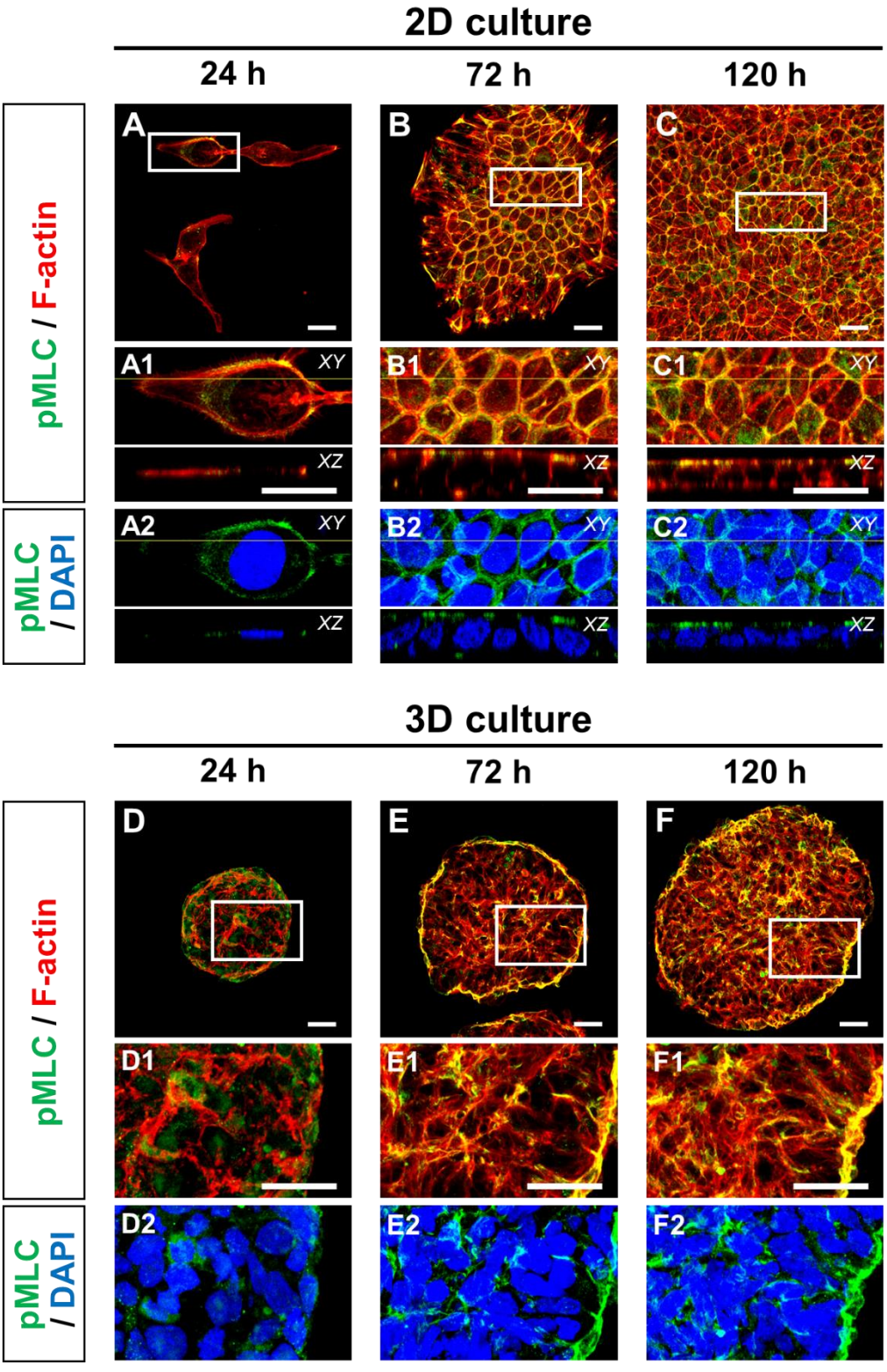

Figure 1.4 Organization of actomyosin cytoskeleton during (A-C) 2D culture and (D-F) 3D culture of hiPSCs. Fluorescence staining images of phosphorylated myosin light chain (pMLC; green) and filamentous actin (F-actin; red) towards cell nuclei (DAPI; blue). Zoom-in images

of the regions with white border are presented in the bottom panels (A1-F1 and A2-F2). *XY* confocal optical sections taken in a plane parallel to the culture substrate. *XZ* confocal optical cross-sections taken in a plane perpendicular to the culture substrate. Scale bars, 25 μm.

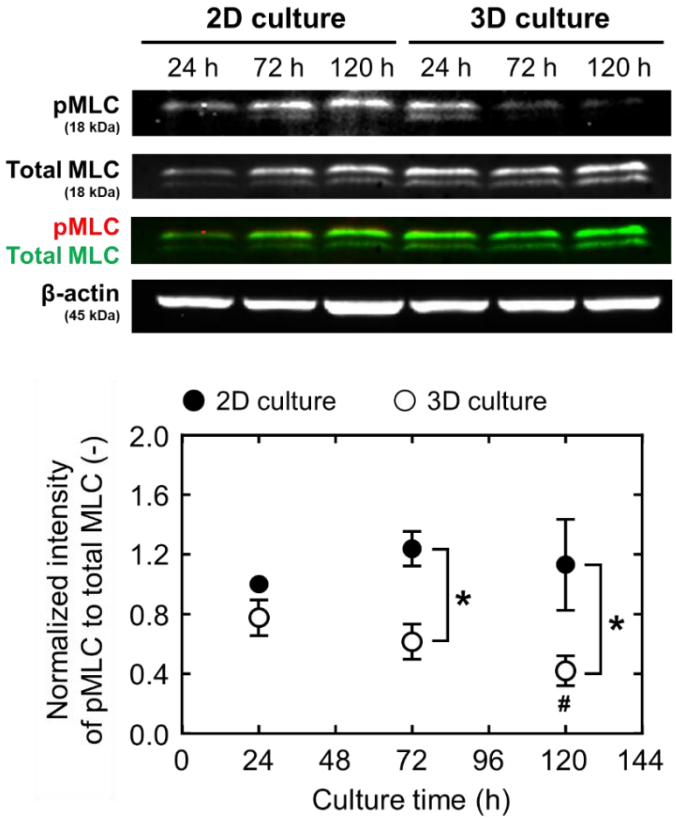

Figure 1.5 Regulation of myosin phosphorylation during 2D and 3D cultures of hiPSCs. Western blot images and quantitative analysis of pMLC. The intensity of pMLC was normalized to that of total MLC. The data are shown as mean ± SD (n = 3). $^{\#,*}$ P-value < 0.05, compared with that measured at 24 h ($^{\#}$), compared between 2D and 3D cultures at the same time points (*).

1.3.4 Epigenetic memory formation and initialization in 2D and 3D cultures

Next, hiPSCs under 2D and 3D cultures were observed for the epigenetic regulation by measuring the global levels of two key bivalent epigenetic marks, H3K4me3 and H3K27me3, which are known to reciprocally control pluripotent state and differentiation potency of pluripotent stem cells (Grandy et al., 2016), by western blotting (**Fig. 1.6**).

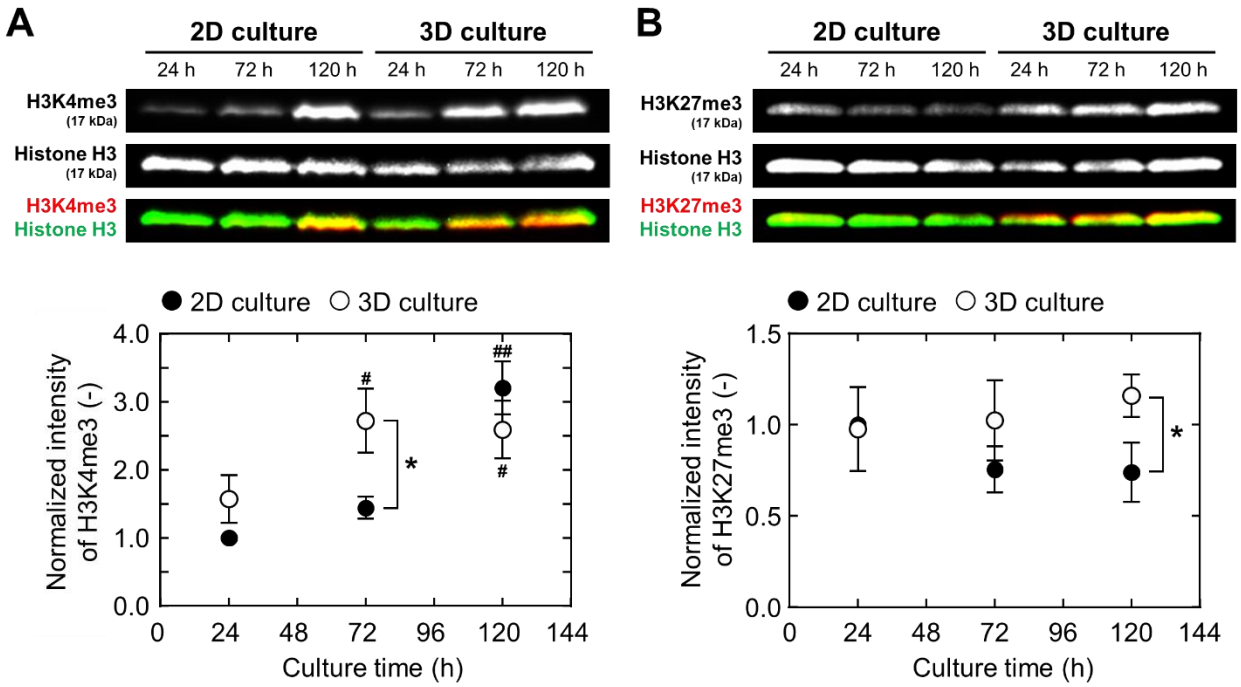

Figure 1.6 Profiles of global H3K4me3 and H3K27me3 during 2D and 3D cultures of hiPSCs. Western blot images and quantitative analysis of (A) H3K4me3 and (B) H3K27me3. The intensity of each target protein was normalized to that of histone H3. The data are shown as mean ± SD (n = 3). $^{\#,*}$ P-value < 0.05, compared with that measured at 24 h ($^{\#}$), compared between 2D and 3D cultures at the same time points (*).

In 2D culture, the active histone mark H3K4me3 was found to be sustained at relatively low levels from 24 to 72 h, and its level was significantly increased at 120 h (**Fig. 1.6A**). Oppositely, the repressive histone mark H3K27me3 was highly detected at 24 h after seeding,

while its level was considerably reduced from 24 to 72 h, and maintained until 120 h (**Fig. 1.6B**). In 3D culture, H3K4me3 level at 24 h was comparable to that in 2D culture; however, its level was found earlier upregulated from 72 h (**Fig. 1.6A**). At the end of culture period (120 h), the levels of H3K4me3 in both 3D and 2D cultures were at relatively high and not significantly different (**Fig. 1.6A**). Remarkably, H3K27me3 levels were maintained along the culture time in 3D culture, and the H3K27me3 level in 3D culture at 120 h was found significantly 1.6-fold higher than that in 2D culture at the same time point (**Fig. 1.6B**).

Moreover, the modifications of epigenetic memory differently obtained in 2D and 3D cultures were further examined for the ability of memory initialization after subculture. hiPSCs in 2D and 3D cultures at 120 h were dissociated into single cells and re-seeded into both 2D and 3D culture conditions (**Fig. 1.7A**). Levels of H3K4me3 and H3K27me3 were then measured in the cells at 24 h after subculture by western blotting (**Fig. 1.7B**). In the cells from 2D culture, the levels of H3K4me3 and H3K27me3 after subculture into both 2D and 3D cultures were reset to the same levels as detected before subculture at 24 h (baseline levels), defined by epigenetic memory initialization (**Fig. 1.7C-D**). Likewise, the cells collected from 3D culture also showed the initialization of H3K4me3 and H3K27me3 levels at 24 h after subculture into 2D and 3D cultures (**Fig. 1.7E-F**)

Taken together, the results unraveled differences in the epigenetic memory formation of hiPSCs regarding the culture conditions and culture durations. The distinct states of epigenetic memory in past culture under the defined culture conditions can be initialized after subculture.

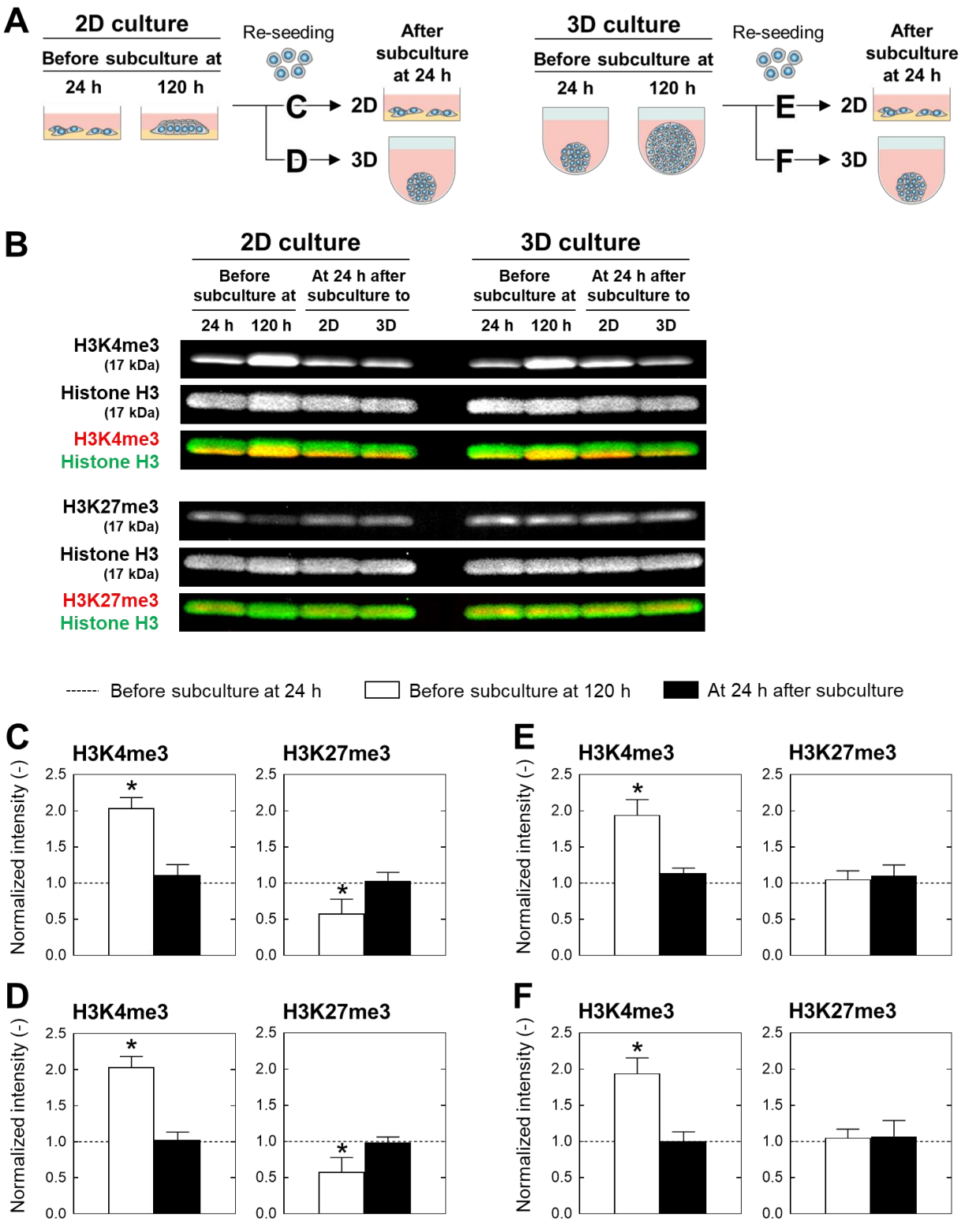

Figure 1.7 Profiles of global H3K4me3 and H3K27me3 after subculture from 2D and 3D cultures of hiPSCs. (A) Schematic diagram showing the experimental procedures used for evaluating epigenetic memory before and after subculture. (B) Western blot images of

H3K4me3 and H3K27me3. Quantitative analysis of H3K4me3 and H3K27me3 before subculture and at 24 h after subculture from 2D culture to (C) 2D and (D) 3D cultures, and from 3D culture to (E) 2D and (F) 3D cultures. The intensity of each target protein was normalized to that of histone H3. The data are shown as mean ± SD (n = 3). * P-value < 0.05, compared the normalized intensity at each time point to that before subculture at 24 h, the baseline value.

1.3.5 Pluripotent state and differentiation potential of hiPSCs in 2D and 3D cultures

To examine the regulation of pluripotent states in hiPSCs under 2D and 3D culture conditions, hiPSCs were grew in stem cell maintenance medium for 120 h and then the expression of pluripotency-associated markers was evaluated by qRT-PCR and immunofluorescence staining.

At 120 h after cell expansion, the mRNA expression of a core pluripotency-associated gene *OCT3/4* in 3D culture was found significantly 1.5-fold higher than that in 2D culture, while the expression of *SOX2* in 2D culture was significantly 1.5-fold higher than that in 3D culture (**Fig. 1.8A**). The expression of *NANOG* in 2D and 3D cultures were at comparable levels. Results of immunofluorescence staining indicated that OCT3/4 and NANOG were detected among the cell population in both culture conditions (**Fig. 1.8B**).

Additionally, the analysis of pluripotency was extended to evaluate the plasticity of pluripotent states in hiPSCs by measuring the mRNA expression of naïve pluripotency-associated genes (*FGF4*, *DPPA5* and *KLF5*) and primed pluripotency-associated genes (*DUSP6*, *SOX11* and *ZIC2*). Strikingly, the results showed that cells under 2D and 3D cultures obtained distinct transcriptional states of pluripotency (**Fig. 1.8A**). In comparison to that in 2D culture, the expression of *FGF4*, *DPPA5*, and *KLF5* was significantly 4.0-, 1.7- and 1.5-fold

higher in 3D culture, respectively. In contrast, the expression of *DUSP6, SOX11* and *ZIC2* was significantly 10.0-, 1.2- and 1.3-fold higher in 2D culture, respectively.

To further investigate the differentiation potential of hiPSCs obtained from 2D and 3D culture conditions, the cultured cells at 120 h were dissociated into single cells and subjected to three-lineage differentiation assay (ectoderm, mesoderm, and endoderm). The differentiation was evaluated by measuring the mRNA expression of lineage-specific genes and immunofluorescence staining of lineage-specific markers. Almost all the mesoderm and endoderm genes showed similar expression levels between lineage-induced cells from 2D and 3D cultures (**Fig. 1.9A**) in agreement with the immunofluorescence staining data displaying the expression patterns of brachyury (mesoderm) and SOX17 (endoderm) (**Fig. 1.9B**). However, after ectoderm induction, cells from 2D culture showed significantly 4.2- and 1.8-fold higher mRNA expression of *PAX6* and *MAP2* than that from 3D culture (**Fig. 1.9A**), in addition, differences in PAX6 expression among differentiated cell population were observed between cells from different culture conditions (**Fig. 1.9B**).

In conclusion, the pluripotent state of hiPSCs under 2D and 3D culture conditions was attuned through regulating the transcriptional expression of naïve and primed pluripotency-associated genes. After three-lineage differentiation induction, the ectoderm gene expression was moderated in the cells from 3D culture, while the mesoderm and endoderm gene expression were similarly maintained in the cells from different culture conditions.

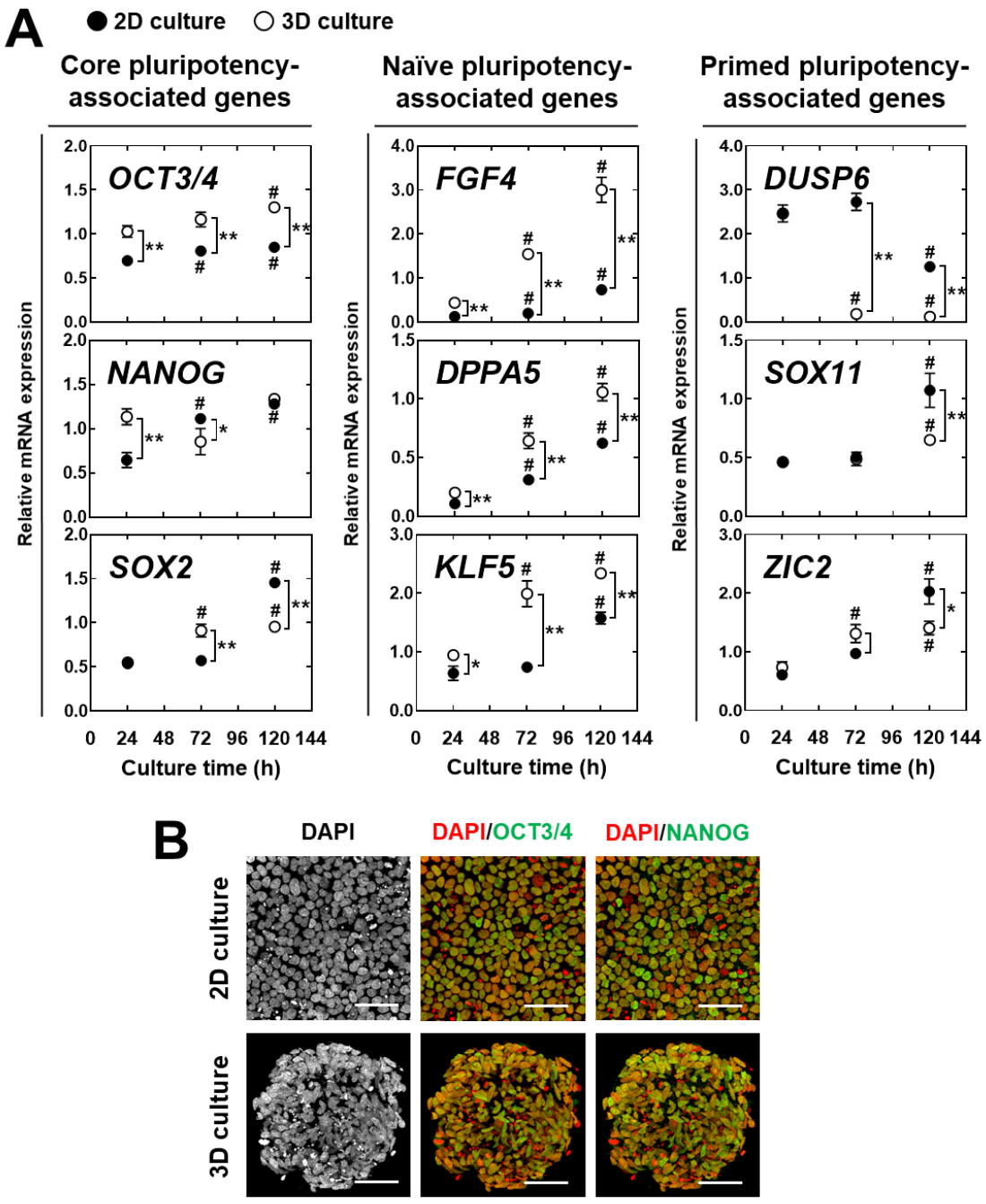

Figure 1.8 Characterization of pluripotency of hiPSCs in 2D and 3D cultures. (A) Relative mRNA expression of core, naïve, and primed pluripotency-associated genes in hiPSCs. (B) Fluorescence staining images of OCT3/4 and NANOG towards cell nuclei (DAPI) in hiPSCs cultured for 120 h. Scale bars, 200 μm. The mRNA expression of each target gene was normalized to that of β-actin. The data are shown as mean ± SD (n = 3). * P-value < 0.05, ** P-value < 0.01, compared between 2D and 3D cultures.

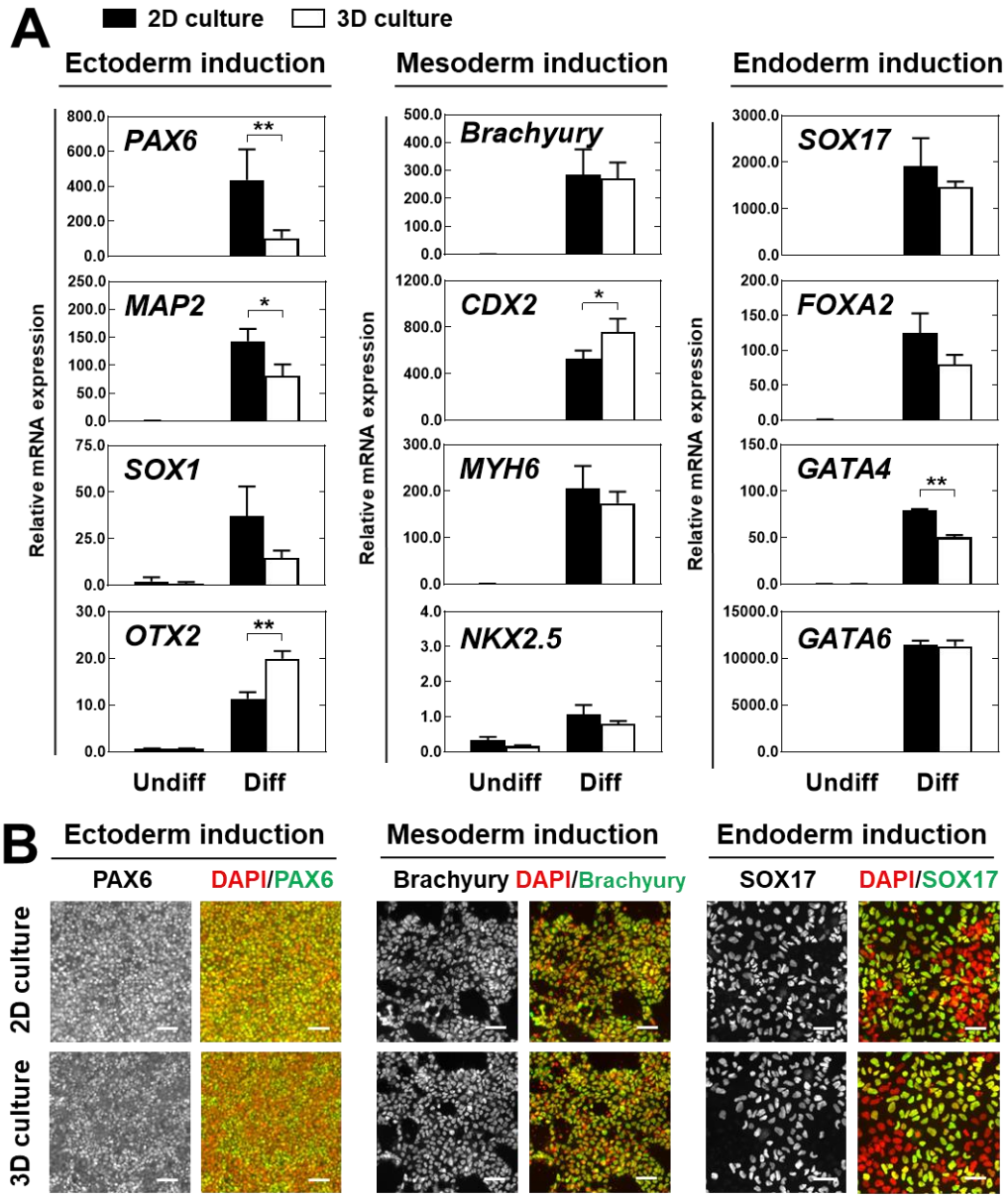

Figure 1.9 Characterization of differentiation potential of hiPSCs obtained from 2D and 3D cultures. (A) Relative mRNA expression of lineage-specific genes in hiPSCs differentiated into ectoderm, mesoderm, and endoderm (Diff), compared with their undifferentiated state (Undiff). (B) Fluorescence staining images of differentiation markers, including PAX6, brachyury, and SOX17, towards cell nuclei (DAPI) in hiPSCs differentiated into ectoderm, mesoderm, and endoderm. Scale bars, 200 μm. The mRNA expression of each target gene was normalized to that of β-actin. The data are shown as mean ± SD (n = 3). * P-value < 0.05, ** P-value < 0.01, compared between 2D and 3D cultures.

1.4 Discussion

Epigenetic memory regulation represents a mechanism of cellular adaptation in response to the culture environmental perturbations (Jain et al., 2013; Kim et al., 2018). The impact of culture conditions on the modulation of cell behaviors, epigenetic memory, and cell quality in hiPSCs was explained as follows:

1.4.1 Regulation of cell behaviors and cytoskeletal contractility in hiPSCs under 2D and 3D culture conditions

hiPSCs responded to different physiological and mechanical properties of cellular environments by distinctly regulating their adhesive and migratory behaviors. The differences in temporal and spatial regulation of cell-cell and cell-substrate adhesion among cells in 2D and 3D environments result in distinctive force distribution and magnitude of physical constraints acting on the cells. In 2D culture, dynamic coordination between cell-substrate and cell-cell interaction reinforces the synchronous and collective cell migration (Aranjuez et al., 2016). During cell migration, activation of Rho GTPase members induced by force transduction in the cell populations is necessary to direct membrane protrusion and cell movement (Das et al., 2015; Mishra et al., 2019). The upregulation of both Rac1 and RhoA observed in 2D culture might indicate the balance of Rac/Rho GTPase antagonism controlling myosin-based cytoskeletal contraction in the migrating cell collectives. Moreover, results here revealed that 2D colonies of hiPSCs kept an intact assembly of actomyosin cortex with apical-basal polarization along cell-cell contacts (**Fig. 1.4B-C**), consistent with the maintenance of myosin motor protein activation over time in 2D culture quantitated by western blotting (**Fig. 1.5**). Regulation of actomyosin-based relaxation and contraction is likely responsible for the dynamic and synergistic behavioral profiles of cells in 2D monolayers.

In contrast to 2D culture, physical limits in confined 3D environments moderate capability of the cells to produce cell protrusions, thereby restricting cell migratory behavior

(Guetta-Terrier et al., 2015; Van Helvert et al., 2018; Wolf et al., 2013). Cell motility and structural dynamics in 3D culture are mainly driven by passive transduction of compressive and contractile forces from the surrounding matrix and intercellular interaction in alliance with deformation of each individual cell (Khatau et al., 2012; Lange & Fabry, 2013; Yamada & Sixt, 2019). The results showed that hiPSCs in 3D culture sustained cadherin-based cell-cell adhesion, whereas reduced the integrin-based cell-substrate adhesion, compared to that in 2D culture (**Fig. 1.3A**). Additionally, RhoA was highly activated, while Rac1 was detected at relatively low levels during 3D culture. In 3D cell structures, actomyosin contraction is essential to aid cell-cell interactions and also create outside-in force transduction, enhancing spheroid integrity and compactness (Dolega et al., 2017; Sodek et al., 2009). Visualization of actomyosin cytoskeleton in 3D culture of hiPSCs (**Fig. 1.4E-F**) demonstrated that formation and accumulation of actomyosin bundles at the periphery of cell aggregates were associated with their structural development and compaction during culture, moreover, these underlined a spatial regulation of actomyosin-generated contraction by which the mechanical forces were transmitted from the outer towards the inner parts of cell aggregates. Compared with 2D culture, the reduction of myosin activation during the late phase of 3D culture (**Fig. 1.5**) was in line with the moderation and partial colocalization of F-actin and myosin detected inside cell aggregates (**Fig. 1.4E-F**). In comparison with the behavioral regulation in 2D monolayer culture, the structural integrity and tensional homeostasis in 3D cell aggregates might be supported by the maintenance of intercellular adhesion and the reorganization and relaxation of actomyosin cytoskeleton in a spatiotemporal manner.

1.4.2 Culture-driven epigenetic memory formation and its initialization after subculture

Epigenetic memory modification can be driven by modulation of cytoskeletal contractility, in turn regulating the properties of cultured cells (Alisafaei et al., 2019). The

actomyosin cytoskeleton-generated intracellular tension can modify organization of nucleocytoskeleton and nuclear translocation of epigenetic regulatory proteins, concertedly reorganizing the epigenetic and chromatin states as well as gene transcriptional profiles (Jain et al., 2013; Sao et al., 2019). Histone methylation H3K4me3 and H3K27me3 are recognized as two key epigenetic signatures directly determining stem cell pluripotency and cell fate decisions (Grandy et al., 2016; Harvey et al., 2019). Specific epigenetic modifications and transcriptional switches of pluripotency-associated genes have been found relevant to the plasticity of pluripotent states in cultured hPSCs (Leitch et al., 2013; Theunissen et al., 2016; Tosolini et al., 2018).

In this chapter, hiPSCs in 2D and 3D cultures exhibited distinct epigenetic memory formation described by the upregulation of H3K4me3 with downregulation of H3K27me3 in 2D culture, and the earlier upregulation of H3K4me3 level with persistence of relatively high H3K27me3 level in 3D culture (**Fig. 1.6**). Compared with cells in 2D culture, the cells in 3D culture with different epigenetic memory status showed the higher expression of naïve pluripotency-associated genes, while sustained the expression of core pluripotent genes (**Fig. 1.8**). In agreement with the relationship between epigenetic memory formation and pluripotency regulation in this current study, prior investigation demonstrated that elevation of global H3K27me3 in hESCs under a naïve culture condition has been linked with a cellular mechanism preventing transition into a lineage-priming state (De Clerck et al., 2019; van Mierlo et al., 2019). The epigenetic memory formed during culture under defined expansion conditions in this chapter has been hypothesized to be convertible, supporting capability of the memory initialization after subculture into new culture environments as shown in **Fig. 1.7**. In consistent with the obtained results, previous studies revealed that epigenetic memory modified in a specific culture condition could be reversible or irreversible depended on time of exposure to the culture environment (Killaars et al., 2019; Li et al., 2016). Taken together, this chapter

annotates the culture-driven epigenetic memory formation during expansion of hiPSCs under 2D monolayer and 3D aggregate cultures, and shows that the cells cultured in these defined conditions could reset the acquired memory from past culture and initialize it after subculture (**Fig. 1.10**). These are critical to further understand how the hiPSC properties could be regulated and maintained during the culture process.

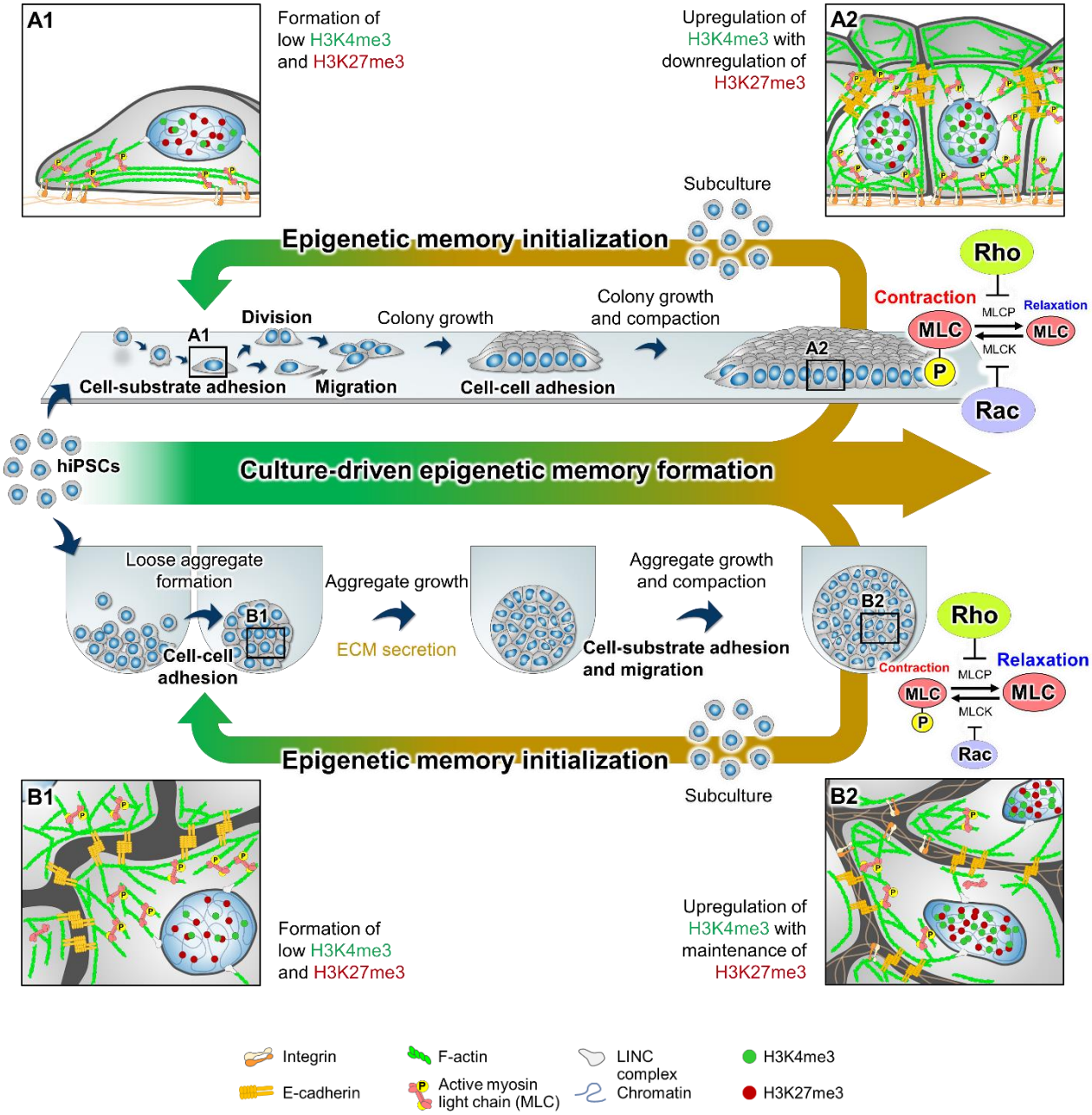

Figure 1.10 Schematic diagram showing epigenetic memory formation during cell expansion and epigenetic memory initialization after subculture in 2D and 3D cultures of hiPSCs.

1.5 Chapter summary

This chapter demonstrates the effect of different culture conditions on the epigenetic memory regulation in hiPSCs. Quantitative analysis of global histone methylation revealed that cells in 2D culture upregulated active H3K4me3 mark and downregulated repressive H3K27me3 mark, whereas the cells in 3D culture significantly earlier upregulated the H3K4me3 but constantly maintained the H3K27me3. After subculture into new culture vessels, the cells collected from both 2D and 3D cultures revealed their ability to reset and initialize the epigenetic memory to baseline levels detected in the initial culture period before subculture. Moreover, compared to cells in 2D culture, the cells in 3D culture demonstrated distinct transcriptional activation of naïve pluripotency signatures. Overall, the obtained findings in this chapter indicate the epigenetic memory formation during expansion of hiPSCs and its initialization after subculture.

Chapter 2

Investigation of epigenetic memory consolidation in prolonged cultures of human iPS cells

2.1 Introduction

Expansion process poses a great challenge for regenerative therapeutic application of hiPSCs. It is critical to ensure proper maintenance of pluripotency and differentiation propensity in the expanded and passaged cells (Cruvinel et al., 2020; Horiguchi & Kino-oka, 2021). The cellular functions are crucially affected by culture environments through adaptive mechanotransduction and epigenetic mechanisms (Hazeltine et al., 2013; Ireland & Simmons, 2015). Changes in the cellular environments and mechanotransduction could dictate cytoskeletal contractility and mechanical nuclear properties, such as nucleoskeletal structure, in turn rearranging intranuclear chromatin organization and accessibility as well as altering gene transcriptional profiles (Boyer et al., 2006; Keller et al., 2018; Meissner, 2010).

The chromatin of PSCs has a dynamic epigenetic plasticity that allows activation or repression of developmental genes, consequently retaining self-renewal or permitting lineage commitment (Atlasi & Stunnenberg, 2017; Spivakov & Fisher, 2007). Acquisition of the active H3K4me3 mark have been shown to be associated with gene expression involved in housekeeping cellular functions, such as cell division and protein transport, and specific pluripotency-related functions in PSCs (Bogliotti et al., 2018; Grandy et al., 2016). Activation of hallmark pluripotency transcription factors including *OCT3/4*, *SOX2* and *NANOG* genes safeguards an undifferentiated state as these pluripotent regulators simultaneously occupy the promoters of differentiation genes, in turn restricting their transcription (Boyer et al., 2005; Hammachi et al., 2012). In concert with the regulation of transcription factors, deposition of

bivalent histone marks characterized by presence of both active H3K4me3 and repressive H3K27me3 marks at gene promoters is responsible for keeping the differentiation genes in a poised state, preventing precocious expression but allowing the genes to be primed for future activation (Grandy et al., 2016; Liu et al., 2016). Along the progression of stem cell growth and division, epigenetic memory governs the inheritance of epigenetic patterns from parent cells to daughter cells (Levenson & Sweatt, 2005; Saxton & Rine, 2019). Alteration of the epigenetic signatures induced by past culture experiences might dysregulate the memory mechanism, fluctuating the cell quality following expansion process (Killaars et al., 2019). Recent studies evidenced that stem cells can imprint information with regards to past culture environments as a reversible or irreversible memory, and that can instruct future environmental sensitization and fate decisions of the cultured cells (Killaars et al., 2019; Lee et al., 2014; Li et al., 2016; Yang et al., 2014). Hence, a unique regulatory pattern of epigenetic modification and inheritance might be at the heart of stabilizing the cellular properties in cultures of PSCs. Although these previous studies have revealed the importance of epigenetic regulation in preserving the cell identity and its heritability during culture, the influence of past culture experiences regarding different growth phases and time spent in culture on the epigenetic memory after subculture and the subsequent cell properties has not yet been elucidated.

This chapter aimed to clarify whether the epigenetic memory formation with respect to different growth phases and time spent in past culture could be consolidated after subculture, and how the epigenetic memory formed in past culture affects the subsequent lineage differentiation of hiPSCs.

2.2 Materials and methods

2.2.1 Cell line and maintenance culture

The hiPSC line 1383D2 provided by the Center for iPS Cell Research and Application at Kyoto University was routinely maintained on iMatrix-511 (Nippi Inc., Japan)-coated polystyrene culture dishes (0.25 μg/cm^2) in stem cell maintenance medium (StemFit AK02N medium; Ajinomoto, Japan) with a seeding density of 7.5 × 10^3 cells/cm^2. Cells were incubated at 37°C and 5% CO_2 in a humidified atmosphere. The medium was changed daily. Cells were subcultured after reaching a confluency of about 80% (2.0 to 3.0 × 10^5 cells/cm^2) every four days. To subculture, cells were treated with 5 mM EDTA/PBS containing 10 μM Y-27632 (Wako Pure Chemical Industries, Japan) for 10 min at RT, and subsequently, a cell dissociation enzyme TrypLE Select^{TM} (Invitrogen, USA) containing 10 μM Y-27632 for 7 min at 37°C. Cells were harvested and dissociated into single cells by gentle pipetting. Finally, cells were re-seeded into StemFit AK02N medium containing 10 μM Y-27632. At 24 h post seeding, the culture medium was replaced with fresh medium without Y-27632.

2.2.2 Experimental cultures

hiPSCs were cultured in two different expansion conditions: low seeding density and high seeding density cultures. Outlines of experimental cultures and evaluation procedures were shown in **Fig. 2.1**. Briefly, single dissociated cells obtained from the maintenance culture were seeded at a density of 2.0 × 10^3 cells/cm^2 (low seeding density) or 4.0 × 10^4 cells/cm^2 (high seeding density) onto dishes coated with iMatrix-511 (0.25 μg/cm^2). Within the first 24 h after seeding, cells were cultured in StemFit AK02N medium supplemented with 10 μM Y-27632. The culture medium was changed every day with fresh medium in the absence of Y-27632. The cultures were further grown for 216 h. To evaluate growth ability, hiPSCs at defined time

points were dissociated into single cells using TrypLE™ Select, and the number of live cells was counted by trypan blue exclusion assay.

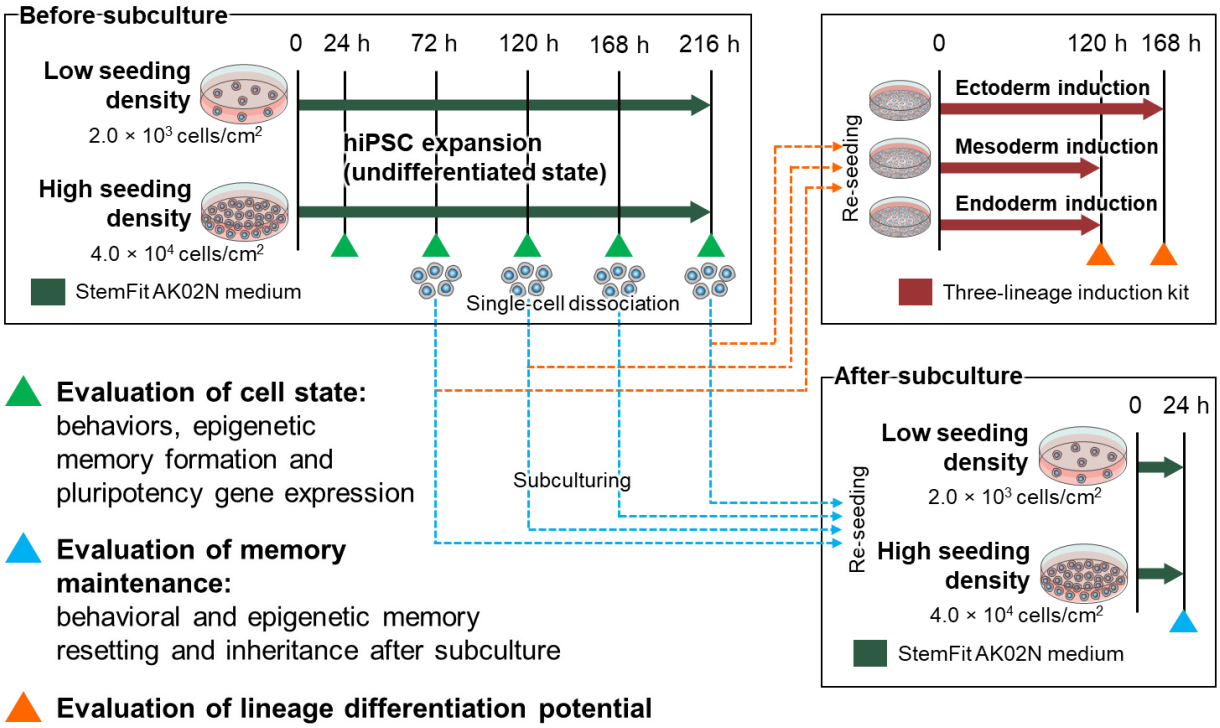

Figure 2.1 Schematic diagram showing the experimental outline in chapter 2.

2.2.3 Assay for trilineage differentiation potential

hiPSCs were differentiated into three germ lineages using Stemdiff™ trilineage differentiation kit (StemCell Technologies, Canada). Firstly, single dissociated cells collected from the expansion cultures at each defined time point were re-seeded onto plates coated with iMatrix-511 (0.25 μg/cm^2) at a density of 2.0 ×10^5 cells/cm^2 for ectoderm and endoderm differentiation, and 5.0 × 10^4 cells/cm^2 for mesoderm differentiation. Following the manufacturer's protocol, for ectoderm differentiation, cells were plated in Stemdiff™ trilineage ectoderm medium with 10 μM Y-27632. For endoderm and mesoderm differentiation, cells were plated in a maintenance culture medium with 10 μM Y-27632. At

the first 24 h after seeding, the media were replaced with each lineage-specific differentiation medium in the absence of Y-27632. The media were changed every day.

2.2.4 Immunofluorescence staining

Cells were fixed on culture plates with 4% paraformaldehyde (Wako Pure Chemical Industries, Japan) for 10 min at RT, and permeabilized with 0.5% Triton X-100 in PBS for 10 min at RT. Subsequently, cells were blocked with Block Ace solution (Dainippon Sumitomo Pharma Co. Ltd., Japan) for 90 min at RT, and then incubated overnight at 4°C with the following primary antibodies: anti-brachyury, anti-lamin A/C (Santa Cruz Biotechnology, USA); anti-lamin B1 (Abcam, USA); anti-PAX6 (Sigma-Aldrich, USA); and anti-SOX17 (Cell Signaling Technology Inc., USA). The treated cells were subjected to washes with TBS and further incubation with fluorescent-dye conjugated secondary antibodies (Thermo Fisher, USA) for 1 h at RT. The cells were then washed with TBS, and stained with 4′,6-diamidino-2-phenylindole (DAPI, Life Technologies, USA) and rhodamine phalloidin (Thermo Fisher, USA) for 30 min at RT to stain the nuclei and F-actin, respectively. Images were acquired using a confocal laser-scanning microscope (FV-1000; Olympus, Japan) with a 60× objective lens.

2.2.5 Protein extraction and western blot analysis

Total cell lysates were prepared using RIPA lysis buffer supplemented with protease and phosphatase inhibitor cocktail (Thermo Scientific, USA). Fractions of nuclear and cytoplasmic proteins were prepared using the Nuclear Extraction Kit (Abcam, USA). Protein concentration was quantified by Bradford assays. Protein lysate (25 or 75 μg protein) was separated by SDS-PAGE and transferred to PVDF membranes (BioRad, USA). The membranes were then blocked with 5% ECL blocking agent (GE Healthcare, USA) in TBS for 60 min at RT and incubated overnight at 4°C with the following primary antibodies: anti-β-actin, anti-histone

H3, anti-integrin β1, anti-tri-methyl-histone H3 (Lys4), anti-tri-methyl-histone H3 (Lys27) (Cell Signaling Technology Inc., USA); anti-E-cadherin, anti-lamin A/C (Santa Cruz Biotechnology, USA); and anti-lamin B1 (Abcam, USA). Blots were incubated with fluorescent-dye conjugated secondary antibodies (BioRad, USA) for 1 h at RT, and visualized using infrared fluorescence with ChemiDoc MP imaging system (BioRad, USA). β-actin and histone H3 were used as an internal control for sample loading. The signal intensity of target protein bands was normalized to the intensity of the internal loading control for that sample, and then the normalized intensity from each lane was divided by the normalized intensity of the sample in lane 1 in order to compare the relative expression across conditions.

2.2.6 Quantitative reverse transcription-polymerase chain reaction

Total RNA was isolated from cultured cells (1.0×10^6 cells) using RNeasy mini kit (Qiagen, Germany) following manufacturer's instruction. cDNA was synthesized from total RNA using PrimeScript RT reagent kit (Takara Bio, Inc., Japan). qRT-PCR analysis was carried out using SYBR Premix Ex Taq (Takara Bio, Inc., Japan) on a 7300 real-time PCR system (Applied Biosystems, USA). Expression values of mRNA were normalized to those of the internal reference gene *ACTB*, and relative expression values were then calculated by the $2^{-\Delta\Delta Ct}$ method. The primers used in this chapter are indicated in **Table 2.1**.

Table 2.1 List of primers used for qRT-PCR in chapter 2

Genes	Forward sequence (5' → 3')	Reverse sequence (5' → 3')
OCT3/4	CAAAACCCGGAGGAGGAGTC	CACATCGGCCTGTGTATATC
NANOG	TGATTTGTGGGCCTGAAGAAAA	GAGGCATCTCAGCAGAAGACA
SOX2	TGGCGAACCATCTCTGTGGT	CCAACGGTGTCAACCTGCAT
PAX6	TCTTTGCTTGGGAAATCCG	CTGCCCGTTCAACATCCTTAG
MAP2	CGAAGCGCCAATGGATTCC	TGAACTATCCTTGCAGACACCT
SOX1	ATGCACCGCTACGACATGG	CTCATGTAGCCCTGCGAGTTG
SOX17	GAGCCAAGGGCGAGTCCCGTA	CCTTCCACGACTTGCCCAGCAT
FOXA2	GTCCGACTGGAGCAGCTACTA	GTACGTGTTCATGCCGTTCATC
GATA4	ACACCCCAATCTCGATATGTTTG	GTTGCACAGATAGTGACCCGT
T	GCAAAAGCTTTCCTTGATGC	ATGAGGATTTGCAGGTGGAC
CDX2	TTCACTACAGTCGCTACATCACCAT	TTGTTGATTTTCCTCTCCTTTGCT
NKX2.5	ACCCTGAGTCCCCTGGATTT	TCACTCATTGCACGCTGCAT
ACTB	AGGCACCAGGGCGTGAT	GCCCACATAGGAATCCTTCTGAC

2.2.7 Statistical analysis

All experimental data are expressed as the mean ± standard deviation (SD). Differences between two groups and multiple groups were assessed using Student's *t* test and one-way analysis of variance followed by Dunnett's or Tukey's multiple comparisons test, respectively. A *P*-value of less than 0.05 or 0.01 was used to indicate statistically significant differences.

2.3 Results

2.3.1 Cell behavioral and nucleoskeletal charataceristics of hiPSCs with different initial seeding densities

In this chapter, cell behavioral changes in the 2D monolayer cultures of hiPSCs with different initial seeding densities were examined. hiPSCs were seeded at two different seeding densities of 2.0×10^3 cells/cm^2 (low seeding density) and 4.0×10^4 cells/cm^2 (high seeding density), and later cultured for 216 h. Compared with cells in low seeding density culture, the hiPSCs in high seeding density culture migrated and earlier interacted and formed cell-cell contact, concomitantly promoting earlier events of colony formation and growth phase transition (**Fig. 2.2A**). Cell densities in low seeding density culture exponentially increased in a time-dependent fashion until 120 h, and subsequently reached a plateau corresponding with the cell confluency, while cell densities in high seeding density culture entered the stationary phase within the first 72 h after seeding (**Fig. 2.2A** and **2.4B**). Contact inhibition was reflected by mostly constant rates of cell growth and decrease in cell mobility. The cells in high seeding density culture were maintained in a prolonged stationary phase from 72 h to 216 h (long-term stationary) with spatial presence of overlapping cell structures.

In addition, expression levels of cell-cell adhesion protein (E-cadherin) and cell-substrate adhesion protein (integrin β1) were measured in the cells at different time points along the culture period to shed light on the dynamics of cell behavioral regulation in different culture conditions and growth phases (**Fig. 2.2B**). In low seeding density culture, the levels of E-cadherin gradually increased during transition from the exponential to stationary phase (72 h to 216 h), while the levels of integrin β1 significantly decreased at 168 h after cells reaching the stationary growth phase. In high seeding density culture, the high levels of E-cadherin were sustained across the culture time without significant changes, whereas the levels of integrin β1 were drastically reduced upon cell confluence (168 h to 216 h) in a similar trend with those in

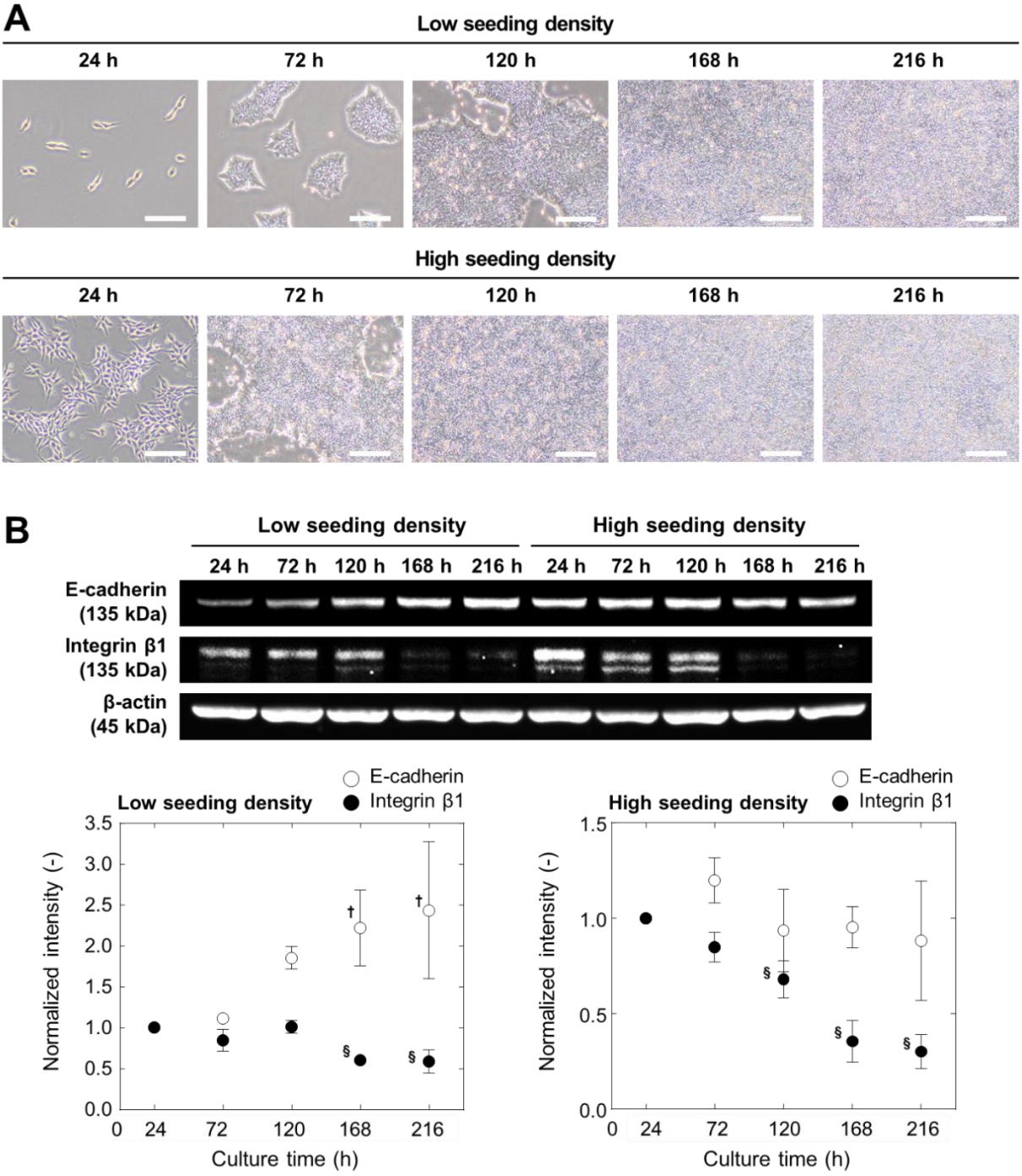

Figure 2.2 Growth-dependent modulation of cell behaviors in hiPSCs. (A) Morphological observation by phase-contrast microscopy in low and high seeding density cultures. Scale bars, 200 μm. (B) Western blot images and quantitative analysis of E-cadherin and integrin β1 in low seeding density and high seeding density cultures. The intensity of each target protein was normalized to that of β-actin. Data are shown as the mean ± SD (n = 3). $^{\dagger, \S}$ P-value < 0.05, compared the normalized intensity at each time point to that at 24 h.

low seeding density culture. Comparing the expression of integrin β1from 24 h to 216 h, its levels in low and high seeding density cultures were significantly decreased by 1.7-fold and 3.3-fold, respectively. These observations described patterns of cell behavioral changes in a function of growth phase transition in hiPSCs with different seeding densities. Changes in E-cadherin and integrin β1 levels along the cultures could indicate the dynamics of cell adhesion and its contribution to the alteration of cell migratory characteristics particularly during the prolonged cultures.

To further ascertain a functional link between cell behavioral modulation and mechanical nuclear properties, structural organization and protein levels of intranuclear lamins (lamin A/C and lamin B1), which are major nucleoskeletal components perceiving and relaying cytoskeleton-driven mechanical signals into the nucleus and chromatin (Sapra et al., 2020; Stephens et al., 2017; Tenga & Medalia, 2020), were investigated by immunostaining (**Fig. 2.3**) and western blotting (**Fig. 2.4**). Lamin B were detected at nuclear rims of all cultured cells among different growth phases. Staining of nuclear lamins revealed growth-dependent changes in nuclear shapes and alignments (**Fig. 2.3**). In both low and high seeding density cultures, cells mainly showed wrinkled nuclear structure in the exponential and early stationary phases at 72 to 120 h in low seeding density culture and at 24 to 96 h in high seeding density culture, while they later showed stretched nuclear structure in the long-term stationary phase at 216 h in low seeding density culture and at 120 to 216 h in high seeding density culture.

Presence of perinuclear localization of lamin A/C was detected temporally after initial cell seeding at 24 to 96 h in low seeding density culture and at 24 to 72 h in high seeding density culture (**Fig. 2.3**). Structural disruption of lamin A/C was observed after colony formation during exponential growth phase and became more apparent after reaching stationary phase in both culture conditions. In confluent cell population, lamin A/C in almost all cells was

diminished but remained in some cells within overlapping structures during long-term stationary phase (216 h) in high seeding density culture.

In consistent with immunostaining images, protein expression of lamin B1 was constantly maintained, while the expression of lamin A/C was decreased upon cell growth progression (**Fig. 2.4**). By the quantitative analysis, the ratios of lamin A/C to lamin B were found significantly decreased in both low and high seeding density cultures. At 216 h the lamin A/C/lamin B1 ratios in low and high seeding density cultures were reduced by 2.9-fold and 3.7-fold, respectively, compared to those at 24 h. Taken together, cell growth progression in both culture conditions elevated cell-cell interactions and nuclear mechanical changes, inducing lamin A/C disruption.

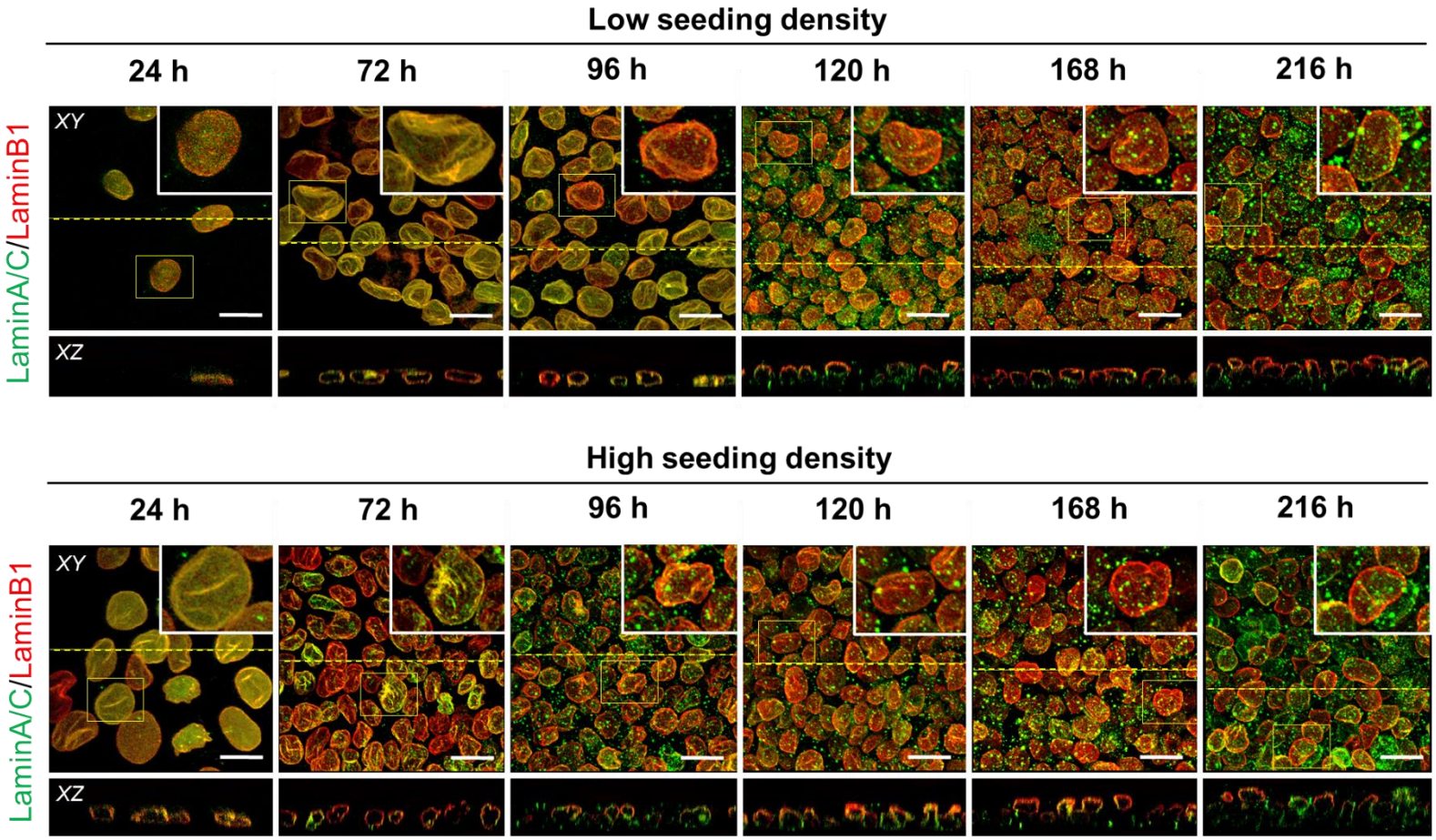

Figure 2.3 Structural reorganization of nucleoskeleton during hiPSC cultures. Fluorescence staining images of nucleoskeleton components (lamin B1 and lamin A/C) along with filamentous actin (F-actin) in low seeding density and high seeding density cultures. The yellow dashed line in the *XY* image plane indicates the location of the *XZ* image plane shown below. Zoom-in images of the regions with yellow border are presented in the top right corner of each panel. Scale bars, 20 μm.

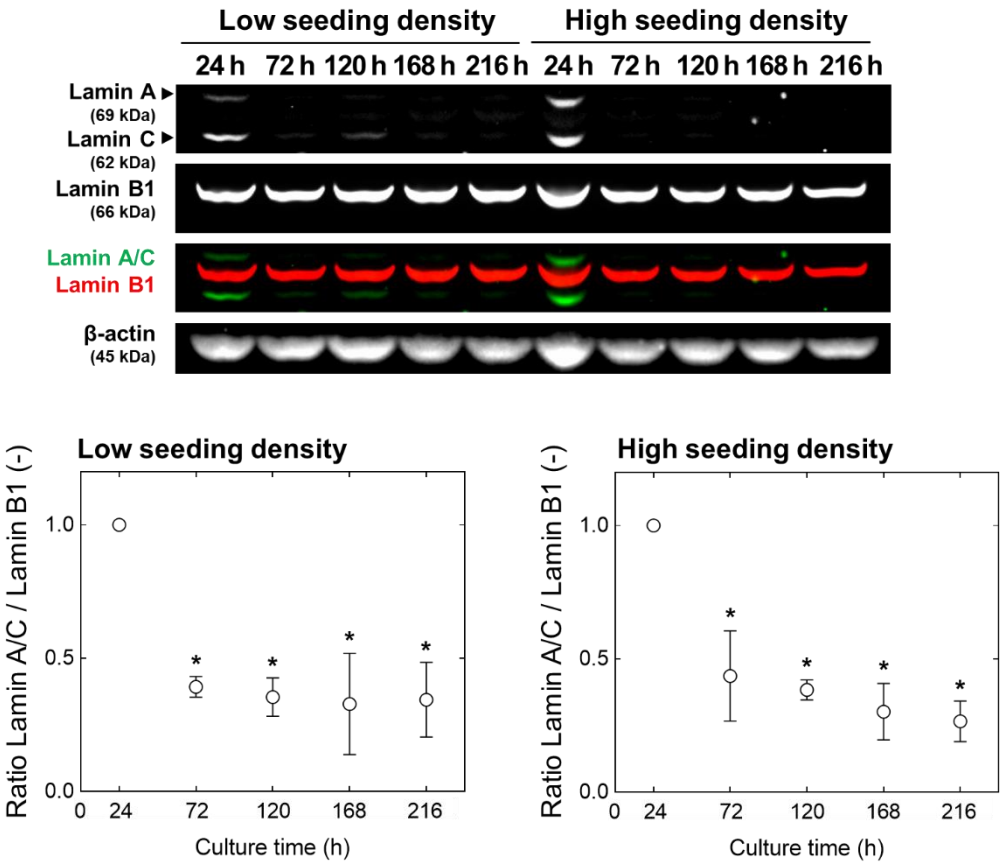

Figure 2.4 Expression of nucleoskeletal proteins during expansion of hiPSCs in low and high seeding density cultures. Western blot images and quantitative analysis of lamin A/C and lamin B1 in low and high seeding density cultures. Data are shown as the mean ± SD (n = 3). * P-value < 0.05, compared the normalized ratio at each time point to that at 24 h.

2.3.2 Epigenetic memory formation during growth phase transition in correlation with the activation of core pluripotent gene expression

To explore the epigenetic memory formation in cultures of hiPSCs with different initial seeding densities and growth phases, the global levels of active H3K4me3 and repressive H3K27me3 histone modifications were evaluated at different time points along the culture period by western blotting (**Fig. 2.5A**). In accordance with the increased cell densities during exponential growth phase, the levels of H3K4me3 were found significantly upregulated, while its levels became constant after cell growth reached the stationary phase in both culture

conditions (**Fig. 2.5B**). In contrast, levels of H3K27me3 were significantly lessened upon cell growth at 120 h and 72 h in low and high seeding density cultures, respectively, and slightly retrieved during stationary phase (**Fig. 2.5B**).

Next, a relationship between the global epigenetic modifications and transcriptional expression associated with the pluripotency regulation was clarified (**Fig. 2.5C**). The ratios of active H3K4me3 to repressive H3K27me3 levels were calculated and plotted against relative expression of core pluripotent genes including *OCT3/4*, *SOX2* and *NANOG*. In low and high seeding density cultures, the H3K4me3/H3K27me3 ratios increased along the transition from exponential to stationary phases, and the maximum ratios were detected at 120 h and 72 h, respectively. The relative expression of *OCT3/4*, *SOX2* and *NANOG* was found positively associated with the increased trends of H3K4me3/H3K27me3 ratios in both culture conditions. Compared among different time points, the relative expression of *OCT3/4*, *SOX2* and *NANOG* in low and high seeding density cultures reached equilibrium at 168 h and 120 h, respectively, and the expression at those time points were found upregulated by 2.2–2.5-fold and 1.5–1.6-fold, compared to those at 24 h, respectively. Overall, the growth-dependent epigenetic memory formation was correlated with the transcriptional activation of core pluripotent genes, and these cooperative epigenetic and transcriptional regulation might play a vital role in activating and retaining the pluripotency during cultures of hiPSCs.

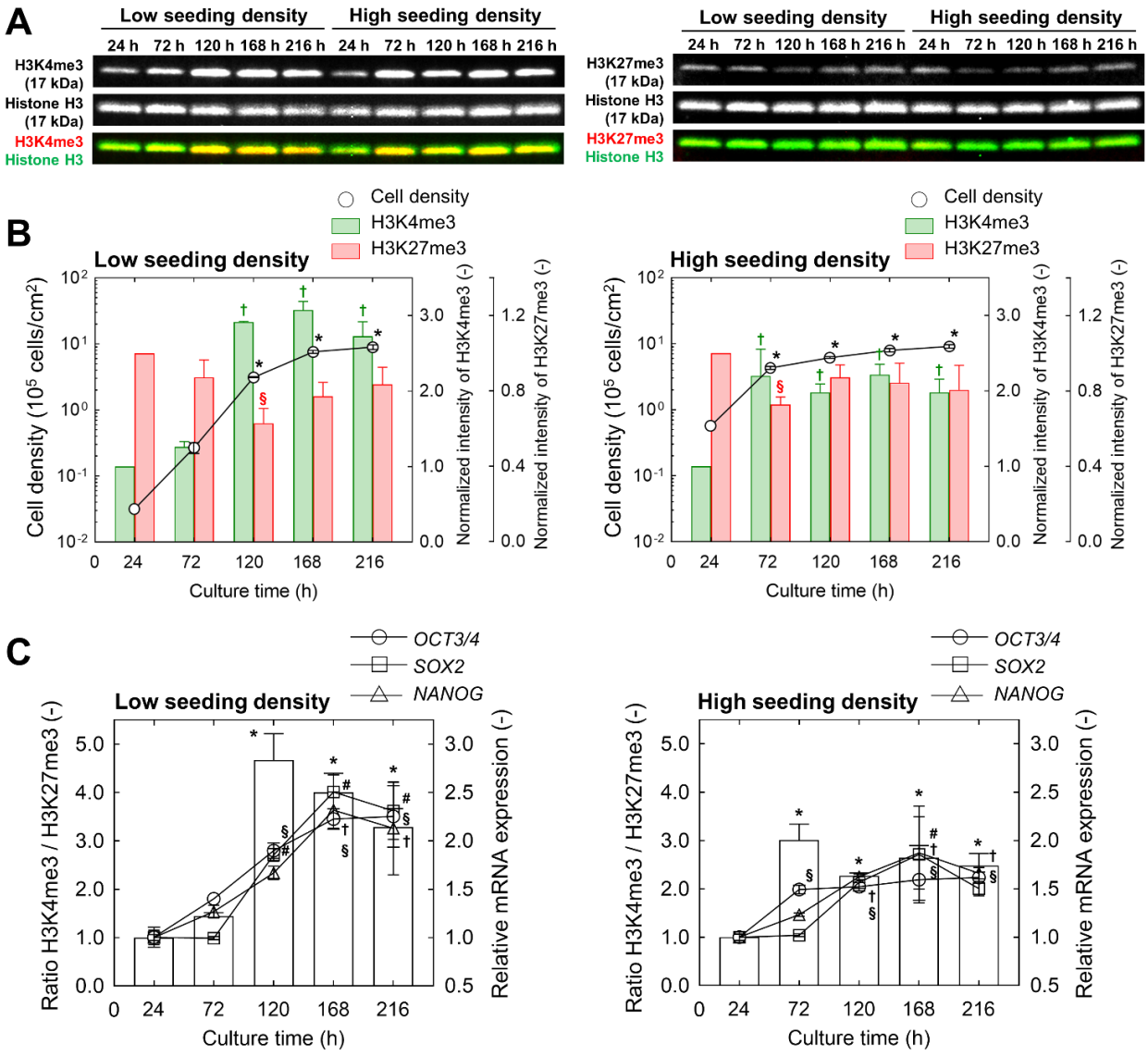

Figure 2.5 Formation of epigenetic memory correlated with cell growth and pluripotent gene expression. (A) Western blot images of H3K4me3 and H3K27me3 during cultures. (B) Growth profiles of hiPSCs (left axis) and quantitative western blot analysis of H3K4me3 and H3K27me3 (right axis) in low and high seeding density cultures, plotted against culture time. The intensity of each target protein was normalized to that of histone H3. Data are shown as the mean ± SD (n = 3). $^{*, \dagger, \S}$ P-value < 0.01, compared the cell density (*), or normalized intensity of H3K4me3 (†) or H3K27me3 (§) at each time point to that at 24 h). (C) Ratio of H3K4me3 to H3K27me3 calculated from normalized western blot data (left axis) and relative mRNA expression of core pluripotency-associated genes (right axis), plotted against culture

time. Data are shown as the mean ± SD (n = 3). $^{*, \dagger, \S, \#}$ P-value < 0.01, compared the ratio of H3K4me3 to H3K27me3 (*), or relative mRNA expression of *OCT3/4* (†), *SOX2* (§) or *NANOG* ($^{\#}$) at each time point to that at 24 h.

2.3.3 Epigenetic memory initialization and consolidation after subculture from different growth phases

In order to examine the memory initialization and consolidation of hiPSCs from past to subsequent cultures and its possible consequence in the conversion from short-term to long-term memories, epigenetic memory (**Fig. 2.6A** and **2.7A**) in the hiPSCs after subculture from different growth phases and different initial seeding densities were investigated. Furthermore, changes in cell behavioral regulation after subculture were observed to determine whether the epigenetic memory formation in past culture could be lasted in the aspect of functional alteration (**Fig. 2.8A**).

The levels of histone methylation and cell behavioral protein expression before subculture at 24 h were considered as an initial baseline reference of original memory in the early phase of culture, while the levels at subculturing time were considered as a past culture memory before subculture, representing recent cell status. The detection levels at 24 h after subculture would be compared with the baseline reference (at 24 h before subculture) and the past culture memory (at subculturing time) to evaluate the memory initialization and consolidation of hiPSCs, which would indicate whether the cells could reset the past culture memory and adapt to new environment or accumulate the memory.

At 24 h after subculture, trends of H3K4me3 (**Fig. 2.6B-C**) and H3K27me3 levels (**Fig. 2.7B-C**) in the cells from different growth phases in both culture conditions were found reduced and increased, respectively. The levels of H3K4me3 and H3K27me3 in the cells from exponential to stationary phase in low seeding density culture (72 h to 168 h; **Fig. 2.6B** and

2.7B) and high seeding density culture (72 h; **Fig. 2.6C** and **2.7C**) could be firmly returned to the baseline levels at 24 h before subculture, indicating the maintenance of epigenetic memory initialization after subculture from early growth phases. However, the levels of H3K4me3 in the cells from stationary phase at 120 h and 168 h in high seeding density culture were fluctuated and increased above the baseline levels (**Fig. 2.6C**), indicating the consolidation of epigenetic memory after subculture. In the cells from long-term stationary phase at 216 h in high seeding density culture, the levels of H3K4me3 were found decreased from the baseline level (**Fig. 2.6C**), indicating the modification of epigenetic memory in the culture prolonged in a long-term stationary phase.

Next, the expression of cell behavior-related proteins after subculture was examined. In the cells from different growth phases in both low and high seeding density cultures, levels of E-cadherin were mostly reset to the baseline levels at 24 h after subculture, while the levels of integrin β1 showed significant differences in the recovery trends (**Fig. 2.8B-C**). The levels of integrin β1 in the cells from exponential to stationary phase in low seeding density cultures (72 h to 168 h) could be returned to the baseline level at 24 h before subculture (**Fig. 2.8B**). In the cells from long-term stationary phase in low seeding density cultures (216 h), the level of integrin β1 slightly decreased from the baseline level. Apparently, the levels of integrin β1 in the cells from long-term stationary phases in high seeding density cultures (120 h to 216 h) were significantly declined below the baseline level (**Fig. 2.8C**).

Taken together, the past culture experience in dependence of growth phase transition and time spent in culture determines the epigenetic memory initialization and consolidation in hiPSCs after subculture and simultaneously change the plasticity of cell behavioral adaptation after subculture.

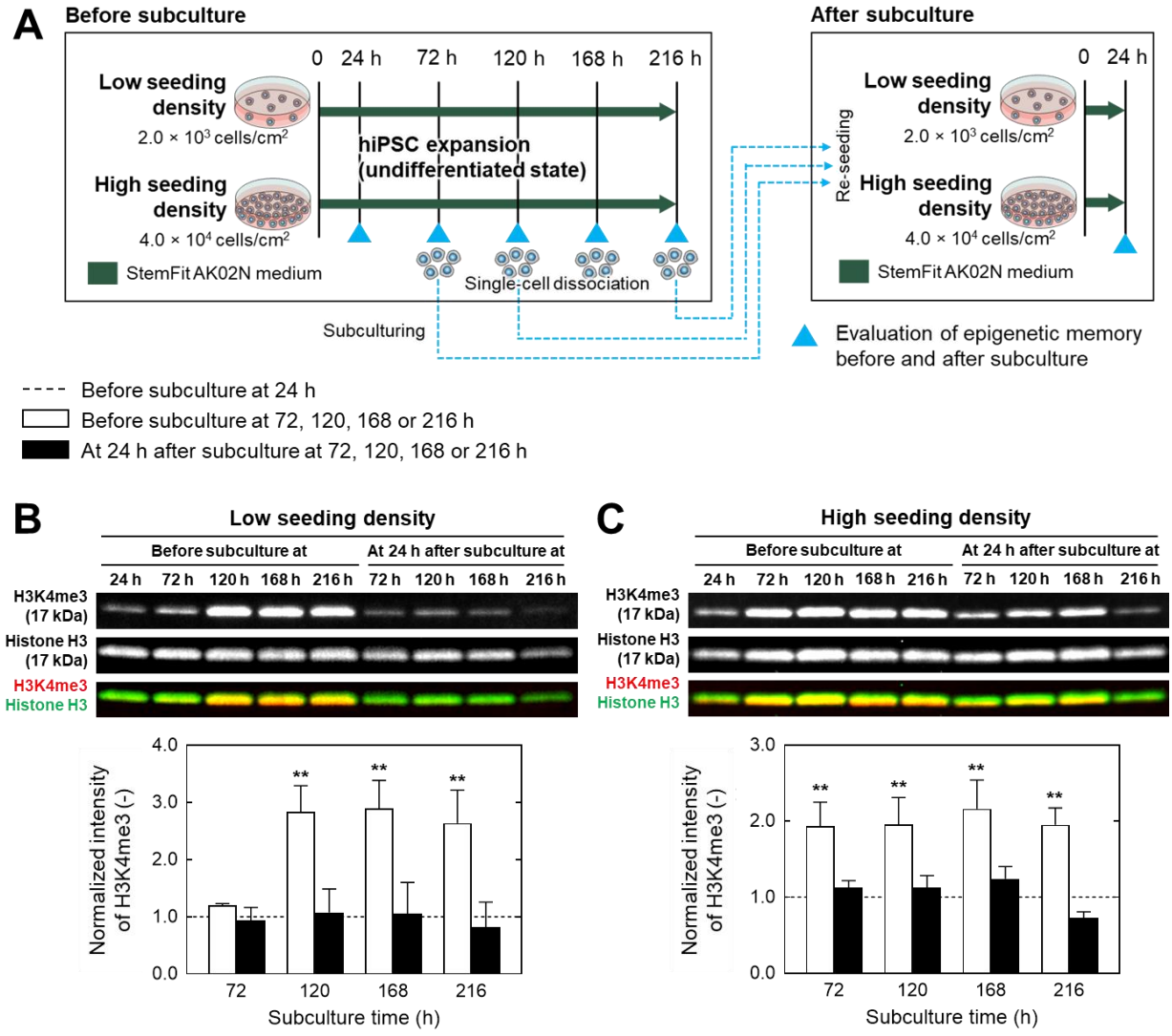

Figure 2.6 Epigenetic memory of H3K4me3 after subculture at different growth phases. (A) Schematic diagram showing the experimental procedures used for evaluating epigenetic memory before and after subculture. Western blot images and quantitative analysis of H3K4me3 in (B) low seeding density and (C) high seeding density cultures at different time points before subculture and at 24 h after subculture. The intensity of each target protein was normalized to that of histone H3, and each normalized value was compared with that measured in cells at 24 h before subculture, as the baseline value. Data are shown as the mean ± SD (n = 3). * P-value < 0.05, ** P-value < 0.01, compared the normalized intensity at each time point to that before subculture at 24 h.

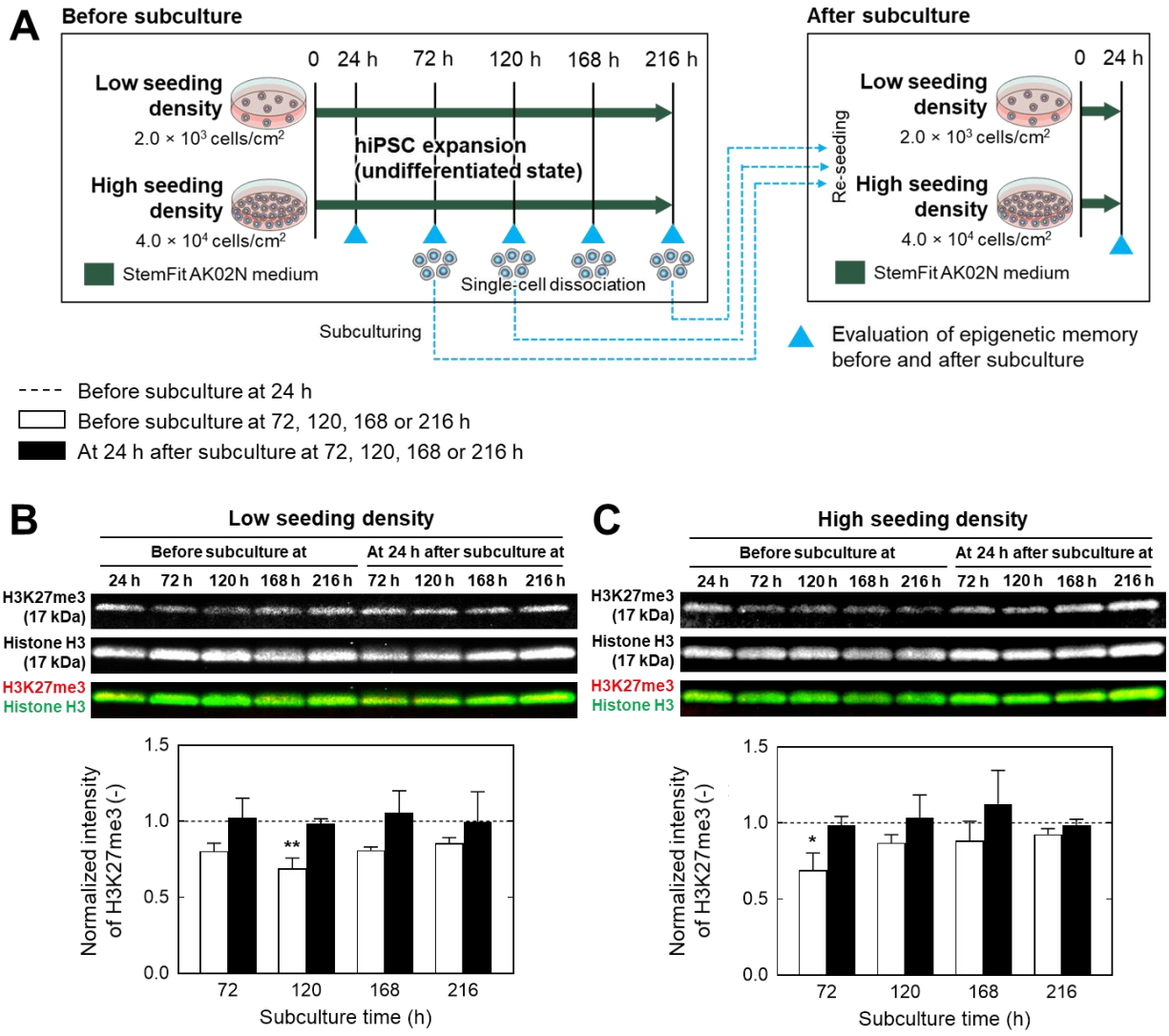

Figure 2.7 Epigenetic memory of H3K27me3 after subculture at different growth phases. (A) Schematic diagram showing the experimental procedures used for evaluating epigenetic memory before and after subculture. Western blot images and quantitative analysis of H3K27me3 in (B) low seeding density and (C) high seeding density cultures at different time points before subculture and at 24 h after subculture. The intensity of each target protein was normalized to that of histone H3, and each normalized value was compared with that measured in cells at 24 h before subculture, as the baseline value. Data are shown as the mean ± SD (n = 3). * P-value < 0.05, ** P-value < 0.01, compared the normalized intensity at each time point to that before subculture at 24 h.

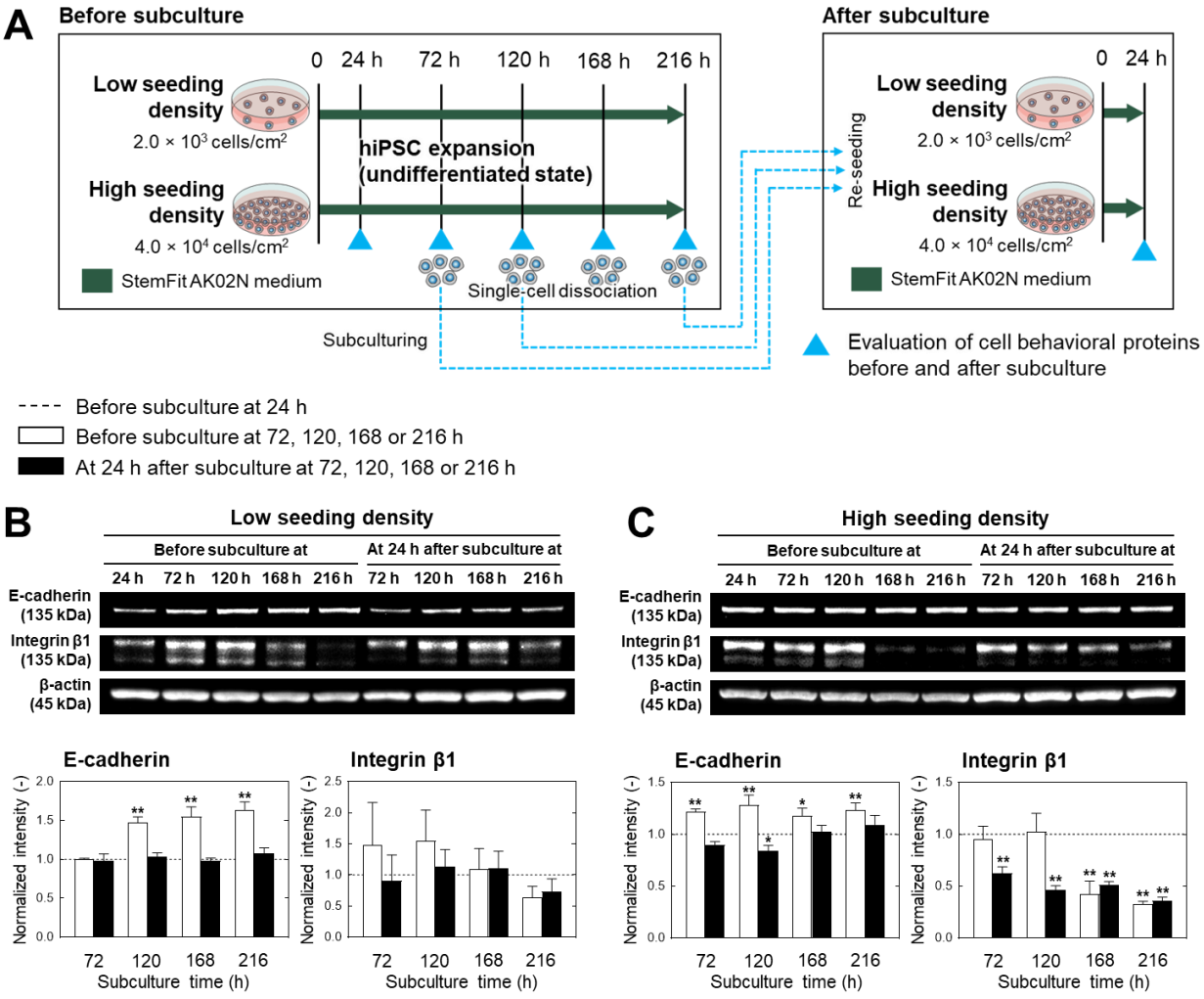

Figure 2.8 Cell behavioral regulation after subculture at different growth phases. (A) Schematic diagram showing the experimental procedures used for evaluating behavioral memory before and after subculture. Western blot images and quantitative analysis of E-cadherin and integrin β1 in (B) low seeding density and (C) high seeding density cultures at different time points before subculture and at 24 h after subculture. The intensity of each target protein was normalized to that of β-actin, and each normalized value was compared with that measured in cells at 24 h before subculture, as the baseline value. Data are shown as the mean ± SD (n = 3). * P-value < 0.05, ** P-value < 0.01, compared the normalized intensity at each time point to that before subculture at 24 h, the baseline value.

2.3.4 Association between epigenetic memory formation in past culture and lineage differentiation potential

To elucidate the association between culture-induced epigenetic memory formation and the transcriptional pluripotency regulation in the undifferentiated state as well as the lineage differentiation preference, hiPSCs at the end of different growth phases (exponential, stationary, and long-term stationary phases) in low and high seeding density cultures were collected for measuring the mRNA expression of core pluripotent genes, and also differentiated into three-germ lineages including ectodermal, mesodermal, and endodermal lineages (**Fig. 2.9A**). The mRNA expression of lineage-specific differentiation genes was measured in the cells after differentiation. The normalized H3K4me3/H3K27me3 ratios measured at each different time point in low and high seeding density cultures were classified into three categories by quartile analysis (low, first quartile; intermediate, interquartile range; and high, fourth quartile), and plotted against the relative expression of pluripotent genes in undifferentiated cells (**Fig. 2.9B**) or the relative expression of lineage differentiation genes in differentiated cells (**Fig. 2.9C**). Upon the increased H3K4me3/H3K27me3 ratios, the expression of pluripotent genes *OCT3/4*, *NANOG*, and *SOX2* was coordinately upregulated (**Fig. 2.9B**). Following the ectodermal differentiation induction, the expression of ectodermal genes *PAX6*, *MAP2*, and *SOX1* was significantly higher in the cells with a low H3K4me3/H3K27me3 ratio (**Fig. 2.9C**). On the contrary, the expression of endodermal genes *FOXA2* and *GATA4* was found significantly increased in the cells with intermediate H3K4me3/H3K27me3 ratios, while the expression of mesodermal genes *Brachyury* and *CDX2* was significantly increased in the cells with high H3K4me3/H3K27me3 ratios (**Fig. 2.9C**). Overall, the ectodermal lineage preference was negatively correlated with the H3K4me3/H3K27me3 ratios, whereas the mesendodermal lineage preference was positively correlated with the H3K4me3/H3K27me3 ratios. Differentiation potential was also evaluated

by the immunostaining of representative differentiation markers PAX6, SOX17 and Brachyury in the cells after lineage induction (**Fig. 2.9D**). The distribution of PAX6-positive cells clearly distinguished the high ectodermal differentiation potential in the cells from low seeding density culture at 72 h with a distinct low H3K4me3/H3K27me3 ratio. In the cells differentiated into mesodermal and endodermal lineages, Brachyury and SOX17 could be detected among the population of differentiated cells. In contrast to other past culture conditions, the cells from low seeding density culture at 72 h showed a significant cell detachment during endodermal induction. These obtained results suggested the distinct states of epigenetic memory in response to the growth phases and past culture experience may be involved in modulating the cellular propensity for subsequent differentiation induction.

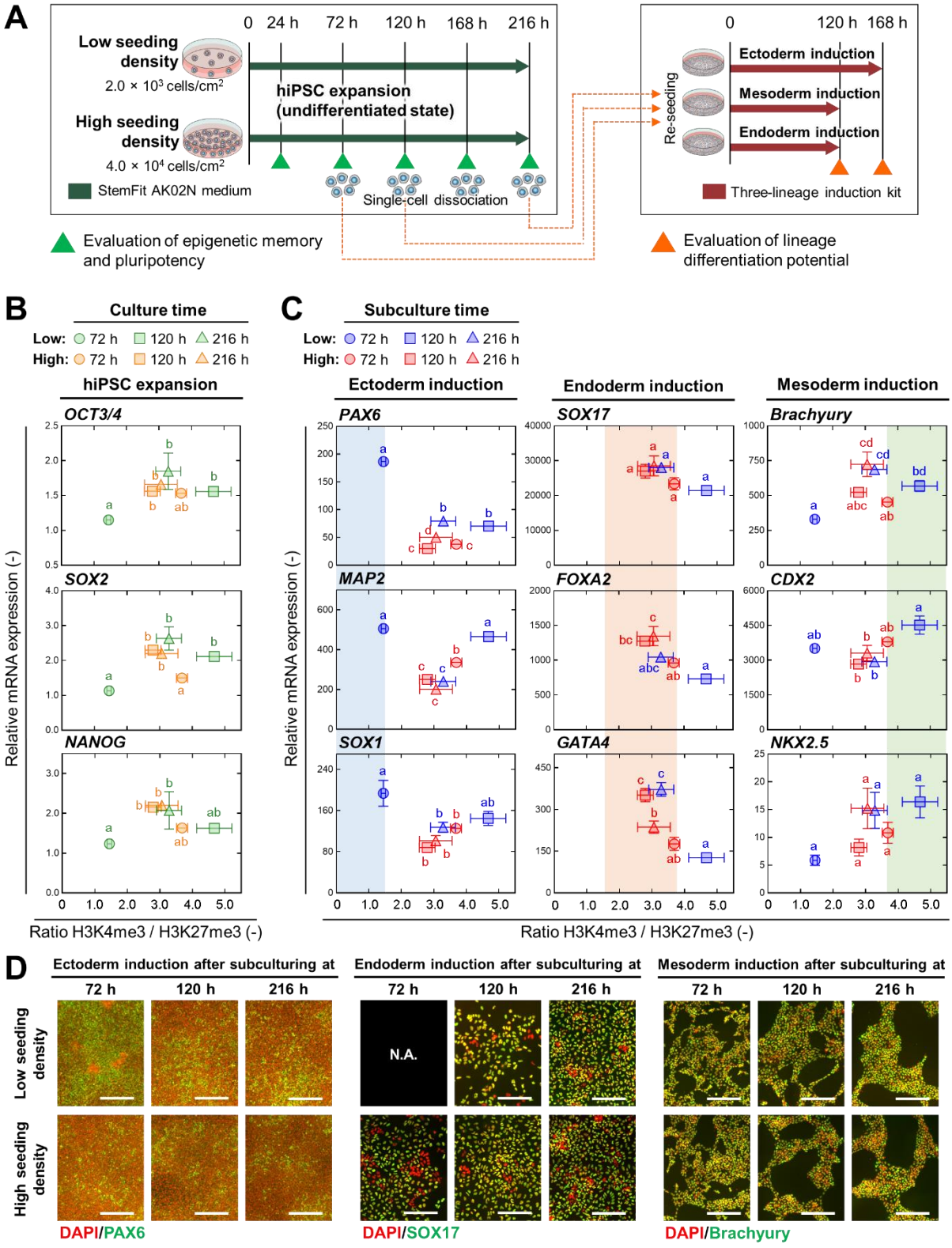

Figure 2.9 Differential transcriptional activation of lineage-specific genes during early differentiation induction linked with the epigenetic memory of hiPSCs in past cultures. (A) Schematic diagram showing the experimental procedures used for investigating the association

between epigenetic memory in past cultures and their pluripotency and tri-lineage differentiation potential. (B) Coordination between relative mRNA expression of core pluripotent genes and the ratio of H3K4me3 to H3K27me3 during hiPSC expansion. Relative mRNA expression of pluripotent genes was normalized with that at 24 h of hiPSC expansion in low seeding density culture. (C) Coordination between relative mRNA expression of lineage-specific genes in hiPSCs differentiated into ectoderm, mesoderm, and endoderm, and the ratio of H3K4me3 to H3K27me3 during hiPSC culture. Relative mRNA expression of differentiation genes was normalized with that of undifferentiated hiPSCs from maintenance culture. Data are shown as the mean ± SD (n = 3). Different alphabet letters indicate statistically significant differences of the relative mRNA expression between conditions (P-value < 0.01, calculated using one-way ANOVA followed by Tukey's test). The H3K4me3/H3K27me3 ratios measured at each different time point in low and high seeding density cultures were normalized with that measured at 24 h in low seeding density as a baseline control, and divided into three categories by quartile analysis (low, first quartile; intermediate, interquartile range; and high, fourth quartile). (D) Fluorescence staining images of differentiation markers including PAX6, Brachyury, and SOX17 along with the cell nuclei (DAPI) of hiPSCs differentiated into the ectoderm, mesoderm, and endoderm, respectively. Scale bars, 200 μm.

2.4 Discussion

Roles of culture experiences regarding cell growth phases and time spent in culture in regulating the epigenetic memory formation during culture and the memory initialization and consolidation after subculture were discussed as follows:

2.4.1 Epigenetic memory formation along growth phase transition and its association with pluripotency regulation and subsequent preferential lineage differentiation.

During growth phase transition, cells receive and integrate multivariate signals from the altered surrounding environments to program epigenetic states and gene regulatory networks, in turn modulating the cell state and potential (Ando et al., 2019; Pauklin & Vallier, 2013; Phadnis et al., 2015). In this chapter, hiPSCs in different initial seeding density cultures demonstrated differences in growth phase progression in correlation with the cell behavioral changes. Transition from exponential to stationary growth phases accompanied with increased cell density and colony compactness, suppressing cell motility while inducing formation of overlapping structures after reaching full confluency (**Fig. 2.2A**). Compared with low seeding density culture, high seeding density culture reinforced a rapid growth phase transition and later maintained the cells in a prolonged stationary phase. E-cadherin-mediated cell-cell adhesion was developed along the colony formation and retained throughout the culture time, while the integrin β1-mediated cell-substrate adhesion was moderated upon stationary phase, as the cells adapted to their ever-changing environment (**Fig. 2.2B**). Alteration in cell adhesion and migratory behaviors during growth was linked with the drastic disruption of nucleoskeleton lamin A/C (**Fig. 2.3** and **2.4**). Physical connection between cytoskeleton and nucleoskeleton as well as their structural changes have been shown to play a role in regulating nuclear architecture and chromatin organization, directly or indirectly affecting epigenetic modification and relevant gene expression (Alisafaei et al., 2019; Pruvost & Moyon, 2021; Toh et al., 2015). Growth-related cell behavioral adaptation and lamin A/C-dependent nuclear deformation

found in different seeding density cultures might underly rearrangement of intranuclear components and contribute to the epigenetic memory formation and maintenance along the growth progression of hiPSCs.

Epigenetic memory formation defined by the global levels of active H3K4me3 and repressive H3K27me3 marks were found highly associated with the growth phase transition, and the distinct states of epigenetic memory could be mirrored by the differential pluripotent gene expression and subsequent preferential lineage differentiation. Prior studies suggested that the H3K4me3/H3K27me3 ratio reflects the chromatin state and gene expression activity (De Gobbi et al., 2011). A higher H3K4me3/H3K27me3 ratio is corresponded in the same fashion with gene transcriptional levels (De Gobbi et al., 2011; Juan et al., 2016). The capacity of PSCs to preserve a balanced regulation between H3K4me3 and H3K27me3 might be necessary to appropriately keep the cells in an undifferentiated state with maintenance of their differentiation propensity (Bogliotti et al., 2018; Liu et al., 2016). Results in this chapter showed that hiPSCs in different seeding density cultures similarly exhibited the increased H3K4me3/H3K27me3 ratios during the transition from exponential to stationary phases, followed by constantly sustained H3K4me3/H3K27me3 ratios in long-term stationary phase (**Fig. 2.5B**). The elevated H3K4me3/H3K27me3 ratios along cell growth were positively correlated with activation of core pluripotent gene expression *OCT3/4*, *SOX2* and *NANOG* (**Fig. 2.5C**). Furthermore, influence of the distinct H3K4me3/H3K27me3 ratios obtained at different growth phases was further evaluated on three-lineage differentiation potential of hiPSCs. Comparative analysis of differentiation gene expression following lineage differentiation induction revealed that cells collected during exponential phase possessed higher ectodermal lineage potential than the cells collected during stationary phase (**Fig. 2.9C**). Distinctively, cells collected at the end of exponential phase and during stationary and long-term stationary phases exhibited higher mesodermal and endodermal lineage potential,

respectively (**Fig. 2.9C**). These results also implied the growth-dependent increment of H3K4me3/H3K27me3 ratios may be responsible for switching the preferential differentiation from ectodermal to mesendodermal lineages. Current measurement of global-level histone methylation confirmed the dynamics of H3K4me3 and H3K27me3 regulation in a growth-dependent manner and suggested its roles in controlling the state and potential of hiPSCs. However, further investigations were still required to unravel the gene-specific epigenetic modifications at genome-wide levels to explore a vast array of molecular and cellular processes in response to the alteration of epigenetic memory during culture. Taken together, the findings indicated that culture experiences substantially impact the subsequent cellular functions including differentiation preference in association with the epigenetic memory formation in past culture.

2.4.2 Past culture experience-induced epigenetic memory consolidation after subculture

Next, the ability of hiPSCs to initialize the epigenetic memory after subculture is considered to be prerequisite for sustaining the cell identity and functional stability following extended expansion and cell passaging. During culture, stem cells could alter and transmit the mechanical and epigenetic memories to the next generation cells in dependence of strength and length of past culture experiences, and these cellular memories could further affect how the cells respond to the new environment in terms of cell behavioral and epigenetic regulation in subsequent cultures (Killaars et al., 2019; Lee et al., 2014; Li et al., 2016; Yang et al., 2014). Previous studies exemplified that the degree of growth confluency in past culture could influence the future cell stemness and differentiation propensity of mesenchymal stem cells (Balint et al., 2015). In this study, the epigenetic memory and cell behavioral adaptation after subculture from different past culture conditions were evaluated in order to illustrate the existence of cell memory process in cultures of hiPSCs. The memory could be modified into a

stable state following prolonged culture in long-term stationary phase, consequently restricting the capability of reinitializing their native epigenetic memory and cell adhesion behaviors after subculture. Based on the current findings, the epigenetic memory at the initial phase of culture after seeding is defined as a sensory memory, which was referred to baseline levels of epigenetic modification and considered as an indicator of the cellular adaptability after subculture. The memory that is formed in past culture and could be initialized to the sensory stage or baseline levels after subculture is defined as a short-term memory, whereas the memory that was consolidated or modified after subculture is instead defined as a long-term memory (**Fig. 2.6-2.7**). Past culture experiences with regards to the growth phase transition, initial seeding densities, and time spent in culture have been shown to govern a process of epigenetic memory initialization and consolidation in the subsequent cultures. Altogether, the obtained findings demonstrate the epigenetic memory consolidation after subculture and importantly underline a plausibility of past culture-induced cell quality fluctuation.

2.5 Chapter summary

Chapter 2 describes the effect of prolonged expansion conditions on the epigenetic memory after subculture. Cells collected from exponential and stationary growth phases maintained the capability of epigenetic memory initialization after subculture; however, the cells collected from long-term stationary growth phase that formed and lasted the epigenetic memory for several days in past culture distinctly showed consolidation of epigenetic memory and changes in cell adhesion behaviors after subculture. These findings clarified the formation and maintenance of epigenetic memory during cell growth progression. In conclusion, the prolonged cell expansion in long-term stationary phase led to the epigenetic memory consolidation after subculture, possibly serving as another key driver of cell quality fluctuation during expansion of hiPSCs.

Concluding remarks

3.1 General conclusion

This study firstly elucidated the culture-driven epigenetic memory formation in hiPSCs under general PSC expansion conditions including 2D monolayer and 3D aggregate cultures. After seeding, hiPSCs in 2D and 3D cultures distinctly adapted to the different culture conditions by modulating integrin-mediated cell adhesion as well as balance of Rac/Rho GTPase antagonism. In contrast to the cells in 2D monolayers, cells in 3D aggregates significantly downregulated myosin phosphorylation and underwent reorganization of actomyosin cytoskeleton within the aggregate structure in a spatiotemporal manner. Quantitative analysis of global histone methylation exhibited distinct epigenetic memory formation between cells in different expansion conditions. Cells in 2D culture displayed remarkable upregulation of active H3K4me3 with downregulation of repressive H3K27me3, whereas cells in 3D culture demonstrated early upregulation of H3K4me3 with persistence of H3K27me3. In addition, cells from 2D and 3D cultures differently showed the transcriptional activation of primed and naïve pluripotency-associated genes, respectively. After subculture into new culture vessels, cells collected from both 2D and 3D cultures revealed their ability to reset and initialize the epigenetic memory to baseline levels detected before subculture. Differences in cell behavioral regulation and epigenetic memory formation of hiPSCs in 2D and 3D conditions represent cellular responses to the different culture environments. Under these defined culture conditions, the cells still retained the epigenetic memory initialization after subculture.

Subsequently, the epigenetic memory of hiPSCs after subculture was further examined in prolonged culture conditions with different cell growth phases. During cell growth progression, the expression of pluripotency-associated genes was activated along with the

formation of epigenetic memory and the disruption of lamin A/C nucleoskeleton. Cells collected from exponential and stationary growth phases maintained the capability of epigenetic memory initialization after subculture; however, the cells collected from long-term stationary growth phase that formed and lasted the epigenetic memory for several days in past culture distinctly showed consolidation of epigenetic memory and changes in cell adhesion behaviors after subculture. In addition, the ratios of H3K4me3 and H3K27me3 at different growth phases in past culture were also found associated with switching the lineage differentiation preference. The findings here clarified the formation and maintenance of epigenetic memory across cell growth progression. The prolonged expansion culture of hiPSCs in long-term stationary phase led to the epigenetic memory consolidation after subculture.

In summary, this thesis demonstrated the epigenetic memory regulation during expansion of hiPSCs and its contribution to the cell state and potential. Cells respond to their surrounding environments under different culture conditions and culture durations by regulating their adhesion behaviors and cytoskeletal contractility. Importantly, culture environments determined the epigenetic memory formation and modulate the pluripotent state of hiPSCs. Acquisition and maintenance of epigenetic memory in past culture are substantially predictive of their memory initializing capability after subculture as well as the subsequent differentiation potential. This study paves the way for controlling and stabilizing the quality of hiPSCs by considering culture environments and epigenetic memory mechanism. Ultimately, the improved understanding may help enable the process design and optimization for expansion and differentiation of hiPSCs to meet quality and stability requirements for manufacturing and downstream applications.

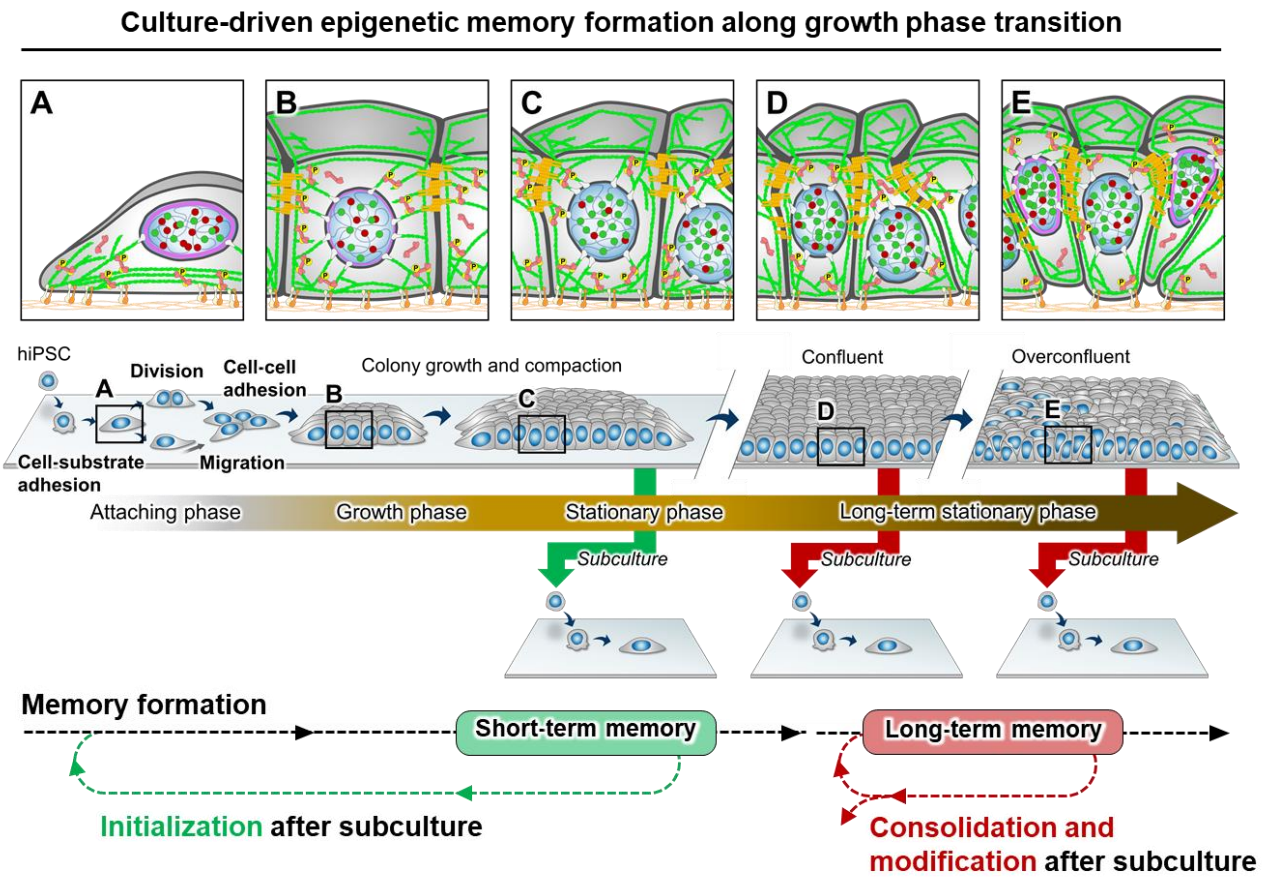

Figure 3.1 Schematic diagram showing the general conclusion of this study.

3.2 Future perspectives

To complement and broaden the current findings, several prospects and considerations are outlined in the following sections:

3.2.1 Application of culture environmental regulation strategy for hiPSC expansion and differentiation processes

The current study demonstrates culture-induced modulation of the state and potential of hiPSCs. Culture environmental factors and balances in cell behavioral regulation are essential to control the self-renewal and cell fate determination upon differentiation of PSCs (Ando et al., 2019; L. Li et al., 2012; Wrighton et al., 2014). Engineering of cell culture environments become increasingly attractive as a programmable platform to regulate stem cell expansion and differentiation processes (García et al., 1999; Mao et al., 2016; Smith et al., 2015; Yu et al., 2018). Previous research documented that HA could be efficiently used to temporally disrupt the E-cadherin-mediated cell-cell connection and subsequently reorganize the arrangement and migratory behaviors during the maintenance culture of hiPSCs (Shuzui et al., 2019). Culture arrangement using HA might be a promising culture strategy for controlling the cell populational quality. Moreover, effects of HA-mediated cell behavioral regulation should be further investigated whether the arrangement could prepare the state of hiPSCs suitable for differentiation induction. The optimization of culture environmental regulation strategy might help stabilize the quality of hiPSCs during expansion and differentiation processes.

3.2.2 Development of non-destructive cell quality evaluation by tracking cell behavioral and nuclear structural changes

Prior studies have demonstrated evidence showing the direct impact of cytoskeletal organization on the epigenetic modification and nuclear structural changes in several types of

cells (Du et al., 2019; Keeling et al., 2017). The chromatin remodeling and 3D nuclear structural organization are well known to be a key determinant of gene regulatory networks and cellular functions (Dultz et al., 2018; Golkaram et al., 2017; Ishihara et al., 2021). As this study showed the distinct cytoskeletal and nucleoskeletal regulation accompanied with the epigenetic modifications and cell state transition, it thus suggests a possibility to classify the individual cell quality among cell population in the culture by evaluating dynamics of cytoskeletal tension and nuclear morphological changes. A correlation between distinct characteristics of cytoskeletal tension, nuclear structures and hiPSC quality must be firstly substantiated. Since the intracellular tensional force generated by cytoskeletal arrangement can be tracked by available live-cell fluorescence-based reporters and the nuclear morphology can also be observed by live-cell imaging, combination of these investigations might serve as a tool for non-destructively and *in situ* monitoring real-time changes in the cellular tension in response to different culture conditions and evaluating the quality of cultured hiPSCs. The proposed approach might be a basis for constructing automated quality assurance in cell culture system.

3.2.3 Elucidation of the cell populational heterogeneity by investigating the epigenetic memory and gene transcriptional profile at single-cell level

The current study elucidated the phenomena of epigenetic memory modifications and gene transcriptional regulation at cell population level using bulk analysis methods. Further prospects of evaluation at single-cell level may hold up a measure of heterogeneity in cell quality, which is particularly existed in rare cell populations (Brielle et al., 2021; Francesconi et al., 2019; R. K. Gupta & Kuznicki, 2020; Zhang & Zhang, 2021). Recently, single-cell characterization of the epigenetic state and gene expression, such as single-cell assay for transposase accessible chromatin and single-cell spatial RNA sequencing, as well as the robust

data analysis methods become widely available. Extensive investigations based on single-cell analysis would provide high-dimensional data fruitful for comprehending both populational and individual cell characteristics in response to the culture conditions and culture operations, and it is important to distinguish the heterogeneity of cellular properties during production of hiPSCs and derivatives.

Nomenclature

α	Attachment efficiency	[-]
μ	Specific growth rate	[h^{-1}]
μ_{app}	Apparent specific growth rate	[h^{-1}]
X_{24}	Number of viable cells at 24 h	[cells]
X_{120}	Number of viable cells at 120 h	[cells]
t	Time	[h]

Abbreviations

2D	Two-dimensional
3D	Three-dimensional
ACTB	Beta-actin
CDX2	Caudal type homeobox 2
DPPA5	Developmental pluripotency-associated 5
DUSP6	Dual specificity phosphatase 6
ECM	Extracellular matrix
EDTA	Ethylenediaminetetraacetic acid
F-actin	Filamentous actin
FGF4	Fibroblast growth factor 4
FOXA2	Forkhead box A2
GATA4	GATA binding protein 4
GATA6	GATA binding protein 6
H3K27me3	Histone H3 trimethylation at lysine 27
H3K4me3	Histone H3 trimethylation at lysine 4
hESCs	Human embryonic stem cells
hiPSCs	Human induced pluripotent stem cells
hPSCs	Human pluripotent stem cells
KLF5	Kruppel-like factor 5
LINC	Linker of nucleoskeleton and cytoskeleton
MAP2	Microtubule-associated protein 2
MLC	Total myosin light chain

Abbreviations (continued)

MYH6	Myosin heavy chain 6
NKX2.5	NK2 transcription factor related, locus 5
OCT3/4	Octamer-binding transcription factor 3/4
OTX2	Orthodenticle homeobox 2
PAX6	Paired box 6
PBS	Phosphate-buffered saline
pMLC	Phosphorylated myosin light chain
PVDF	Polyvinylidene difluoride
qRT-PCR	Quantitative reverse transcription-polymerase chain reaction
RIPA	Radioimmunoprecipitation assay
ROCK	Rho-associated protein kinase
RT	Room temperature
SD	Standard deviation
SDS-PAGE	Sodium dodecyl sulphate–polyacrylamide gel electrophoresis
SOX1	Sex determining region Y-box 1
SOX11	Sex determining region Y-box 11
SOX17	Sex determining region Y-box 17
SOX2	Sex determining region Y-box 2
TBS	Tris-buffered saline
TBST	TBS containing 0.1% Tween-20
ZIC2	Zic family member 2
μm	micrometer

References

Adil, M. M., & Schaffer, D. V. (2017). Expansion of human pluripotent stem cells. *Curr. Opin. Chem.*, *15*, 24–35. https://doi.org/10.1016/j.coche.2016.11.002

Alam, S. G., Zhang, Q., Prasad, N., Li, Y., Chamala, S., Kuchibhotla, R., KC, B., Aggarwal, V., Shrestha, S., Jones, A. L., Levy, S. E., Roux, K. J., Nickerson, J. A., & Lele, T. P. (2016). The mammalian LINC complex regulates genome transcriptional responses to substrate rigidity. *Sci. Rep.*, *6*(1). https://doi.org/10.1038/srep38063

Alisafaei, F., Jokhun, D. S., Shivashankar, G. V., & Shenoy, V. B. (2019). Regulation of nuclear architecture, mechanics, and nucleocytoplasmic shuttling of epigenetic factors by cell geometric constraints. *Proc. Natl. Acad. Sci.*, *116*(27), 13200–13209. https://doi.org/10.1073/pnas.1902035116

Amabile, G., & Meissner, A. (2009). Induced pluripotent stem cells: current progress and potential for regenerative medicine. *Trends Mol. Med.*, *15*(2), 59–68. https://doi.org/10.1016/j.molmed.2008.12.003

Ando, Y., Okeyo, K. O., & Adachi, T. (2019). Modulation of adhesion microenvironment using mesh substrates triggers self-organization and primordial germ cell-like differentiation in mouse ES cells. *APL Bioeng.*, *3*(1), 016102. https://doi.org/10.1063/1.5072761

Ankam, S., Teo, B. K. K., Pohan, G., Ho, S. W. L., Lim, C. K., & Yim, E. K. F. (2018). Temporal changes in nucleus morphology, lamin A/C and histone methylation during nanotopography-induced neuronal differentiation of stem cells. *Front. Bioeng. Biotechnol.*, *6*. https://doi.org/10.3389/fbioe.2018.00069

Aranda, P., Agirre, X., Ballestar, E., Andreu, E. J., Román-Gómez, J., Prieto, I., Martín-Subero, J. I., Cigudosa, J. C., Siebert, R., Esteller, M., & Prosper, F. (2009). Epigenetic signatures associated with different levels of differentiation potential in human stem cells. *PLoS One*, *4*(11), e7809. https://doi.org/10.1371/journal.pone.0007809

Aranjuez, G., Burtscher, A., Sawant, K., Majumder, P., & McDonald, J. A. (2016). Dynamic myosin activation promotes collective morphology and migration by locally balancing oppositional forces from surrounding tissue. *Mol. Biol. Cell*, *27*(12), 1898–1910. https://doi.org/10.1091/mbc.e15-10-0744

Atlasi, Y., & Stunnenberg, H. G. (2017). The interplay of epigenetic marks during stem cell differentiation and development. *Nat. Rev. Genet.*, *18*(11), 643–658. https://doi.org/10.1038/nrg.2017.57

Azuara, V., Perry, P., Sauer, S., Spivakov, M., Jørgensen, H. F., John, R. M., Gouti, M., Casanova, M., Warnes, G., Merkenschlager, M., & Fisher, A. G. (2006). Chromatin signatures of pluripotent cell lines. *Nat. Cell Biol.*, *8*(5), 532–538. https://doi.org/10.1038/ncb1403

Baghbaderani, B. A., Syama, A., Sivapatham, R., Pei, Y., Mukherjee, O., Fellner, T., Zeng, X., & Rao, M. S. (2016). Detailed characterization of human induced pluripotent stem cells manufactured for therapeutic applications. *Stem Cell Rev.*, *12*(4), 394–420. https://doi.org/10.1007/s12015-016-9662-8

Balint, R., Richardson, S. M., & Cartmell, S. H. (2015). Low-density subculture: a technical note on the importance of avoiding cell-to-cell contact during mesenchymal stromal cell expansion. *J. Tissue Eng. Regen. Med.*, *9*(10), 1200–1203. https://doi.org/10.1002/term.2051

Banerji, C. R. S., Miranda-Saavedra, D., Severini, S., Widschwendter, M., Enver, T., Zhou, J. X., & Teschendorff, A. E. (2013). Cellular network entropy as the energy potential in Waddington's differentiation landscape. *Sci. Rep.*, *3*(1). https://doi.org/10.1038/srep03039

Bar-Nur, O., Russ, H., Efrat, S., & Benvenisty, N. (2011). Epigenetic memory and preferential lineage-specific differentiation in induced pluripotent stem cells derived from human pancreatic islet beta cells. *Cell Stem Cell*, *9*(1), 17–23. https://doi.org/10.1016/j.stem.2011.06.007

Barrand, S., & Collas, P. (2010). Chromatin states of core pluripotency-associated genes in pluripotent, multipotent and differentiated cells. *Biochem. Biophys. Res. Commun.*, *391*(1), 762–767. https://doi.org/10.1016/j.bbrc.2009.11.134

Bernstein, B. E., Mikkelsen, T. S., Xie, X., Kamal, M., Huebert, D. J., Cuff, J., Fry, B., Meissner, A., Wernig, M., Plath, K., Jaenisch, R., Wagschal, A., Feil, R., Schreiber, S. L., & Lander, E. S. (2006). A Bivalent Chromatin Structure Marks Key Developmental Genes in Embryonic Stem Cells. *Cell*, *125*(2), 315–326. https://doi.org/10.1016/j.cell.2006.02.041

Bertero, A., Madrigal, P., Galli, A., Hubner, N. C., Moreno, I., Burks, D., Brown, S., Pedersen, R. A., Gaffney, D., Mendjan, S., Pauklin, S., & Vallier, L. (2015). Activin/Nodal signaling and NANOG orchestrate human embryonic stem cell fate decisions by controlling the H3K4me3 chromatin mark. *Genes Dev.*, *29*(7), 702–717. https://doi.org/10.1101/gad.255984.114

Bhanu, N. V., Sidoli, S., & Garcia, B. A. (2016). Histone modification profiling reveals differential signatures associated with human embryonic stem cell self-renewal and differentiation. *Proteomics*, *16*(3), 448–458. https://doi.org/10.1002/pmic.201500231

Bogliotti, Y. S., Wu, J., Vilarino, M., Okamura, D., Soto, D. A., Zhong, C., Sakurai, M., Sampaio, R. V., Suzuki, K., Izpisua Belmonte, J. C., & Ross, P. J. (2018). Efficient derivation of stable primed pluripotent embryonic stem cells from bovine blastocysts. *Proc. Natl. Acad. Sci.*, *115*(9), 2090–2095. https://doi.org/10.1073/pnas.1716161115

Boyer, L. A., Lee, T. I., Cole, M. F., Johnstone, S. E., Levine, S. S., Zucker, J. P., Guenther, M. G., Kumar, R. M., Murray, H. L., Jenner, R. G., Gifford, D. K., Melton, D. A., Jaenisch, R., & Young, R. A. (2005). Core transcriptional regulatory circuitry in human embryonic stem cells. *Cell*, *122*(6), 947–956. https://doi.org/10.1016/j.cell.2005.08.020

Boyer, L. A., Plath, K., Zeitlinger, J., Brambrink, T., Medeiros, L. A., Lee, T. I., Levine, S. S., Wernig, M., Tajonar, A., Ray, M. K., Bell, G. W., Otte, A. P., Vidal, M., Gifford, D. K., Young, R. A., & Jaenisch, R. (2006). Polycomb complexes repress developmental regulators in murine embryonic stem cells. *Nature*, *441*(7091), 349–353. https://doi.org/10.1038/nature04733

Brielle, S., Bavli, D., Motzik, A., Kan-Tor, Y., Sun, X., Kozulin, C., Avni, B., Ram, O., & Buxboim, A. (2021). Delineating the heterogeneity of matrix-directed differentiation toward soft and stiff tissue lineages via single-cell profiling. *Proc. Natl. Acad. Sci.*, *118*(19), e2016322118. https://doi.org/10.1073/pnas.2016322118

Chan, S. W., Rizwan, M., & Yim, E. K. F. (2020). Emerging methods for enhancing pluripotent stem cell expansion. *Frontiers in Cell and Developmental Biology*, *8*. https://doi.org/10.3389/fcell.2020.00070

Chanet, S., Miller, C. J., Vaishnav, E. D., Ermentrout, B., Davidson, L. A., & Martin, A. C. (2017). Actomyosin meshwork mechanosensing enables tissue shape to orient cell force. *Nat. Commun.*, *8*(1). https://doi.org/10.1038/ncomms15014

Chang, P. H., Chao, H. M., Chern, E., & Hsu, S. H. (2021). Chitosan 3D cell culture system promotes naïve-like features of human induced pluripotent stem cells: A novel tool to sustain pluripotency and facilitate differentiation. *Biomaterials*, *268*, 120575. https://doi.org/10.1016/j.biomaterials.2020.120575

Cheedipudi, S., Genolet, O., & Dobreva, G. (2014). Epigenetic inheritance of cell fates during embryonic development. *Front. Genet.*, *5*. https://doi.org/10.3389/fgene.2014.00019

Chen, X., Ye, S., & Ying, Q. L. (2015). Stem cell maintenance by manipulating signaling pathways: past, current and future. *BMB Rep.*, *48*(12), 668–676. https://doi.org/10.5483/bmbrep.2015.48.12.215

Creighton, H., & Waddington, C. H. (1958). The strategy of the genes. *AIBS Bulletin*, *8*(2), 49. https://doi.org/10.2307/1291959

Crowder, S., Leonardo, V., Whittaker, T., Papathanasiou, P., & Stevens, M. (2016). Material cues as potent regulators of epigenetics and stem cell function. *Cell Stem Cell*, *18*(1), 39–52. https://doi.org/10.1016/j.stem.2015.12.012

Cruvinel, E., Ogusuku, I., Cerioni, R., Rodrigues, S., Gonçalves, J., Góes, M. E., Alvim, J. M., Silva, A. C., Lino, V. D. S., Boccardo, E., Goulart, E., Pereira, A., Dariolli, R., Valadares, M., & Biagi, D. (2020). Long-term single-cell passaging of human iPSC fully supports pluripotency and high-efficient trilineage differentiation capacity. *SAGE Open Med.*, *8*, 205031212096645. https://doi.org/10.1177/2050312120966456

Damodaran, K., Venkatachalapathy, S., Alisafaei, F., Radhakrishnan, A. V., Sharma Jokhun, D., Shenoy, V. B., & Shivashankar, G. V. (2018). Compressive force induces reversible chromatin condensation and cell geometry–dependent transcriptional response. *Mol. Biol. Cell*, *29*(25), 3039–3051. https://doi.org/10.1091/mbc.e18-04-0256

Das, T., Safferling, K., Rausch, S., Grabe, N., Boehm, H., & Spatz, J. P. (2015). A molecular mechanotransduction pathway regulates collective migration of epithelial cells. *Nat. Cell Biol.*, *17*(3), 276–287. https://doi.org/10.1038/ncb3115

de Clerck, L., Taelman, J., Popovic, M., Willems, S., van der Jeught, M., Heindryckx, B., de Sutter, P., Marks, H., Deforce, D., & Dhaenens, M. (2019). Untargeted histone profiling during naive conversion uncovers conserved modification markers between mouse and human. *Sci. Rep.*, *9*(1). https://doi.org/10.1038/s41598-019-53681-6

de Gobbi, M., Garrick, D., Lynch, M., Vernimmen, D., Hughes, J. R., Goardon, N., Luc, S., Lower, K. M., Sloane-Stanley, J. A., Pina, C., Soneji, S., Renella, R., Enver, T., Taylor, S., Jacobsen, S. E. W., Vyas, P., Gibbons, R. J., & Higgs, D. R. (2011). Generation of bivalent chromatin domains during cell fate decisions. *Epigenetics Chromatin*, *4*(1). https://doi.org/10.1186/1756-8935-4-9

Dean, C. (2017). What holds epigenetic memory? *Nat. Rev. Mol. Cell Biol.*, *18*(3), 140. https://doi.org/10.1038/nrm.2017.15

Dolega, M. E., Delarue, M., Ingremeau, F., Prost, J., Delon, A., & Cappello, G. (2017). Cell-like pressure sensors reveal increase of mechanical stress towards the core of

multicellular spheroids under compression. *Nat. Commun.*, *8*(1). https://doi.org/10.1038/ncomms14056

Du, J., Fan, Y., Guo, Z., Wang, Y., Zheng, X., Huang, C., Liang, B., Gao, L., Cao, Y., Chen, Y., Zhang, X., Li, L., Xu, L., Wu, C., Weitz, D. A., & Feng, X. (2019). Compression generated by a 3D supracellular actomyosin cortex promotes embryonic stem cell colony growth and expression of Nanog and Oct4. *Cell Syst.*, *9*(2), 214–220.e5. https://doi.org/10.1016/j.cels.2019.05.008

Duggal, G., Warrier, S., Ghimire, S., Broekaert, D., van der Jeught, M., Lierman, S., Deroo, T., Peelman, L., van Soom, A., Cornelissen, R., Menten, B., Mestdagh, P., Vandesompele, J., Roost, M., Slieker, R. C., Heijmans, B. T., Deforce, D., de Sutter, P., de Sousa Lopes, S. C., & Heindryckx, B. (2015). Alternative routes to induce naïve pluripotency in human embryonic stem cells. *Stem Cells*, *33*(9), 2686–2698. https://doi.org/10.1002/stem.2071

Dultz, E., Mancini, R., Polles, G., Vallotton, P., Alber, F., & Weis, K. (2018). Quantitative imaging of chromatin decompaction in living cells. *Mol. Biol. Cell*, *29*(14), 1763–1777. https://doi.org/10.1091/mbc.e17-11-0648

Dundes, C. E., & Loh, K. M. (2020). Bridging naïve and primed pluripotency. *Nat. Cell Biol.*, *22*(5), 513–515. https://doi.org/10.1038/s41556-020-0509-9

Duval, K., Grover, H., Han, L. H., Mou, Y., Pegoraro, A. F., Fredberg, J., & Chen, Z. (2017). Modeling physiological events in 2D vs. 3D cell culture. *Physiology*, *32*(4), 266–277. https://doi.org/10.1152/physiol.00036.2016

Francesconi, M., di Stefano, B., Berenguer, C., de Andrés-Aguayo, L., Plana-Carmona, M., Mendez-Lago, M., Guillaumet-Adkins, A., Rodriguez-Esteban, G., Gut, M., Gut, I. G., Heyn, H., Lehner, B., & Graf, T. (2019). Single cell RNA-seq identifies the origins of heterogeneity in efficient cell transdifferentiation and reprogramming. *Elife*, *8*. https://doi.org/10.7554/Elife.41627

Friman, E. T., Deluz, C., Meireles-Filho, A. C., Govindan, S., Gardeux, V., Deplancke, B., & Suter, D. M. (2019). Dynamic regulation of chromatin accessibility by pluripotency transcription factors across the cell cycle. *Elife*, *8*. https://doi.org/10.7554/Elife.50087

Gafni, O., Weinberger, L., Mansour, A. A., Manor, Y. S., Chomsky, E., Ben-Yosef, D., Kalma, Y., Viukov, S., Maza, I., Zviran, A., Rais, Y., Shipony, Z., Mukamel, Z., Krupalnik, V., Zerbib, M., Geula, S., Caspi, I., Schneir, D., Shwartz, T., . . . Hanna, J. H. (2013). Derivation of novel human ground state naive pluripotent stem cells. *Nature*, *504*(7479), 282–286. https://doi.org/10.1038/nature12745

Galvanauskas, V., Grincas, V., Simutis, R., Kagawa, Y., & Kino-oka, M. (2017). Current state and perspectives in modeling and control of human pluripotent stem cell expansion processes in stirred-tank bioreactors. *Biotechnol. Prog.*, *33*(2), 355–364. https://doi.org/10.1002/btpr.2431

García, A. J., Vega, M. D., & Boettiger, D. (1999). Modulation of Cell proliferation and differentiation through substrate-dependent changes in fibronectin conformation. *Mol. Biol. Cell*, *10*(3), 785–798. https://doi.org/10.1091/mbc.10.3.785

Gilbert, S. F. (2000). Diachronic Biology Meets Evo-Devo: C. H. Waddington's approach to evolutionary developmental biology. *Am. Zool.*, *40*(5), 729–737. https://doi.org/10.1093/icb/40.5.729

Golkaram, M., Jang, J., Hellander, S., Kosik, K. S., & Petzold, L. R. (2017). The role of chromatin density in cell population heterogeneity during stem cell differentiation. *Sci. Rep.*, *7*(1). https://doi.org/10.1038/s41598-017-13731-3

Grandy, R. A., Whitfield, T. W., Wu, H., Fitzgerald, M. P., VanOudenhove, J. J., Zaidi, S. K., Montecino, M. A., Lian, J. B., van Wijnen, A. J., Stein, J. L., & Stein, G. S. (2016). Genome-wide studies reveal that H3K4me3 modification in bivalent genes is dynamically regulated during the pluripotent cell cycle and stabilized upon differentiation. *Mol. Cell. Biol.*, *36*(4), 615–627. https://doi.org/10.1128/mcb.00877-15

Guetta-Terrier, C., Monzo, P., Zhu, J., Long, H., Venkatraman, L., Zhou, Y., Wang, P., Chew, S. Y., Mogilner, A., Ladoux, B., & Gauthier, N. C. (2015). Protrusive waves guide 3D cell migration along nanofibers. *J. Cell Biol.*, *211*(3), 683–701. https://doi.org/10.1083/jcb.201501106

Gunhanlar, N., Shpak, G., van der Kroeg, M., Gouty-Colomer, L. A., Munshi, S. T., Lendemeijer, B., Ghazvini, M., Dupont, C., Hoogendijk, W. J. G., Gribnau, J., de Vrij, F. M. S., & Kushner, S. A. (2017). A simplified protocol for differentiation of electrophysiologically mature neuronal networks from human induced pluripotent stem cells. *Mol. Psychiatry*, *23*(5), 1336–1344. https://doi.org/10.1038/mp.2017.56

Gupta, M., Sarangi, B. R., Deschamps, J., Nematbakhsh, Y., Callan-Jones, A., Margadant, F., Mège, R. M., Lim, C. T., Voituriez, R., & Ladoux, B. (2015). Adaptive rheology and ordering of cell cytoskeleton govern matrix rigidity sensing. *Nat. Commun.*, *6*(1). https://doi.org/10.1038/ncomms8525

Gupta, R. K., & Kuznicki, J. (2020). Biological and medical importance of cellular heterogeneity deciphered by single-cell RNA sequencing. *Cells*, *9*(8), 1751. https://doi.org/10.3390/cells9081751

Hammachi, F., Morrison, G., Sharov, A., Livigni, A., Narayan, S., Papapetrou, E., O'Malley, J., Kaji, K., Ko, M., Ptashne, M., & Brickman, J. (2012). Transcriptional activation by Oct4 is sufficient for the maintenance and induction of pluripotency. *Cell Rep.*, *1*(2), 99–109. https://doi.org/10.1016/j.celrep.2011.12.002

Harvey, A., Caretti, G., Moresi, V., Renzini, A., & Adamo, S. (2019). Interplay between metabolites and the epigenome in regulating embryonic and adult stem cell potency and maintenance. *Stem Cell Rep.*, *13*(4), 573–589. https://doi.org/10.1016/j.stemcr.2019.09.003

Hazeltine, L. B., Selekman, J. A., & Palecek, S. P. (2013). Engineering the human pluripotent stem cell microenvironment to direct cell fate. *Biotechnol/ Adv.*, *31*(7), 1002–1019. https://doi.org/10.1016/j.biotechadv.2013.03.002

Horiguchi, I., & Kino-oka, M. (2021). Current developments in the stable production of human induced pluripotent stem cells. *Engineering*, *7*(2), 144–152. https://doi.org/10.1016/j.eng.2021.01.001

Huang, C. Y., Liu, C. L., Ting, C. Y., Chiu, Y. T., Cheng, Y. C., Nicholson, M. W., & Hsieh, P. C. H. (2019). Human iPSC banking: barriers and opportunities. *J. Biomed. Sci.*, *26*(1). https://doi.org/10.1186/s12929-019-0578-x

Ireland, R. G., & Simmons, C. A. (2015). Human pluripotent stem cell mechanobiology: manipulating the biophysical microenvironment for regenerative medicine and tissue engineering applications. *Stem Cells*, *33*(11), 3187–3196. https://doi.org/10.1002/stem.2105

Ishihara, S., Sasagawa, Y., Kameda, T., Yamashita, H., Umeda, M., Kotomura, N., Abe, M., Shimono, Y., & Nikaido, I. (2021). Local states of chromatin compaction at transcription start sites control transcription levels. *Nucleic Acids Res.*, *49*(14), 8007–8023. https://doi.org/10.1093/nar/gkab587

Jain, N., Iyer, K. V., Kumar, A., & Shivashankar, G. V. (2013). Cell geometric constraints induce modular gene-expression patterns via redistribution of HDAC3 regulated by actomyosin contractility. *Proc. Natl. Acad. Sci.*, *110*(28), 11349–11354. https://doi.org/10.1073/pnas.1300801110

Jensen, C., & Teng, Y. (2020). Is it time to start transitioning from 2D to 3D cell culture? *Front. Mol. Biosci.*, *7*. https://doi.org/10.3389/fmolb.2020.00033

Ji, P., Manupipatpong, S., Xie, N., & Li, Y. (2016). Induced pluripotent stem cells: generation strategy and epigenetic mystery behind reprogramming. *Stem Cells Int.*, *2016*, 1–11. https://doi.org/10.1155/2016/8415010

Juan, A., Wang, S., Ko, K., Zare, H., Tsai, P. F., Feng, X., Vivanco, K., Ascoli, A., Gutierrez-Cruz, G., Krebs, J., Sidoli, S., Knight, A., Pedersen, R., Garcia, B., Casellas, R., Zou, J., & Sartorelli, V. (2016). Roles of H3K27me2 and H3K27me3 examined during fate specification of embryonic stem cells. *Cell Rep.*, *17*(5), 1369–1382. https://doi.org /10.1016/j.celrep.2016.09.087

Kaneko, S., Kakinuma, S., Asahina, Y., Kamiya, A., Miyoshi, M., Tsunoda, T., Nitta, S., Asano, Y., Nagata, H., Otani, S., Kawai-Kitahata, F., Murakawa, M., Itsui, Y., Nakagawa, M., Azuma, S., Nakauchi, H., Nishitsuji, H., Ujino, S., Shimotohno, K., . . . Watanabe, M. (2016). Human induced pluripotent stem cell-derived hepatic cell lines as a new model for host interaction with hepatitis B virus. *Sci. Rep.*, *6*(1). https://doi.org/10.1038/srep29358

Kanie, K., Sakai, T., Imai, Y., Yoshida, K., Sugimoto, A., Makino, H., Kubo, H., & Kato, R. (2019). Effect of mechanical vibration stress in cell culture on human induced pluripotent stem cells. *Regen. Ther.*, *12*, 27–35. https://doi.org/10.1016/j.reth.2019. 05.002

Kato, Y., Kim, M. H., & Kino-oka, M. (2018). Comparison of growth kinetics between static and dynamic cultures of human induced pluripotent stem cells. *J. Biosci. Bioeng.*, *125*(6), 736–740. https://doi.org/10.1016/j.jbiosc.2018.01.002

Kato, Y., Matsumoto, T., & Kino-oka, M. (2019). Effect of liquid flow by pipetting during medium change on deformation of hiPSC aggregates. *Regen. Ther.*, *12*, 20–26. https://doi.org/10.1016/j.reth.2019.03.004

Keeling, M. C., Flores, L. R., Dodhy, A. H., Murray, E. R., & Gavara, N. (2017). Actomyosin and vimentin cytoskeletal networks regulate nuclear shape, mechanics and chromatin organization. *Sci. Rep.*, *7*(1). https://doi.org/10.1038/s41598-017-05467-x

Keller, A., Dziedzicka, D., Zambelli, F., Markouli, C., Sermon, K., Spits, C., & Geens, M. (2018). Genetic and epigenetic factors which modulate differentiation propensity in human pluripotent stem cells. *Hum. Reprod. Update*, *24*(2), 162–175. https://doi.org /10.1093/humupd/dmx042

Khatau, S. B., Bloom, R. J., Bajpai, S., Razafsky, D., Zang, S., Giri, A., Wu, P. H., Marchand, J., Celedon, A., Hale, C. M., Sun, S. X., Hodzic, D., & Wirtz, D. (2012). The distinct roles of the nucleus and nucleus-cytoskeleton connections in three-dimensional cell migration. *Sci. Rep.*, *2*(1). https://doi.org/10.1038/srep00488

Killaars, A. R., Grim, J. C., Walker, C. J., Hushka, E. A., Brown, T. E., & Anseth, K. S. (2018). Extended exposure to stiff microenvironments leads to persistent chromatin remodeling

in human mesenchymal stem cells. *Adv. Sci.*, *6*(3), 1801483. https://doi.org/10.1002/advs.201801483

Killaars, A. R., Walker, C. J., & Anseth, K. S. (2020). Nuclear mechanosensing controls MSC osteogenic potential through HDAC epigenetic remodeling. *Proc. Natl. Acad. Sci.*, *117*(35), 21258–21266. https://doi.org/10.1073/pnas.2006765117

Kim, I. G., Gil, C. H., Seo, J., Park, S. J., Subbiah, R., Jung, T. H., Kim, J. S., Jeong, Y. H., Chung, H. M., Lee, J. H., Lee, M. R., Moon, S. H., & Park, K. (2018). Mechanotransduction of human pluripotent stem cells cultivated on tunable cell-derived extracellular matrix. *Biomaterials*, *150*, 100–111. https://doi.org/10.1016/j.biomaterials.2017.10.016

Kim, K., Doi, A., Wen, B., Ng, K., Zhao, R., Cahan, P., Kim, J., Aryee, M. J., Ji, H., Ehrlich, L. I. R., Yabuuchi, A., Takeuchi, A., Cunniff, K. C., Hongguang, H., Mckinney-Freeman, S., Naveiras, O., Yoon, T. J., Irizarry, R. A., Jung, N., . . . Daley, G. Q. (2010). Epigenetic memory in induced pluripotent stem cells. *Nature*, *467*(7313), 285–290. https://doi.org/10.1038/nature09342

Kim, M. H., & Kino-oka, M. (2020). Bioengineering considerations for a nurturing way to enhance scalable expansion of human pluripotent stem cells. *Biotechnol. J.*, *15*(4), 1900314. https://doi.org/10.1002/biot.201900314

Koaykul, C., Kim, M. H., Kawahara, Y., Yuge, L., & Kino-oka, M. (2019). Maintenance of neurogenic differentiation potential in passaged bone marrow-derived human mesenchymal stem cells under simulated microgravity conditions. *Stem Cells Dev.*, *28*(23), 1552–1561. https://doi.org/10.1089/scd.2019.0146

Kropp, C., Massai, D., & Zweigerdt, R. (2017). Progress and challenges in large-scale expansion of human pluripotent stem cells. *Process Biochem.*, *59*, 244–254. https://doi.org/10.1016/j.procbio.2016.09.032

Kshitiz, Afzal, J., Chang, H., Goyal, R., & Levchenko, A. (2016). Mechanics of Microenvironment as instructive cues guiding stem cell behavior. *Current Stem Cell Rep.*, *2*(1), 62–72. https://doi.org/10.1007/s40778-016-0033-9

Lange, J. R., & Fabry, B. (2013). Cell and tissue mechanics in cell migration. *Exp. Cell Res.*, *319*(16), 2418–2423. https://doi.org/10.1016/j.yexcr.2013.04.023

Le, H. Q., Ghatak, S., Yeung, C. Y. C., Tellkamp, F., Günschmann, C., Dieterich, C., Yeroslaviz, A., Habermann, B., Pombo, A., Niessen, C. M., & Wickström, S. A. (2016). Mechanical regulation of transcription controls Polycomb-mediated gene silencing

during lineage commitment. *Nat. Cell Biol.*, *18*(8), 864–875. https://doi.org/10.1038/ncb3387

Le, M. N. T., & Hasegawa, K. (2019). Expansion culture of human pluripotent stem cells and production of cardiomyocytes. *Bioengineering*, *6*(2), 48. https://doi.org/10.3390/bioengineering6020048

Lee, J., Abdeen, A. A., & Kilian, K. A. (2014). Rewiring mesenchymal stem cell lineage specification by switching the biophysical microenvironment. *Sci. Rep.*, *4*(1). https://doi.org/10.1038/srep05188

Lei, Y., & Schaffer, D. V. (2013). A fully defined and scalable 3D culture system for human pluripotent stem cell expansion and differentiation. *Proc. Natl. Acad. Sci.*, *110*(52), E5039–E5048. https://doi.org/10.1073/pnas.1309408110

Leitch, H. G., McEwen, K. R., Turp, A., Encheva, V., Carroll, T., Grabole, N., Mansfield, W., Nashun, B., Knezovich, J. G., Smith, A., Surani, M. A., & Hajkova, P. (2013). Naive pluripotency is associated with global DNA hypomethylation. *Nat. Struct. Biol.*, *20*(3), 311–316. https://doi.org/10.1038/nsmb.2510

Levenson, J. M., & Sweatt, J. D. (2005). Epigenetic mechanisms in memory formation. *Nat. Rev. Neurosci.*, *6*(2), 108–118. https://doi.org/10.1038/nrn1604

Li, C., & Wang, J. (2013). Quantifying Waddington landscapes and paths of non-adiabatic cell fate decisions for differentiation, reprogramming and transdifferentiation. *J. R. Soc. Interface*, *10*(89), 20130787. https://doi.org/10.1098/rsif.2013.0787

Li, C. X., Talele, N. P., Boo, S., Koehler, A., Knee-Walden, E., Balestrini, J. L., Speight, P., Kapus, A., & Hinz, B. (2016). MicroRNA-21 preserves the fibrotic mechanical memory of mesenchymal stem cells. *Nat. Mater.*, *16*(3), 379–389. https://doi.org/10.1038/nmat4780

Li, L., Bennett, S. A., & Wang, L. (2012). Role of E-cadherin and other cell adhesion molecules in survival and differentiation of human pluripotent stem cells. *Cell Adh. Migr.*, *6*(1), 59–73. https://doi.org/10.4161/cam.19583

Lipsitz, Y. Y., Woodford, C., Yin, T., Hanna, J. H., & Zandstra, P. W. (2018). Modulating cell state to enhance suspension expansion of human pluripotent stem cells. *Proc. Natl. Acad. Sci.*, *115*(25), 6369–6374. https://doi.org/10.1073/pnas.1714099115

Liu, L. P., & Zheng, Y. W. (2019). Predicting differentiation potential of human pluripotent stem cells: Possibilities and challenges. *World J. Stem Cells*, *11*(7), 375–382. https://doi.org/10.4252/wjsc.v11.i7.375

Liu, X., Wang, C., Liu, W., Li, J., Li, C., Kou, X., Chen, J., Zhao, Y., Gao, H., Wang, H., Zhang, Y., Gao, Y., & Gao, S. (2016). Distinct features of H3K4me3 and H3K27me3 chromatin domains in pre-implantation embryos. *Nature*, *537*(7621), 558–562. https://doi.org/10.1038/nature19362

Mao, A. S., Shin, J. W., & Mooney, D. J. (2016). Effects of substrate stiffness and cell-cell contact on mesenchymal stem cell differentiation. *Biomaterials*, *98*, 184–191. https://doi.org/10.1016/j.biomaterials.2016.05.004

McEwen, K., Leitch, H., Amouroux, R., & Hajkova, P. (2013). The impact of culture on epigenetic properties of pluripotent stem cells and pre-implantation embryos. *Biochem. Soc. Trans.*, *41*(3), 711–719. https://doi.org/10.1042/bst20130049

McKee, C., Brown, C., & Chaudhry, G. R. (2019). Self-assembling scaffolds supported long-term growth of human primed embryonic stem cells and upregulated core and naïve pluripotent markers. *Cells*, *8*(12), 1650. https://doi.org/10.3390/cells8121650

Meissner, A. (2010). Epigenetic modifications in pluripotent and differentiated cells. *Nat. Biotechnol.*, *28*(10), 1079–1088. https://doi.org/10.1038/nbt.1684

Messmer, T., von Meyenn, F., Savino, A., Santos, F., Mohammed, H., Lun, A. T. L., Marioni, J. C., & Reik, W. (2019). Transcriptional heterogeneity in naive and primed human pluripotent stem cells at single-cell resolution. *Cell Rep.*, *26*(4), 815–824.e4. https://doi.org/10.1016/j.celrep.2018.12.099

Mikkelsen, T. S., Ku, M., Jaffe, D. B., Issac, B., Lieberman, E., Giannoukos, G., Alvarez, P., Brockman, W., Kim, T. K., Koche, R. P., Lee, W., Mendenhall, E., O'Donovan, A., Presser, A., Russ, C., Xie, X., Meissner, A., Wernig, M., Jaenisch, R., . . . Bernstein, B. E. (2007). Genome-wide maps of chromatin state in pluripotent and lineage-committed cells. *Nature*, *448*(7153), 553–560. https://doi.org/10.1038/nature06008

Mirbagheri, M., Adibnia, V., Hughes, B. R., Waldman, S. D., Banquy, X., & Hwang, D. K. (2019). Advanced cell culture platforms: a growing quest for emulating natural tissues. *Mater. Horiz.*, *6*(1), 45–71. https://doi.org/10.1039/c8mh00803e

Mishra, A. K., Mondo, J. A., Campanale, J. P., & Montell, D. J. (2019). Coordination of protrusion dynamics within and between collectively migrating border cells by myosin II. *Mol. Biol. Cell*, *30*(19), 2490–2502. https://doi.org/10.1091/mbc.e19-02-0124

Nath, S. C., Horie, M., Nagamori, E., & Kino-oka, M. (2017). Size- and time-dependent growth properties of human induced pluripotent stem cells in the culture of single aggregate. *J. Biosci. Bioeng.*, *124*(4), 469–475. https://doi.org/10.1016/j.jbiosc.2017.05.006

Nichols, J., & Smith, A. (2009). Naive and Primed Pluripotent States. *Cell Stem Cell*, *4*(6), 487–492. https://doi.org/10.1016/j.stem.2009.05.015

Ortmann, D., Brown, S., Czechanski, A., Aydin, S., Muraro, D., Huang, Y., Tomaz, R. A., Osnato, A., Canu, G., Wesley, B. T., Skelly, D. A., Stegle, O., Choi, T., Churchill, G. A., Baker, C. L., Rugg-Gunn, P. J., Munger, S. C., Reinholdt, L. G., & Vallier, L. (2020). Naive pluripotent stem cells exhibit phenotypic variability that is driven by genetic variation. *Cell Stem Cell*, *27*(3), 470–481.e6. https://doi.org/10.1016/j.stem.2020.07.019

Pauklin, S., & Vallier, L. (2013). The cell-cycle state of stem cells determines cell fate propensity. *Cell*, *155*(1), 135–147. https://doi.org/10.1016/j.cell.2013.08.031

Phadnis, S. M., Loewke, N. O., Dimov, I. K., Pai, S., Amwake, C. E., Solgaard, O., Baer, T. M., Chen, B., & Pera, R. A. R. (2015). Dynamic and social behaviors of human pluripotent stem cells. *Sci. Rep.*, *5*(1). https://doi.org/10.1038/srep14209

Polak, J. M., & Mantalaris, S. (2008). Stem cells bioprocessing: an important milestone to move regenerative medicine research into the clinical arena. *Pediatr. Res.*, *63*(5), 461–466. https://doi.org/10.1203/pdr.0b013e31816a8c1c

Pruvost, M., & Moyon, S. (2021). Oligodendroglial epigenetics, from lineage specification to activity-dependent myelination. *Life*, *11*(1), 62. https://doi.org/10.3390/life11010062

Rada-Iglesias, A., & Wysocka, J. (2011). Epigenomics of human embryonic stem cells and induced pluripotent stem cells: insights into pluripotency and implications for disease. *Genome Med.*, *3*(6), 36. https://doi.org/10.1186/gm252

Rehakova, D., Souralova, T., & Koutna, I. (2020). Clinical-grade human pluripotent stem cells for cell therapy: characterization strategy. *Int. J. Mol. Sci.*, *21*(7), 2435. https://doi.org/10.3390/ijms21072435

Roberts, G. A., Ozkan, B., Gachulincová, I., O'Dwyer, M. R., Hall-Ponsele, E., Saxena, M., Robinson, P. J., & Soufi, A. (2021). Dissecting OCT4 defines the role of nucleosome binding in pluripotency. *Nat. Cell Biol.*, *23*(8), 834–845. https://doi.org/10.1038/s41556-021-00727-5

Rohani, L., Borys, B. S., Razian, G., Naghsh, P., Liu, S., Johnson, A. A., Machiraju, P., Holland, H., Lewis, I. A., Groves, R. A., Toms, D., Gordon, P. M. K., Li, J. W., So, T., Dang, T., Kallos, M. S., & Rancourt, D. E. (2020). Stirred suspension bioreactors maintain naïve pluripotency of human pluripotent stem cells. *Commun. Biol.*, *3*(1). https://doi.org/10.1038/s42003-020-01218-3

Sao, K., Jones, T. M., Doyle, A. D., Maity, D., Schevzov, G., Chen, Y., Gunning, P. W., & Petrie, R. J. (2019). Myosin II governs intracellular pressure and traction by distinct tropomyosin-dependent mechanisms. *Mol. Biol. Cell*, *30*(10), 1170–1181. https://doi.org/10.1091/mbc.e18-06-0355

Sapra, K. T., Qin, Z., Dubrovsky-Gaupp, A., Aebi, U., Müller, D. J., Buehler, M. J., & Medalia, O. (2020). Nonlinear mechanics of lamin filaments and the meshwork topology build an emergent nuclear lamina. *Nat. Commun.*, *11*(1). https://doi.org/10.1038/s41467-020-20049-8

Saxton, D. S., & Rine, J. (2019). Epigenetic memory independent of symmetric histone inheritance. *Elife*, *8*. https://doi.org/10.7554/Elife.51421

Scesa, G., Adami, R., & Bottai, D. (2021). iPSC preparation and epigenetic memory: does the tissue origin matter? *Cells*, *10*(6), 1470. https://doi.org/10.3390/cells10061470

Seki, T., & Fukuda, K. (2016). Induced pluripotent stem cells for clinical use. *Pluripotent Stem Cells - From the Bench to the Clinic*. Published. https://doi.org/10.5772/62505

Shi, Y., Inoue, H., Wu, J. C., & Yamanaka, S. (2016). Induced pluripotent stem cell technology: a decade of progress. *Nat. Rev. Drug Discov.*, *16*(2), 115–130. https://doi.org/10.1038/nrd.2016.245

Shibata, S., Hayashi, R., Okubo, T., Kudo, Y., Katayama, T., Ishikawa, Y., Toga, J., Yagi, E., Honma, Y., Quantock, A. J., Sekiguchi, K., & Nishida, K. (2018). Selective laminin-directed differentiation of human induced pluripotent stem cells into distinct ocular lineages. *Cell Rep.*, *25*(6), 1668–1679.e5. https://doi.org/10.1016/j.celrep.2018.10.032

Shih, Y. R. V., Tseng, K. F., Lai, H. Y., Lin, C. H., & Lee, O. K. (2011). Matrix stiffness regulation of integrin-mediated mechanotransduction during osteogenic differentiation of human mesenchymal stem cells. *J. Bone Miner. Res.*, *26*(4), 730–738. https://doi.org/10.1002/jbmr.278

Shuzui, E., Kim, M. H., Azuma, K., Fujinaga, Y., & Kino-oka, M. (2019). Maintenance of an undifferentiated state of human-induced pluripotent stem cells through botulinum hemagglutinin-mediated regulation of cell behavior. *J. Biosci. Bioeng.*, *127*(6), 744–751. https://doi.org/10.1016/j.jbiosc.2018.11.014

Smith, Q., Stukalin, E., Kusuma, S., Gerecht, S., & Sun, S. X. (2015). Stochasticity and spatial interaction govern stem cell differentiation dynamics. *Sci. Rep.*, *5*(1). https://doi.org/10.1038/srep12617

Sodek, K. L., Ringuette, M. J., & Brown, T. J. (2009). Compact spheroid formation by ovarian cancer cells is associated with contractile behavior and an invasive phenotype. *Int. J. Cancer Res.*, *124*(9), 2060–2070. https://doi.org/10.1002/ijc.24188

Spivakov, M., & Fisher, A. G. (2007). Epigenetic signatures of stem-cell identity. *Nat. Rev. Genet.*, *8*(4), 263–271. https://doi.org/10.1038/nrg2046

Sreenivasappa, H., Chaki, S. P., Lim, S. M., Trzeciakowski, J. P., Davidson, M. W., Rivera, G. M., & Trache, A. (2014). Selective regulation of cytoskeletal tension and cell–matrix adhesion by RhoA and Src. *Integr. Biol.*, *6*(8), 743. https://doi.org/10.1039/c4ib00019f

Stephens, A. D., Banigan, E. J., Adam, S. A., Goldman, R. D., & Marko, J. F. (2017). Chromatin and lamin A determine two different mechanical response regimes of the cell nucleus. *Mol. Biol. Cell*, *28*(14), 1984–1996. https://doi.org/10.1091/mbc.e16-09-0653

Takahashi, K. (2012). Cellular reprogramming – lowering gravity on Waddington's epigenetic landscape. *J. Cell Sci.*, https://doi.org/10.1242/jcs.084822

Takahashi, K., & Yamanaka, S. (2006). Induction of pluripotent stem cells from mouse embryonic and adult fibroblast cultures by defined factors. *Cell*, *126*(4), 663–676. https://doi.org/10.1016/j.cell.2006.07.024

Takahashi, S., Kobayashi, S., & Hiratani, I. (2018). Epigenetic differences between naïve and primed pluripotent stem cells. *Cell. Mol. Life Sci.*, *75*(7), 1191–1203. https://doi.org/10.1007/s00018-017-2703-x

Tanosaki, S., Tohyama, S., Kishino, Y., Fujita, J., & Fukuda, K. (2021). Metabolism of human pluripotent stem cells and differentiated cells for regenerative therapy: a focus on cardiomyocytes. *Inflamm. Regen.*, *41*(1). https://doi.org/10.1186/s41232-021-00156-9

Tenga, R., & Medalia, O. (2020). Structure and unique mechanical aspects of nuclear lamin filaments. *Curr. Opin. Struct. Biol.*, *64*, 152–159. https://doi.org/10.1016/j.sbi.2020.06.017

Theunissen, T., Friedli, M., He, Y., Planet, E., O'Neil, R., Markoulaki, S., Pontis, J., Wang, H., Iouranova, A., Imbeault, M., Duc, J., Cohen, M., Wert, K., Castanon, R., Zhang, Z., Huang, Y., Nery, J., Drotar, J., Lungjangwa, T., . . . Jaenisch, R. (2016). Molecular criteria for defining the naive human pluripotent state. *Cell Stem Cell*, *19*(4), 502–515. https://doi.org/10.1016/j.stem.2016.06.011

Toh, K. C., Ramdas, N. M., & Shivashankar, G. V. (2015). Actin cytoskeleton differentially alters the dynamics of lamin A, HP1α and H2B core histone proteins to remodel

chromatin condensation state in living cells. *Integr. Biol.*, *7*(10), 1309–1317. https://doi.org/10.1039/c5ib00027k

Tosolini, M., Brochard, V., Adenot, P., Chebrout, M., Grillo, G., Navia, V., Beaujean, N., Francastel, C., Bonnet-Garnier, A., & Jouneau, A. (2018). Contrasting epigenetic states of heterochromatin in the different types of mouse pluripotent stem cells. *Sci. Rep.*, *8*(1). https://doi.org/10.1038/s41598-018-23822-4

Valamehr, B., Abujarour, R., Robinson, M., Le, T., Robbins, D., Shoemaker, D., & Flynn, P. (2012). A novel platform to enable the high-throughput derivation and characterization of feeder-free human iPSCs. *Sci. Rep.*, *2*(1). https://doi.org/10.1038/srep00213

van Helvert, S., Storm, C., & Friedl, P. (2017). Mechanoreciprocity in cell migration. *Nat. Cell Biol.*, *20*(1), 8–20. https://doi.org/10.1038/s41556-017-0012-0

van Mierlo, G., Dirks, R. A., de Clerck, L., Brinkman, A. B., Huth, M., Kloet, S. L., Saksouk, N., Kroeze, L. I., Willems, S., Farlik, M., Bock, C., Jansen, J. H., Deforce, D., Vermeulen, M., Déjardin, J., Dhaenens, M., & Marks, H. (2019). Integrative proteomic profiling reveals PRC2-dependent epigenetic crosstalk maintains ground-state pluripotency. *Cell Stem Cell*, *24*(1), 123–137.e8. https://doi.org/10.1016/j.stem.2018.10.017

Vining, K. H., & Mooney, D. J. (2017). Mechanical forces direct stem cell behaviour in development and regeneration. *Nat. Rev. Mol. Cell Biol.*, *18*(12), 728–742. https://doi.org/10.1038/nrm.2017.108

Wang, L., Xu, X., Cao, Y., Li, Z., Cheng, H., Zhu, G., Duan, F., Na, J., Han, J. D. J., & Chen, Y. G. (2017). Activin/Smad2-induced histone H3 Lys-27 trimethylation (H3K27me3) reduction is crucial to initiate mesendoderm differentiation of human embryonic stem cells. *J. Biol. Chem.*, *292*(4), 1339–1350. https://doi.org/10.1074/jbc.m116.766949

Warrier, S., van der Jeught, M., Duggal, G., Tilleman, L., Sutherland, E., Taelman, J., Popovic, M., Lierman, S., Chuva De Sousa Lopes, S., van Soom, A., Peelman, L., van Nieuwerburgh, F., de Coninck, D. I. M., Menten, B., Mestdagh, P., van de Sompele, J., Deforce, D., de Sutter, P., & Heindryckx, B. (2017). Direct comparison of distinct naive pluripotent states in human embryonic stem cells. *Nat. Commun.*, *8*(1). https://doi.org/10.1038/ncomms15055

Weinberger, L., Ayyash, M., Novershtern, N., & Hanna, J. H. (2016). Dynamic stem cell states: naive to primed pluripotency in rodents and humans. *Nat. Rev. Mol. Cell Biol.*, *17*(3), 155–169. https://doi.org/10.1038/nrm.2015.28

Weissbein, U., Plotnik, O., Vershkov, D., & Benvenisty, N. (2017). Culture-induced recurrent epigenetic aberrations in human pluripotent stem cells. *PLoS Genet.*, *13*(8), e1006979. https://doi.org/10.1371/journal.pgen.1006979

Wolf, K., te Lindert, M., Krause, M., Alexander, S., te Riet, J., Willis, A. L., Hoffman, R. M., Figdor, C. G., Weiss, S. J., & Friedl, P. (2013). Physical limits of cell migration: Control by ECM space and nuclear deformation and tuning by proteolysis and traction force. *J. Cell Biol.*, *201*(7), 1069–1084. https://doi.org/10.1083/jcb.201210152

Wrighton, P. J., Klim, J. R., Hernandez, B. A., Koonce, C. H., Kamp, T. J., & Kiessling, L. L. (2014). Signals from the surface modulate differentiation of human pluripotent stem cells through glycosaminoglycans and integrins. *Proc. Natl. Acad. Sci.*, *111*(51), 18126–18131. https://doi.org/10.1073/pnas.1409525111

Wu, F., Su, R. Q., Lai, Y. C., & Wang, X. (2017). Engineering of a synthetic quadrastable gene network to approach Waddington landscape and cell fate determination. *Elife*, *6*. https://doi.org/10.7554/Elife.23702

Yamada, K. M., & Sixt, M. (2019). Mechanisms of 3D cell migration. *Nat. Rev. Mol. Cell Biol.*, *20*(12), 738–752. https://doi.org/10.1038/s41580-019-0172-9

Yang, C., Tibbitt, M. W., Basta, L., & Anseth, K. S. (2014). Mechanical memory and dosing influence stem cell fate. *Nat. Mater.*, *13*(6), 645–652. https://doi.org/10.1038/nmat3889

Yeo, J. C., & Ng, H. H. (2012). The transcriptional regulation of pluripotency. *Cell Res.*, *23*(1), 20–32. https://doi.org/10.1038/cr.2012.172

Yoshida, S., Miyagawa, S., Fukushima, S., Kawamura, T., Kashiyama, N., Ohashi, F., Toyofuku, T., Toda, K., & Sawa, Y. (2018). Maturation of human induced pluripotent stem cell-derived cardiomyocytes by soluble factors from human mesenchymal stem cells. *Mol. Ther.*, *26*(11), 2681–2695. https://doi.org/10.1016/j.ymthe.2018.08.012

Yu, L., Li, J., Hong, J., Takashima, Y., Fujimoto, N., Nakajima, M., Yamamoto, A., Dong, X., Dang, Y., Hou, Y., Yang, W., Minami, I., Okita, K., Tanaka, M., Luo, C., Tang, F., Chen, Y., Tang, C., Kotera, H., & Liu, L. (2018). Low cell-matrix adhesion reveals two subtypes of human pluripotent stem cells. *Stem Cell Rep.*, *11*(1), 142–156. https://doi.org/10.1016/j.stemcr.2018.06.003

Zhang, L., & Zhang, S. (2020). Imputing single-cell RNA-seq data by considering cell heterogeneity and prior expression of dropouts. *J. Mol. Cell Biol.*, *13*(1), 29–40. https://doi.org/10.1093/jmcb/mjaa052

Lists of publications

Thanuthanakhun, N., Kino-oka, M., Borwornpinyo, S., Ito, Y., & Kim, M. H. (2021). The impact of culture dimensionality on behavioral epigenetic memory contributing to pluripotent state of iPS cells. *J. Cell. Physiol.*, *236*(7), 4985–4996. https://doi.org/10.1002/jcp.30211

Kim, M. H., Thanuthanakhun, N., Fujimoto, S., & Kino-oka, M. (2021). Effect of initial seeding density on cell behavior-driven epigenetic memory and preferential lineage differentiation of human iPSCs. *Stem Cell Res.*, *56*, 102534. https://doi.org/10.1016/j.scr.2021.102534

Acknowledgements

Utmost and heartfelt appreciation are extended to all relevant persons for their support, help and encouragement that directly or indirectly contributed to the completion of this study.

I would like to express my sincere gratitude to my supervisor, Prof. Masahiro Kino-oka, for giving me the opportunity to be a part of BioProcess Systems Engineering laboratory at Osaka University since my Master's study and providing invaluable guidance and advice throughout the years.

I am also most grateful to my research director, Assoc. Prof. Mee-Hae Kim, who has mentored me with great patience and given me endless of support. Her advisement has helped me to grow both academically and personally.

I would like to extend my deepest appreciation to my dissertation committee members, Prof. Kazuhito Fujiyama and Prof. Hajime Watanabe, for their constructive comments and helpful input in finalizing this study.

I would like to give special thanks to Asst. Prof. Ikki Horiguchi for always providing me honest feedback on my research as well as technical and miscellaneous support.

I would like to thank Mr. Chaiyong Koaykul, Ms. Fitria Dwi Ayuningtyas, Ms. Parichut Thummarati, Mr. Shun Fujimoto, Ms. Sathidaphorn Sungwallek, and all members in BioProcess Systems Engineering laboratory for their research assistantship and constant encouragement.

I would like to acknowledge the Government of Japan's Ministry of Education, Culture, Sports, Science and Technology (MEXT) for providing me with a full scholarship for my study and stay in Japan.

I owe a great deal of gratitude to my previous teachers at Mahidol University, Thailand for a huge contribution to my success ever since. I must also recognize all my friends here in Japan and back at home in Thailand for the unconditional friendship and motivational conversations. Without their support, I would not have been able to go through all challenges and difficulties along my journey.

Last but not the least, it is my privilege to express a deep sense of gratitude to my parents and family for their love and for instilling in me the courage and perseverance to achieve my goal.

Naruchit Thanuthanakhun